Immunological and functional consequences of von Willebrand factor binding to complement C1q

Inauguraldissertation

zur

Erlangung der Würde eines Doktors der Philosophie

vorlegt der

Philosophisch-Naturwissenschaftlichen Fakultät

der Universität Basel

von

Claudia Donat

2020

Genehmigt von der Philosophisch-Naturwissenschaftlichen Fakultät
auf Antrag von

Prof. Dr. Marten Trendelenburg

Prof. Dr. Radek Skoda

Assoz. Prof. Dr. Verena Schröder

Basel, den 18. Februar 2020

Prof. Dr. Martin Spiess
Dekan

Table of Contents

List of Figures

List of Abbreviations

ABC	adenosine triphosphate (ATP)-binding cassette
ADAMTS13	a disintegrin and metalloproteinase with a thrombospondin type 1 motif, member 13
ADP	adenosine diphosphate
AF	Alexa Fluor®
aHUS	atypical hemolytic uremic syndrome
AnV	AnnexinV
APC	allophycocyanin
ApoE	apoplipoprotein E
aPTT	activated partial thromboplastin time
AU	arbitrary aggregation units
AUC	area under the curve
B cell	B lymphocyte
BSA	bovine serum albumin
BW	body weight
C1qa$^{-/-}$	C1q-deficient
CANTOS	Canakinumab Antiinflammatory Thrombosis Outcome Study
CC	cholesterol crystals
cC1q	collagen-like domain of C1q
CD	cluster of differentiation
CK	cysteine knots
CRP	C-reactive protein
d	days
DAF	decay-accelerating factor
DAMPs	damage-associated molecular patterns
DAPI	4′,6-diamidino-2-phenylindole
DCs	dendritic cells
DMEM	Dulbecco's Modified Eagle Media
e.g.	exempli gratia
EDTA	ethylenediaminetetraacetic acid
EKNZ	Ethikkommission Nordwest- und Zentralschweiz
ELISA	enzyme-linked immunosorbent assay
FACS	fluorescence-activated cell sorting

FC	fragment crystallizable
FCS	fetal calf serum
FITC	fluorescein isothiocyanate
FLICA	fluorochrome-labeled inhibitors of caspases
gC1q	globular head domain of C1q
GM-CSF	granulocyte-macrophage colony-stimulating factor
gMFI	geometric mean fluorescence intensity
GP	glycoprotein complex
HAE	hereditary angioedema
HIV	human immunodeficiency virus
HMDMs	human monocyte-derived macrophages
hr	hour
HSA	human serum albumin
i.p.	intraperitoneal
i.v.	intravenous
Ig	immunoglobulin
IL	interleukin
IQR	interquartile range
JAK	Janus kinase
LAIR1	leukocyte-associated immunoglobulin-like receptor 1
LDL	low-density lipoprotein
LPS	lipopolysaccharide
LRP-1	low-density lipoprotein receptor-related protein 1
MAC	membrane-attack complex
MBL	mannose-binding lectin
MerTK	tyrosine-protein-kinase Mer
MHC II	major histocompatibility complex class II
mRNA	messenger ribonucleic acid
NLRP3	NOD (nucleotide oligomerization domain)-, LRR (leucine-rich repeat)-, and PYD (pyrin domain)-containing protein 3
ns	not significant
OCT	optimal cutting temperature
OD	optical density
PAMPs	pattern-associated molecular patterns
PBS	phosphate buffered saline

PBSTBF	PBS/Tween/BSA/FCS
PCR	polymerase chain reaction
PD-L1	programmed death ligand 1
PE	phycoerythrin
PeCy	phycoerythrin-cyanine
PI	propidium iodide
PNH	paroxysmal nocturnal hemoglobinuria
PS	phosphatidylserine
PT	prothrombin time
PTX	pentraxin
px²	square pixels
r	Spearman's rank correlation coefficient
ROS	reactive oxygen species
RT	room temperature
SAP	serum amyloid P component
SIRS	systemic inflammatory response syndrome
SLE	systemic lupus erythematosus
SMCs	smooth muscle cells
SR-A1	scavenger receptor A1
SSC	side scatter
STAT	signal transducer and activator of transcription
T cell	T lymphocytes
TCC	terminal complement complex
TF	tissue factor
TMA	thrombotic microangiopathy
TNFα	tumor necrosis factor α
TTP	thrombotic thrombocytopenic purpura
TxA2	thromboxane A2
VTE	venous thromboembolism
vWD	von Willebrand disease
vWF	von Willebrand factor
WPBs	Weibel-Palade bodies
WT	wild type

Summary

This dissertation investigates the immunological and functional consequences of the binding of von Willebrand factor to complement C1q.

Whereas C1q, the pattern recognition molecule of the classical complement pathway, is a crucial player of the innate immune system, von Willebrand factor (vWF) is vital for the initiation of primary hemostasis and functional coagulation.

Although it has been shown that vWF binds to C1q, the impact of the C1q-vWF interaction remains poorly understood.

The reciprocal activation of the complement and coagulation systems has been increasingly shown not only in health but also in a growing number of inflammatory diseases, but the precise pathogenic mechanisms are still incompletely clarified.

Therefore, I aimed at determining the implications of the C1q-vWF binding:

In a first study, we elucidated the interaction between C1q and vWF in the context of atherosclerosis. By using complexes of cholesterol crystals, C1q and vWF as an *in vitro* model, I was able to demonstrate that these complexes decrease phagocytosis and secretion of inflammatory cytokines by human macrophages.

In this way, our results show that C1q-vWF formation could have a favorable effect in an atherosclerotic setting.

In a second study, I examined the interaction between C1q and vWF in the context of hemostasis. By performing quantitative and functional hemostatic tests in C1q-deficient mice, we were able to demonstrate that C1q enhances primary hemostasis, potentially in a vWF-dependent manner.

These findings suggest that C1q exerts a hemostasis-mediating role and provide a possible explanation for thromboembolic complications in inflammatory disorders.

In conclusion, both studies contribute to a better understanding of the C1q-vWF interaction and point towards an impact in atherosclerosis and hemostasis.

General introduction

The complement system

The complement system is an essential part of the innate immune system. The fact that the sum of soluble complement proteins accounts for nearly 5% of the total plasma protein concentration in the human body underlines its importance [1]. The three main physiological activities of the complement system are i) to directly defend against infections, ii) to bridge innate and adaptive immunity, and iii) to clear immune complexes and apoptotic cells [2]. The complement system is composed of approximately 30 proteins, mainly serine proteases in form of pro-enzymes, present in plasma and on cell surfaces. In this manner, initiation of the complement pathway is followed by amplification and propagation. Therefore, regulatory proteins are crucial for finetuning and confinement [3].

The complement proteins can be activated through three different pathways, all of them merging into a shared terminal pathway (**Figure 1**).

The classical pathway of complement is initiated by recognition and binding of the C1 complex ($C1qC1r_2C1s_2$) to a pathogen's cell surface directly or indirectly, e.g. via an antigen-antibody complex or C-reactive protein (CRP). Subsequently, C1r cleaves C1s, which in turn cleaves C4 into C4a and C4b fragments and enables the cleavage of C2 into C2a and C2b, respectively. Formation of C4bC2a on the cell surface acts as a convertase for C3, producing C3a and C3b.

For the lectin pathway, initiation is triggered through binding of mannose-binding lectin (MBL), collectins or ficolins to carbohydrate structures on a pathogen's surface. Activation of the lectin pathway leads to the formation of the same C3 convertase as in the classical pathway.

The alternative pathway is initiated by a spontaneous hydrolysis of soluble C3 in fluid phase, generating $C3(H_20)$. Binding of factor B to $C3(H_20)$ enables its cleavage through factor D to form C3bBb, the alternative C3 convertase. Moreover, the activation of the alternative pathway can occur through binding of factor B to C3b, originated from the classical or lectin pathways.

Thus, all three pathways generate a C3 convertase. The resulting C3b is covalently bound to a cell surface and secondarily binds C3 convertases, forming a C5 convertase (C4bC2aC3b or $C3b_2Bb$). This results in the formation of C5a and C5b. The latter recruits C6, C7, C8 and C9 that polymerize to form the C5b-9 complex, also known as terminal complement complex (TCC) or membrane-attack complex

(MAC). Consequently, MAC formation results in disruption of the cell membrane and lysis of the cell. Moreover, the effector molecules C3b, C3a, C5a and C4a exert important functions. C3b is an opsonin that acts as an eat-me signal for complement receptor-expressing phagocytes by binding to the surface of a pathogen. C3a, C5a and C4a are anaphylatoxins that lead to the recruitment of immune cells and therefore mediate a local inflammatory response. Because of its powerful effects, the complement system is tightly regulated in order to ensure the protection of the host. On the one hand, host cells are resistant against low-grade activation. On the other hand, specialized proteins are responsible for the regulation of the complement system. E.g. C4-binding protein and complement receptor 1 can perturb formation of the C3 convertase by displacing C2a by binding to C4b and factor H and decay-accelerating factor (DAF) by displacing Bb through binding to C3b, whereas protectin (CD59) prevents the formation of MAC [4].

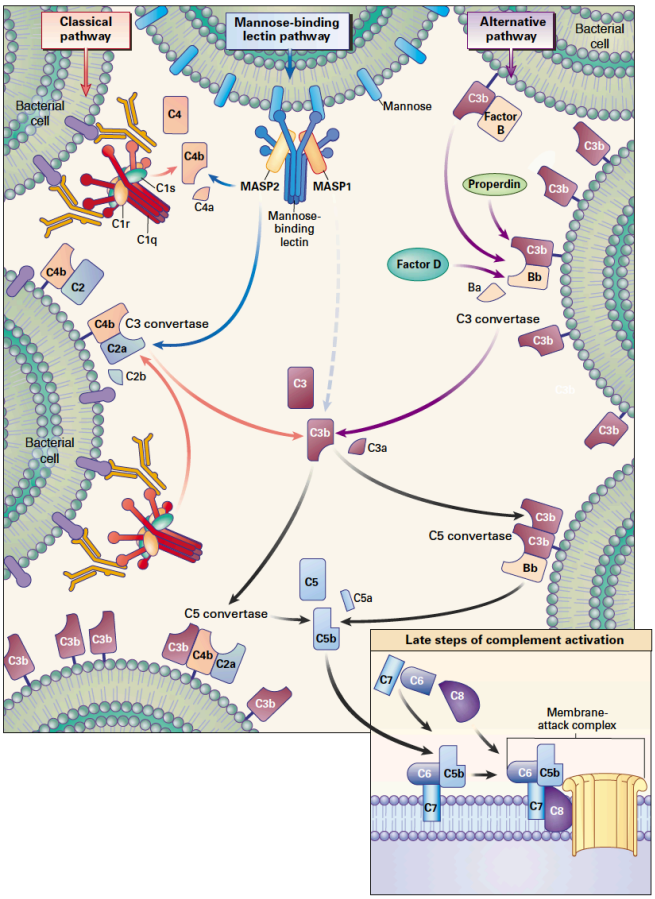

Figure 1: The complement system.

The complement system can be divided into three pathways: the classical, lectin and alternative pathways. All three pathways culminate into late steps of complement activation characterized by formation of the membrane-attack complex (MAC). Abbreviations: MASP-1/2: mannan-binding lectin-associated serine protease-1/2.
Reproduced with permission from Walport [2], © Massachusetts Medical Society.

C1q

Structure

C1q is a 460 kDa glycoprotein, composed of 18 polypeptide chains with its hexameric structure resembling a bouquet of tulips. Six A (34 kDa), six B (32 kDa) and six C (27 kDa) chains form non-covalently linked subunits, with each trimer of one A, B and C chain being covalently linked by disulfide bonds as depicted in **Figure 2** [5-7]. Each chain is comprised of a collagen-like (cC1q) domain near the N-terminus as well as a globular (gC1q) domain at the C-terminus [5, 8], responsible for the interaction with a plethora of ligands.

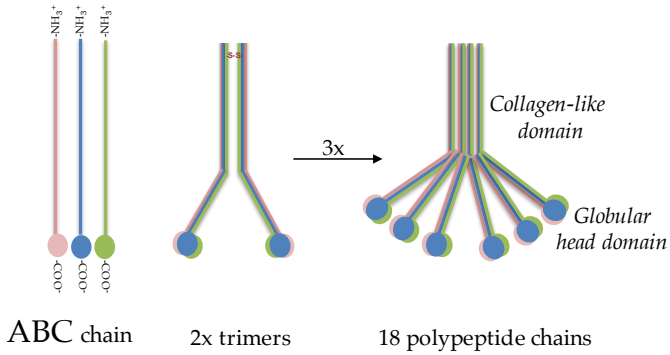

Figure 2: Schematic structure of C1q.

The tulip-like structure of the C1q molecule is depicted. The globular head domain represents the tulip heads, whereas the collagen-like domain represents the tulip stalks. Abbreviations: -S-S-: disulfide bonds.

Biosynthesis

Within the human body, C1q is present in the circulating blood at a physiological concentration of 80-150 µg/ml. Whereas the majority of C1q is bound within the C1 complex, a fraction of C1q is unbound and circulates in tissues [9]. C1q is mainly synthesized by myeloid cells, particularly by cultured monocytes, tissue macrophages and dendritic cells [10], but also by epithelial cells [11], fibroblasts [12], mesenchymal cells [13], microglia cells [14], trophoblasts [15], osteoclasts [16], Kupffer cells [17] and mast cells [18]. The molecule is synthesized as a transmembrane protein that is membrane-anchored until it is enzymatically cleaved into its soluble form [19].

Complement activation

One of the main functions of C1q, and the one that led to its discovery, is the initiation of the classical pathway of the complement system. For this function, the Ca^{2+}-dependent C1 initiation complex is formed by binding of serine proteases C1r and C1s to the cC1q domain ($C1qC1r_2C1s_2$). In detail, binding of the gC1q domain to fragment crystallizable (Fc) regions of antibodies (immunoglobulin (Ig) of IgG or IgM isotype) on an immune complex induces a conformational change in C1r, allowing C1r autoactivation and subsequent C1s cleavage [20]. In this regard, C1q is viewed as a pattern recognition molecule and thus essential in early stages of infection.

Complement-independent functions

Complement-independent functions of C1q were first described in the 1980s with studies demonstrating that C1q, in the absence of C1r and C1s, increases phagocytosis of various targets by phagocytes [21-23]. Over the last decades, the gC1q domain has been described to bind not only IgG and IgM but also structures such as CRP, serum amyloid P component (SAP) , pentraxin (PTX) 3, phosphatidylserine (PS), human immunodeficiency virus (HIV)-1 gp41, apoptotic cells and many more (reviewed in [24]). In this way, C1q acts as an opsonin: while the gC1q domain recognizes the ligands mentioned above, the cC1q domain signals to receptors present on cells, such as cC1qR/calreticulin, hereby mediating phagocytosis [25]. To date, a vast number of studies underlines that opsonization with C1q enhances phagocytosis independent of complement activation (reviewed in [26]).

Next to its established role as a pattern recognition molecule, C1q is involved in the regulation of cell processes of various cell types. C1q has been described to induce migration and adhesion of fibroblasts to extracellular matrix [27, 28]. Furthermore, it has been demonstrated that high concentrations of C1q stimulate the migration of neutrophils and eosinophils within injured areas [29].

Peerschke and co-workers have also investigated the interaction between C1q and platelets and revealed that platelet adhesion and aggregation is upregulated due to the presence of C1q [30, 31]. For microglial cells, Färber and colleagues demonstrated the ability of C1q to induce an increase in pro-inflammatory cytokine secretion by these cells and also to mitigate their proliferation [32].

Moreover, C1q steadily gains credit to function as a bridge between innate and adaptive immunity. Accumulating work has provided evidence that C1q is capable

of modulating various immune cells and their cross-talk. Studies have shown that dendritic cells (DCs) express C1q receptors cC1qR/calreticulin and gC1qR and that C1q is able to induce maturation of DCs [33, 34]. In the context of T lymphocytes (T cells), it has been demonstrated that C1q-deficient mice exhibited an impaired interferon (IFN) γ production by T cells and a hampered CD8+ T cell proliferation [35, 36]. Furthermore, C1q is implicated in the modulation of B lymphocytes (B cells). It has been shown that C1q triggers IgG production by B cells whereas a lack of C1q in C1q-deficient mice leads to a positive selection of B1b B cells, in turn increasing IgM autoantibody production and escape from self-tolerance [37, 38].

C1q in health and disease

Over the years, multitudinous studies have highlighted different roles for C1q in physiological settings. For instance, C1q has been described to be important for development, in particular for synaptic pruning of the central nervous system [39] and aging [40]. Moreover, it has been demonstrated that C1q contributes to tissue repair by enhancing angiogenesis [41]. Additionally, during pregnancy, C1q acts as a molecular bridge between endovascular trophoblasts and decidual epithelial cells and is therefore crucial for embryo implementation into the endometrium [15, 42, 43].

On the other hand, C1q has been studied in many pathophysiological contexts as well. In cancer research, C1q can be regarded as a pro- or anti-tumorigenic factor depending on the type of cancer [44]. With regard to neurodegenerative diseases, C1q has been shown to play a role in disorders such as Alzheimer's disease, Parkinson's disease, Huntington's disease and prion disease (reviewed by Cho et al. [45]). Systemic lupus erythematosus (SLE) is yet another disorder where C1q and the complement system are strongly involved in pathogenesis. SLE is a chronic autoimmune disease commonly characterized by hypocomplementemia and the presence of autoantibodies, e.g. against C1q or other complement proteins [46]. Hereditary C1q deficiency in humans has been described to be the strongest genetic susceptibility factor for SLE [47, 48], underlining the importance of C1q in this disorder. Of note, while C1q deficiency is rare, anti-C1q autoantibodies can be found in roughly one-third of SLE patients [49]. With greatly improved clinical management over the last decades, premature morbidity and mortality in SLE is now increasingly ascribed to cardiovascular complications [50, 51]. Cardiovascular diseases, in particular atherosclerosis and thrombosis, have an increased prevalence in SLE, however the occurrence cannot be sufficiently explained by traditional risk

factors [52, 53]. Therefore, next to complement components, hemostatic factors are under investigation.

Hemostasis

The coagulation system functions in a concerted interplay between serine proteases, cofactors, and other molecules amplifying one another's activity on the surface of cells in order to terminate bleeding caused by initial trauma. It can be divided into primary hemostasis, resulting in initial platelet plug formation, and secondary hemostasis, resulting in fibrin generation and stable, secondary hemostatic plug formation. On the other hand, natural anticoagulants and the mechanism of fibrinolysis limit the formation of the blood clot and the propagation of the thrombus [54].

Primary hemostasis

Primary hemostasis is achieved by interaction of platelets, adhesive molecules and the vessel wall. Platelets circulating in the blood do not adhere to intact endothelium. Upon vascular injury, neurogenic reflex mechanisms cause vasoconstriction and the release of local mediators. Simultaneously, collagen and von Willebrand factor (vWF) are exposed from the subendothelium and promote adhesion of platelets by interaction with platelet glycoprotein complex (GP) IB. Hereby, platelets undergo a conformational change that increases their surface area tremendously [55-58]. Adhesion of platelets results in their activation that is accompanied by secretion of their α granules (containing factors such as P-selectin, fibrinogen, factor V and VIII and vWF) and δ granules (containing factors such as adenosine diphosphate (ADP), serotonin and Ca^{2+}) as well as the production of thromboxane A2 (TxA2). Subsequent binding of released Ca^{2+} to phospholipids is crucial for the conversion of coagulation factors into their active forms during secondary hemostasis. TxA2 and ADP are released from and bind to platelets, which results in activation of GP IIb/IIIa receptors and hence enables binding of fibrinogen. This mechanism reinforces aggregation of platelets to consequently form the initial platelet plug [56] (**Figure 3**).

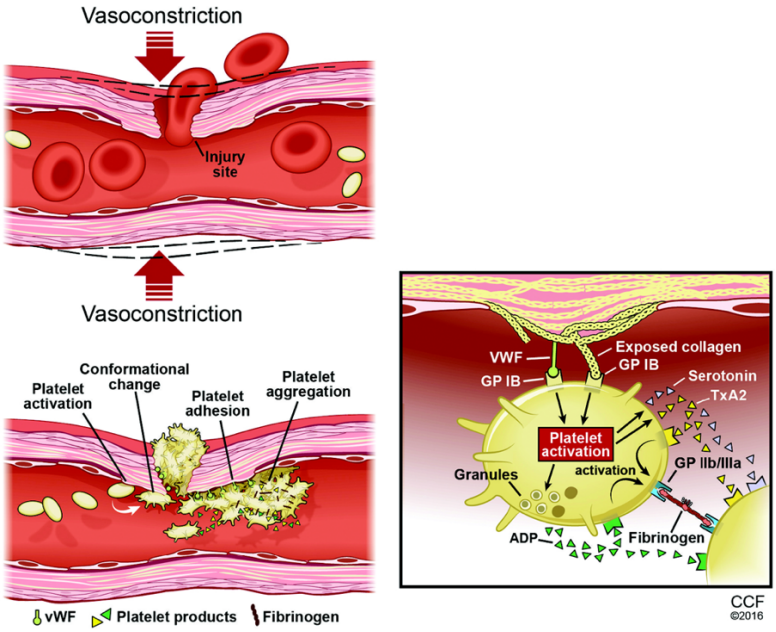

Figure 3: Primary hemostasis.

Biological effects of primary hemostasis are depicted. Initial injury results in vasoconstriction, platelet activation and aggregation and eventually primary platelet plug formation. Abbreviations: vWF: von Willebrand factor, GP IB: glycoprotein IB receptor, TxA2: thromboxane A2, GP IIb/IIIa: glycoprotein IIb/IIIa receptor (integrin $\alpha_{IIB}ß_3$), ADP: adenosine diphosphate.
Reproduced with permission from Bermudez et al. [59], © Licensee InTech.

Secondary hemostasis

Secondary hemostasis comprises various proteins that interact in a complex manner to finally convert soluble fibrinogen into insoluble fibrin, which stabilizes the initial platelet plug. Traditionally, secondary hemostasis was classified into the contact activation pathway (intrinsic) and the tissue factor pathway (extrinsic), with both pathways converging into a common pathway [54]. However, even though this concept provides a rationale for the understanding of *in vitro* coagulation tests, it fails to include the fundamental role of cell-based surfaces of *in vivo* coagulation and leaves clinical observations unexplained [60].

In the extrinsic pathway, tissue factor (TF), which is expressed in the subendothelial tissue, is exposed due to vascular tissue trauma [58]. TF binds to factor VII, thereby activating it in the presence of Ca^{2+}. The factor VIIa ("a" depicting the activated form) in turn activates the common pathway.

On the other hand, the intrinsic pathway is triggered by blood trauma or collagen contact. Through direct contact, factor XII becomes activated. This causes activation of factor XI. Factor XIa further activates factor IX. Factor IXa forms the tenase complex together with cofactor factor VIII on a phospholipid surface to activate the common pathway.

In the common pathway, factor X is activated via extrinsic or intrinsic pathway-derived factors. Factor Xa forms the prothrombinase complex together with cofactor factor V, phospholipids of tissues and platelets and Ca^{2+}. This complex converts prothrombin (factor II) into thrombin (factor IIa), which subsequently cleaves the soluble fibrinogen into insoluble fibrin. Fibrin monomers polymerize and become cross-linked by factor XIIIa, consequently transforming the initial instable platelet plug into a stable clot [54, 57, 61] (**Figure 4**).

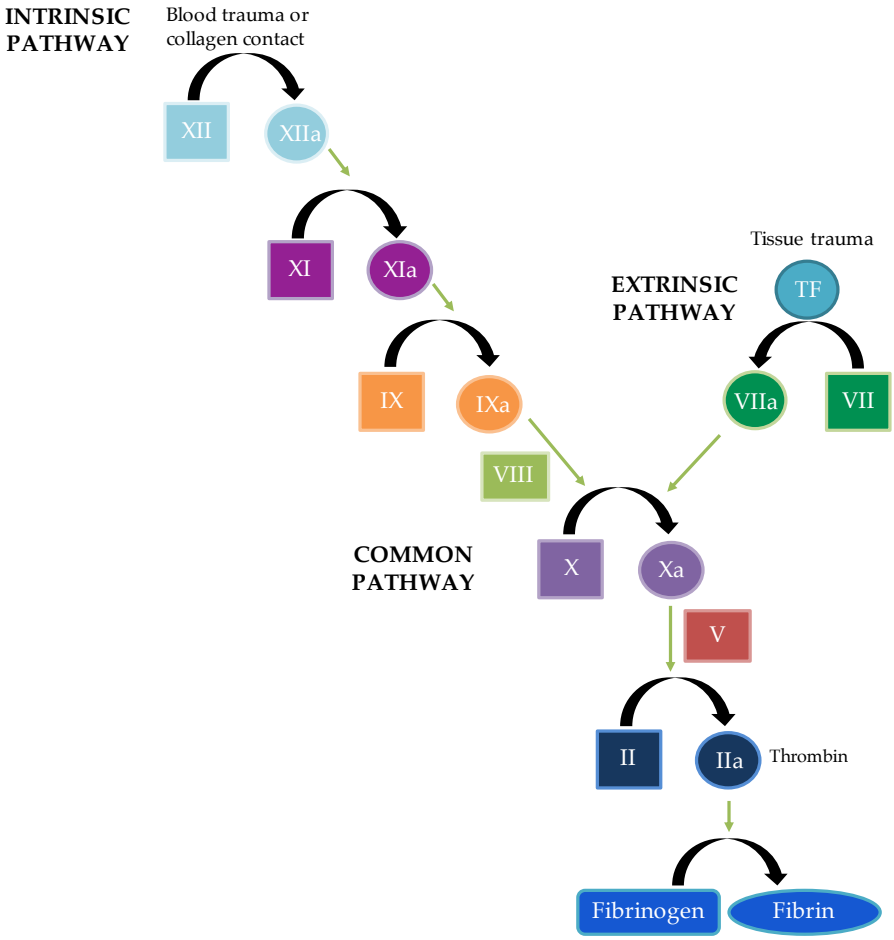

Figure 4: Classical model of secondary hemostasis.

The classical model of the secondary hemostasis is divided into the intrinsic and extrinsic pathways, both converging into the common pathway. Abbreviations: TF: tissue factor, a: activated.

This classical model of secondary hemostasis is still important for clinical *in vitro* tests such as prothrombin time (PT), investigating the extrinsic pathway, or the activated partial thromboplastin time (aPTT), investigating the intrinsic pathway, respectively.

Nowadays, the current understanding is based on a cell-based model, which considers the intrinsic pathway to contribute to initial thrombin formation by the extrinsic pathway rather than to occur in parallel [57].

For the cell-based model, the initiation phase is set off by exposure of blood to TF on TF expressing cells. Circulating factor VII binds to TF and becomes activated. The TF-factor VIIa-complex can in turn activate factor IX and factor X, hereby bridging extrinsic and intrinsic pathways. Factor Xa further converts prothrombin into thrombin. This initiation can be terminated by TF pathway inhibitor.

In the amplification phase, platelets become activated by thrombin, which is generated during the initiation phase, and vWF. Activated platelets release factor V and VIII from their granules so that platelets finally carry factors XIa, VIIIa and Va on their surface.

During the propagation phase, assembly of the tenase (IXa-VIIIa) and prothrombinase (Xa-Va) complex occurs on the surface of activated platelets. Hereby, a sufficient production of thrombin and fibrin, respectively, is ensured [54, 62] (**Figure 5**).

In order to counterbalance the amplification of coagulation and to prevent harmful thrombosis, the human body has anticoagulant and fibrinolytic mechanisms. Within the anticoagulant system, antithrombin, tissue factor plasminogen inhibitor, the protein C pathway and the protein Z dependent protease inhibitor play important roles. For fibrinolysis, fibrin is cleaved by the main protease plasmin. Plasmin itself is formed from its pro-form plasminogen by tissue plasminogen activator or urokinase [54].

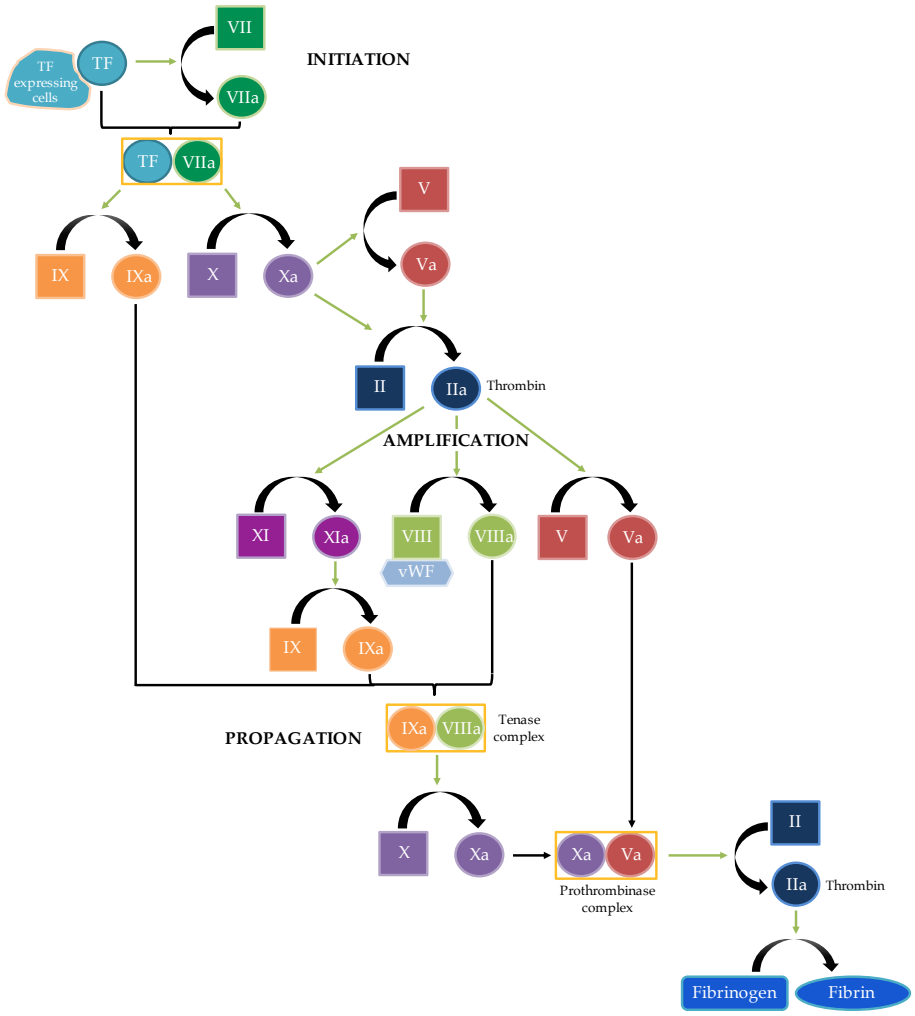

Figure 5: Cell-based model of secondary hemostasis.

The cell-based model of secondary hemostasis can be divided into i) initiation phase (occurring on TF-bearing cells), ii) amplification phase (occurring on activated platelets) and iii) propagation phase (occurring on activated platelets).
Abbreviations: TF: tissue factor; a: activated.

von Willebrand factor

Structure and biosynthesis

vWF is a multimeric glycoprotein composed of 40-200 mosaic domain structured monomers with a total molecular weight exceeding 20.000 kDa [63]. A single monomer consists of three A, three B, six C and four D domains arranged in the following sequence: D1-D2-D'D3-A1-A2-A3-D4-C1-C2-C3-C4-C5-C6 [64, 65]. It is synthesized as a pre-pro form, consisting of a signal peptide, pro-peptide and mature vWF [66]. vWF dimers are formed by bridging their cysteine knots (CK) via disulfide bonds, whereas multimers are formed by linking dimers at their D'D3 domains via disulfide bonds (**Figure 6**). A unique feature of vWF is its ability to undergo a conformational change dependent on environmental flow forces. While

vWF is irregularly coiled under static conditions, it extends into an elongated shape under shear stress such as in the blood stream [67, 68], thereupon exposing certain functional domains.

vWF is exclusively produced within Weibel-Palade bodies (WPBs) of endothelial cells and within α granules of megakaryocytes, progenitors of platelets [69, 70]. Synthesized vWF can be either stored or directly secreted into the plasma, where it circulates at a concentration of approximately 10 μg/ml in healthy individuals [71].

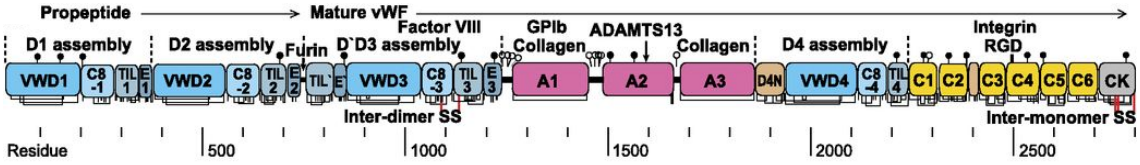

Figure 6: Schematic structure of mosaic vWF domains.

The structure of the vWF domains of a monomer is depicted and binding sites for dimerization, multimerization and ligand interaction declared.
Abbreviations: vWF: von Willebrand factor, GPIb: glycoprotein Ib receptor, ADAMTS13: a disintegrin and metalloproteinase with thrombospondin motifs 13, RGD: arginyl-glycyl-aspartic acid, SS: disulfide bond.
Reproduced with permission from Springer [72], © the American Society of Hematology

Function

vWF contributes essentially to the regulation of hemostasis and thrombosis by two main functions: The first function lies in the vWF-platelet interaction during primary hemostasis, whereas the second function is vWF's cofactor activity for factor VIII during secondary hemostasis [54]. These functions are based on the interplay between the specialized domains of the vWF monomer and their ligands. For instance, interaction between collagen and vWF takes places on vWF's A1 and A3 domains [73]. The interaction with platelets is mediated by binding of the A1 domain to platelet receptor GPIB receptor as well as binding of the C4 domain to the platelet receptor GPIIb/IIIa (integrin $\alpha_{IIB}ß_3$) [74, 75]. Moreover, the coactivity function of vWF for factor VIII is carried out by binding of vWF's D'D3 domain to factor VIII [76]. To balance the potent function of vWF, biosynthesis and activity in the blood are limited by degradation of vWF multimers into smaller fragments by the metalloprotease ADAMTS13, also known as vWF-cleaving protease, which cleaves vWF at its A2 domain [77].

vWF in health and disease

Over the years, additional versatile functions of vWF have been revealed. Turner and Moake elucidated a link between vWF and the alternative pathway of the complement system, demonstrating attachment of complement components C3, C5, factor B, D, H, I and properdin to ultra-large vWF strings [78]. Moreover, an impact of vWF on angiogenesis, smooth muscle cell proliferation and tumor cell apoptosis has been proposed (reviewed in [79]).

Since adequate hemostasis is dependent on the balance between vWF production and degradation, an imbalance on either side can have severe effects. Decreased levels or impaired function of vWF results in von Willebrand disease (vWD), the most common inherited bleeding disorder. The distinct types of vWD are caused by different defects: Type 1 and 3 are characterized by null alleles leading to reduced (type 1) or absent (type 3) vWF synthesis. Type 2 vWD is characterized by missense mutations in certain domains leading to a deficiency of high-molecular weight vWF multimers (type 2A), enhanced, spontaneous binding of platelet receptor GP IB (type 2B), decreased collagen binding or platelet adhesion (type 2M) or decreased factor VIII binding (type 2N) [80]. Depending on the type of vWD, the age and the sex of the patients, symptoms vary accordingly. While the most common symptoms are epistaxis and bruising in children, bleeding from minor small wounds, hematomas and menorrhagia are most commonly observed in adults [81, 82]. In 60-80% of patients, bleeding after surgery has been reported [82]. Bleeding symptoms of patients with vWD are usually treated with desmopressin, which increases the endogenous coagulation factor concentrations, or with infusion of exogenous coagulation factors in form of vWF or factor VIII-vWF concentrates [80].

Acquired von Willebrand syndrome (formerly referred to as VWD type 2A) is another distinct pathological condition observed in patients with underlying cardiovascular, endocrine and hematological diseases, where patients present with similar symptoms due to a variety of pathogenic mechanisms [83].

On the other hand, deficiency in ADAMTS13 leads to an abundance of vWF multimers and may cause thrombotic thrombocytopenic purpura (TTP), a hemostatic disorder that can be life-threatening when untreated, characterized by the formation of blood clots in blood vessels [84].

To summarize, the presence, amount and form of vWF is highly important for the proper function of primary and secondary hemostasis.

Cross-talk between complement and hemostasis

Complement and coagulation are two distinct systems that share several structural and functional features. It has been postulated that both pathways originate from a common ancestral developmental-immune cascade [85]. Structurally, both systems are proteolytic cascades of serine proteases of the chymotrypsin family with highly conserved catalytic sites of histidine, serine and asparagine [85]. Moreover, the pathways can be organized into initiation, amplification and propagation phases, where the pathways can reinforce themselves by consecutive activation of cascade components. Additionally, both powerful multi-component systems are finely regulated by a series of inhibitors and regulators.

Functionally, both systems act as an innate defense against external danger such as pathogens. The pathways are intended to act locally, therefore initiation is triggered through complement/coagulation components on surface receptors of cells only in the presence of foreign or altered structures, further leading to specialized, biological effects.

Up to date, manifold interplays between complement and coagulation have been described, with the cross-talk occurring via target cells or inflammatory mediators. On the one hand, many complement components have been described to possess procoagulant properties. For instance, C3a is able to induce activation and aggregation of platelets [86]. C5a as well as TCC can trigger TF expression by endothelial cells [87, 88]. Moreover, C4 binding protein can form a complex with protein S, hence resulting in an inhibitory effect on an anti-coagulant mechanism [89]. On the other hand, it has been shown that coagulation components can cleave complement components *in vitro*. This has been demonstrated for several factors such as factor XIIa and thrombin [90, 91]. The observations that inflammatory responses can be activated due to injury accompanied by bleeding, or that thrombus formation can act as a physical barrier to prevent bacteria from spreading underlines the synergy between both systems [92, 93].

Next to growing evidence in basic research, the implication of the cross-talk can be observed in clinics. The example of systemic inflammatory response syndrome (SIRS) demonstrates the concomitance of systemic inflammation and dysbalanced hemostasis [94]. Furthermore, diseases involving complement abnormalities, such as atypical hemolytic uremic syndrome (aHUS) [95], paroxysmal nocturnal hemoglobinuria (PNH) [96] and hereditary angioedema (HAE) [97], are associated with thrombotic complications, which are believed to be caused by complement-induced hyperactivation of platelets. Moreover, patients suffering from SLE show

an increased risk for hemostasis-associated comorbidities such as thrombosis and atherosclerosis [98].

To summarize, the implication of both complement and coagulation in a number of diseases highlights the advantages of a better understanding of the cross-talk in order to promote development of tailored therapies and to improve patient management in those clinical settings.

C1q-vWF interaction

C1q and vWF are pivotal initiation molecules of their appertaining pathways. The finding of a nucleotide sequence homology between autoantibodies against C1q (anti-C1q) derived from a SLE patient [99] and the C1 domain of vWF [100] led to the investigation of binding studies of C1q and vWF.

Kölm et al. demonstrated that interaction between C1q and vWF requires the exposure of a cryptic epitope on C1q's collagen-like domain. This epitope is exposed as a result of a conformational change caused by binding of C1q's globular-head domain to a surface. Using digestion studies, the collagen-like domain of C1q could be identified as the main binding site for vWF binding. Inhibition assays have led to the conclusion that binding of vWF to C1q can occur at C1q's A08 region, a 13 amino acid peptide sequence at the N-terminus of the A chain. Importantly, the C1q-vWF complex formation has been demonstrated to ensure C1q's and vWF's main functions, namely complement activation, and recruitment of platelets, respectively. Until now, C1q-vWF binding could be demonstrated *ex vivo* on the surface of red blood cells and within glomeruli of SLE patients with active lupus nephritis as well as *in vitro* on surfaces such as ELISA plates, apoptotic cells and cholesterol crystals [100]. However, the functional consequences of the C1q-vWF in physiological and pathophysiological settings remain unknown.

Atherosclerosis

Atherosclerosis is a chronic, inflammatory disease that is characterized by narrowing of the arteries due to deposition of fat, cholesterol, Ca^{2+} and cell debris in the vessel wall, resulting in plaque formation. A common hallmark of all stages of atherosclerosis is the presence of cholesterol crystals (CC). Progression of atherosclerosis can lead to acute occlusion due to thrombus formation and rupture of the plaque, consequently culminating into myocardial infarction or stroke [101, 102]. As a stereotype of cardiovascular diseases, it accounts for approximately 50% of overall mortality in western society and therefore presents a tremendous health burden [103]. While the cause of the disease remains unknown, many risk factors are described to contribute to its pathogenesis. Next to genetical predisposition, increasing age, male gender, hypertension and diabetes (factors with strong genetic components), smoking, lack of exercise as well as high fat diet (environmental factors) are the most common risk factors [104].

In terms of pathophysiology, development of atherosclerotic plaques initially starts with the permeation and accumulation of lipoproteins into the subendothelium of arteries at prone sites. These trapped lipoproteins, such as low-density lipoprotein (LDL), can undergo oxidation and acetylation processes where they trigger expression of adhesion molecules and secretion of chemokines by the endothelial monolayer. This activation attracts blood monocytes that then migrate into the intima. In the intimal space, these monocytes mature into macrophages where they phagocytose encountered modified lipoproteins. The sustained uptake of lipoproteins results in the formation of lipid-laden macrophages, termed "foam cells", visible as fatty streaks in the arteries. By overwhelming the recycling capacity of macrophages, the saturation of cholesterol becomes exceeded and leads to its crystallization and formation of cholesterol crystals (CC). Over time, formation of foam cells and CC causes secretion of extracellular matrix molecules that promotes further retention of lipoproteins. Moreover, ongoing inflammatory processes, leading to recruitment and defective egress of immune cells, together with the migration and proliferation of smooth muscle cells (SMCs) feed the growth of the atherosclerotic lesion. With the lesions advancing, dying cells release their cell content including extracellular lipids. These dying cells are removed by phagocytes in a process termed efferocytosis that becomes defective in atherosclerosis and causes the phagocytes to become necrotic. These secondary necrotic cells in combination with the released lipids finally fuel the formation of the lipid or

necrotic core. Ultimately, rupture of the fibrous cap triggers coagulation and thus leads to luminal thrombosis and arterial occlusion [105, 106] (**Figure 7**).

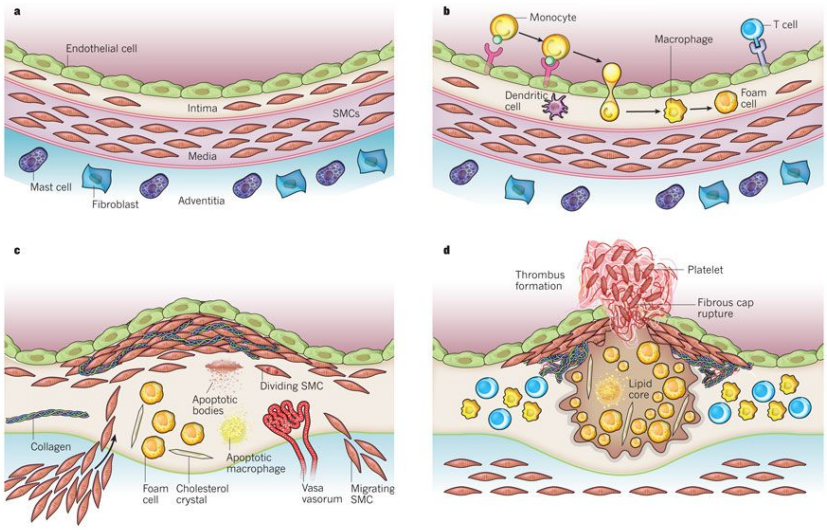

Figure 7: Development of atherosclerotic lesions.

Four stages of the development of atherosclerotic lesions are depicted: from a) normal artery to b) initiation of lesions to c) lesion progression and finally to d) thrombus formation. Abbreviations: SMC: smooth muscle cell.
Reproduced with permission from Libby et al. [105] © Macmillan Publishers Limited

Traditionally, the therapy regime for patients suffering from atherosclerosis is mainly based on lifestyle changes as well as medication with cholesterol-lowering statins [107]. Given the complexity of the disease, it appears logical that these measures are only partially successful. Therefore, new approaches are currently under investigation, e.g. approaches that aim to interfere with inflammation and foam cell development in order to combat atherosclerosis progression [108, 109].

C1q in atherosclerosis

Even though it has been well established that the complement system is involved in atherosclerosis, the exact role of complement in the pathogenesis is still not fully understood. While absent in the healthy arterial intima, multiple complement molecules can be found in tissues of atherosclerotic lesions. Furthermore, transgenic animal models demonstrate that all three complement pathways are implicated in atherogenesis. However, it is difficult to discriminate between complement-dependent and complement-independent effects. While the classic and lectin pathways have been attributed protective characteristics by removing cell debris and apoptotic cells from atherosclerotic plaques, the alternative pathway, the terminal complement complex (TCC) as well as the anaphylatoxins C5a and C3a appear to rather drive disease progression [110-112].

With regard to C1q, data derived from *in vitro* and *in vivo* studies suggest a dual role in atherosclerosis. Notably, C1q was found to be expressed in human atherosclerotic tissues [113-115] providing evidence of C1q to contribute to atherosclerosis. A number of *in vitro* studies have demonstrated beneficial effects of C1q in models of atherosclerosis. For example, C1q enhances the clearance of atherogenic lipoproteins, namely oxidized LDL and modified LDL, and in the same time increases the expression of cholesterol efflux transporters ABC-A1 and ABC-G1 [116]. Furthermore, C1q has been described to polarize macrophages towards an anti-inflammatory phenotype during ingestion of atherogenic lipoproteins [117]. Moreover, a transcriptome study revealed that human macrophages secrete less pro-inflammatory IL-6 via the JAK-STAT pathway when ingesting C1q-coated modified LDL [118, 119]. Additionally, Pulanco et al. could show that C1q promotes survival and efferocytosis of macrophages and therefore hypothesized a protective role in early atherosclerosis [120].

On the other hand, experimental models with atherosclerosis-prone (LDL-deficient or ApoE-deficient) mice are used to debate the role of C1q *in vivo*. In a model of early atherosclerosis, it has been described that $LDL^{-/-}/C1qa^{-/-}$ mice manifest with greater aortic root lesion size [121, 122]. Furthermore, a reduction in disease markers such as inflammatory cytokines, chemokines, cholesterol and triglycerides and a decrease in atherosclerotic lesion size could be demonstrated for $C1qa^{+/+}$ compared to $C1qa^{-/-}$ mice [123].

On the contrary, a number of studies illuminate a potentially harmful contribution of C1q. C1q receptors gC1qR and cC1qR, which are expressed on the surface of platelets, have been shown to cause activation and aggregation of platelets *in vitro* [30, 31, 124]. Moreover, the presence of C1q on CC in human plasma was demonstrated to result in downstream activation of complement and TCC generation [125]. *In vivo*, an association study on a cohort with familial hypercholesterolemia has revealed that a single nucleotide polymorphism in the C1qR1 gene represents a risk factor for coronary heart disease [126]. Furthermore, several studies in animals and humans have demonstrated that the activation of complement, e.g. initiated through C1q, drives atheroprogression [127-130].

In conclusion, these findings suggest beneficial as well as detrimental effects for the presence of C1q, notably dependent on its respective context.

vWF in atherosclerosis

A plethora of work has been carried out to elucidate a potential proatherogenic role of vWF. First, animal models of vWF deficiency in pigs and mice were used to address this question. Whereas Fuster et al. have shown beneficial effects of vWF in pigs [131-133], Griggs et al. did not observe protective effects against atherosclerosis by vWF deficiency [134-136]. In mice, Methia et al. as well as Qin et al. could demonstrate that the absence of vWF has a positive influence on atherogenesis [137, 138]. However, those studies in vWF-deficient animals strongly vary in their study design (animals on normal or high cholesterol diet with injury or no injury induced and different sites of manifestations investigated).

Second, anti-vWF agents have been administered to several animal species. Here, reduction of neointimal formation, inhibition of intima thickening or decrease in intimal hyperplasia could be observed in the majority of the studies [139].

Third, studies on vWD in humans were undertaken. In analogy to animal studies, observed effects in humans are controversial and strongly dependent on the cohort and the study design. Whereas Bilora and colleagues have shown that vWD patients manifest with less plaques than healthy controls [140, 141], Sramek et al. did not find differences in carotid intima media thickness in vWD patients versus healthy controls [142, 143].

Moreover, studies investigating the association of vWF plasma levels with an increased risk for cardiovascular events have come to different conclusions. On the one hand, vWF has been shown to be associated with an increased risk of cardiac death and proposed to be useful for risk stratification in patients with atherosclerotic carotid artery disease [144, 145]. On the other hand, studies have claimed that vWF is unsuitable as a biomarker to predict myocardial infarction and that vWF is not associated with plaque ulceration in carotid artery disease [146, 147]. Thus, the number of studies showing controversial data is continuously growing.

To summarize, neither an unequivocal atheroprogressive nor an atheroprotective effect could be demonstrated so far.

Part I

C1q-vWF interaction in the context of atherosclerosis

Abstract

Complement C1q, the initiation molecule of the classical pathway, exerts various immunomodulatory functions independent of complement activation. Non-classical functions of C1q include the clearance of apoptotic cells and cholesterol crystals (CC), as well as the modulation of cytokine secretion by immune cells such as macrophages. Moreover, C1q has been shown to act as a binding partner for von Willebrand factor (vWF), initiation molecule of primary hemostasis. However, the consequences of this C1q-vWF interaction on the phagocytosis of CC by macrophages has remained elusive until now.

Here, we used CC-C1q-vWF complexes to study immunological effects on human monocyte-derived macrophages (HMDMs). HMDMs were investigated by analyzing surface receptor expression, phagocytosis of CC complexes, cytokine secretion and caspase-1 activity.

We found that vWF only bound to CC in a C1q-dependent manner. Exposure of macrophages to CC-C1q-vWF complexes resulted in an upregulated expression of phagocytosis-mediating receptors MerTK, LRP-1 and SR-A1 as well as CD14, LAIR1 and PD-L1 when compared to CC-C1q without vWF, whereas phagocytosis of CC-C1q complexes was hampered in the presence of vWF. In addition, we observed a diminished caspase-1 activation and subsequent reduction in pro-inflammatory IL-1β cytokine secretion, IL-1β/IL-1RA ratio and IL-1α/IL-1RA ratio.

In conclusion, our results demonstrate that vWF binding to C1q substantially modulates the effects of C1q on HMDMs. In this way, the C1q-vWF interaction might be beneficial in dampening inflammation, e.g. in the context of atherosclerosis.

Introduction

The complement system is a highly effective part of the innate immune system. The multiple functions of complement include defense against bacterial infections, bridging innate and adaptive immunity and the clearance of immune complexes and components of inflammation [2]. The complement system can be activated through three distinct pathways: the classical, the lectin and the alternative pathway. All three pathways converge in a shared terminal response resulting in the formation of C5a and C3a as potent inflammatory effector molecules and C5b-9 as membrane attack complex. However, each pathway is initiated through different characteristic recognition molecules [148]. The initiation of the classical pathway is triggered by C1q through sensing of bound antibodies as well as pathogen- and damage-associated molecular patterns (PAMPs/DAMPs). In addition, more recent research has shown a number of functions for C1q that are independent of downstream complement activation [149]. On the one hand, opsonization with C1q enhances the clearance of diverse structures, namely immune complexes [23] and apoptotic cells [150] as well as atherogenic lipoproteins [116] and CC [151] by phagocytes. On the other hand, anti-inflammatory properties for C1q have been well described. For example, bound C1q decreases the release of pro-inflammatory cytokines and increases the production of anti-inflammatory mediators by phagocytes [152, 153]. Additionally, the presence of C1q on apoptotic cells skews macrophage polarization towards an anti-inflammatory phenotype [154].

Apart from C1q's extensively studied involvement in immunity, a complex cross-talk between complement and coagulation is becoming more and more evident [155]. Complement components have been found to induce hemostasis and *vice versa* coagulation factors can trigger complement activation, thereby combining two powerful plasma cascades. Within the hemostatic cascade, von Willebrand factor (vWF) acts as an important starter molecule by mediating platelet adhesion and aggregation. Immune cells, such as macrophages, are competent to take up and clear vWF through scavenger receptors [156, 157]. Moreover, vWF has been shown to interact with complement factor H [78, 158] and therefore can modulate the activation of complement via the alternative pathway [159]. Furthermore, a direct interaction between vWF and C1q was found by our group, demonstrating that C1q, bound to surfaces such as apoptotic cells, acts as a binding partner for vWF [100]. The C1q-vWF interaction also seems to occur on the surface of CC.

CC can be found as a characteristic feature in the intima of atherosclerotic arteries from early lesions to late plaque [160] and are widely used in *in vitro* models of atherosclerosis [161-163]. Formation of CC occurs upon fatty streak development by an increased uptake and exhausted efflux of cholesterol by lipid-laden macrophages known as foam cells. In *in vitro* and *in vivo* models of atherosclerosis, CC have been implicated in the activation of the NOD (nucleotide oligomerization domain)-, LRR (leucine-rich repeat)-, and PYD (pyrin domain)-containing protein 3 (NLRP3) inflammasome and downstream cytokine secretion, consequently triggering local and systemic inflammation [164-166]. While the role of CC and macrophages in atherosclerosis appears unambiguous, C1q can play a dual role. On the one hand, C1q bound to oxidized LDL or CC has been shown to activate the classical pathway, and in this context to drive the progression of atherosclerosis in animal models [128, 167]. On the other hand, C1q has also been described to be protective in early atherosclerosis *in vivo* [121, 122] and to increase cholesterol efflux transporter expression *in vitro* [116], suggesting atheroprotective properties. Similarly, the role of vWF in atherosclerosis is still a matter of debate. Although various studies suggest that vWF deficiency provides protection from atherosclerosis in animals, in humans, an unequivocal protective effect of vWF deficiency on atherosclerosis has not been demonstrated so far [139].

In summary, CC, macrophages, C1q and vWF have all been implicated in atherosclerosis. Nevertheless, the consequences of the interaction between C1q and vWF, especially on phagocytes, remain to be determined. In order to better understand this interaction, the aim of our study was to investigate the immunological effect of complexes consisting of cholesterol crystals, C1q and von Willebrand factor (CC-C1q-vWF complexes) by studying receptor expression, phagocytosis and cytokine secretion of macrophages.

Hypothesis

With our current knowledge about C1q's capacity to extensively impact on immune cells in the context of SLE and atherosclerosis, especially demonstrating protective, anti-inflammatory properties in human macrophages [117, 153, 154, 168], we proposed that the additional presence of vWF affects the immune response. Therefore, we hypothesized that vWF, in form of C1q-vWF complexes, plays an important role in altering the immunoregulatory effect of C1q. Based on preliminary findings obtained by our group, we speculated that the binding of vWF

to C1q on the surface of CC, in form of CC-C1q-vWF complexes, is capable of exerting beneficial effects on HMDMs by limiting the inflammatory response in the context of atherosclerosis.

Material and Methods

Morphology of HMDMs

After 7 d, HMDMs were harvested with PBS/10 mM EDTA and reseeded in DMEM+ at a cell concentration of 50,000 cells/well onto 96-well plates. Plates were previously coated with 5 µg/ml human serum albumin (HSA) (Sigma Aldrich) or purified C1q (Complement Technology, Tyler, Tx, USA) in coating buffer (0.1M Na_2CO_3 buffer, pH 9.6) overnight at 4°C. 10 µg/ml recombinant vWF (provided by Baxalta, Lexington, MA, USA (former Baxter; characterization by [169]) in PBS was added to C1q coated wells and incubated for 1 hr at RT. Plates were washed with PBS before adding HMDMs. After 18 hr, morphology of HMDMs was assessed with an inverted phase-contrasted microscope, Olympus IX50 (Olympus, Hamburg, Germany). For cell size analysis, a magnification of 10x was used and analyzed by Fiji 2.00 software.

Preparation of CC

Cholesterol (suitable for cell culture, Sigma Aldrich, St. Louis, MO, USA) was dissolved in 95% ethanol at 60°C (12.5g/l), sterile filtered and allowed to crystallize at room temperature (RT) for 7 days (d). Excess liquid was removed from the suspension, followed by drying for 5 d. Finally, CC were ground and stored as CC stock at -20°C until use.

Preparation of CC, CC-C1q and CC-C1q-vWF Complexes for Characterization of C1q and vWF Binding

Dry stock CC were weighed and suspended in PBS (Life Technology, Carlsbad, CA, USA) at a concentration of 1.6 mg/ml, vortexed and sonicated until a visually homogenous suspension was achieved. This CC suspension was split in three factions for generation of CC, CC-C1q complexes and CC-C1q-vWF complexes. Fractions were washed with PBS by centrifugation (1000 x g, 5 min, RT) and resuspended at the same concentration. For generation of CC-C1q complexes, 50 µg/ml purified C1q, diluted in PBS, was added and incubated for 1 hr at RT on a shaker (700 rpm). Afterwards, CC and CC-C1q complexes were washed (as

described above). For generation of CC-C1q-vWF complexes, 10 μg/ml recombinant vWF, diluted in PBS, was added to washed CC-C1q complexes, vortexed rigorously and further incubated for 1 hr at RT on a shaker (700 rpm). After another washing step, CC complexes were further incubated with monoclonal mouse anti-C1q (clone 32A6 cell supernatant [170]), diluted 1:20 in PBS, or polyclonal rabbit anti-vWF (Abcam, Cambridge, UK), diluted 1:1000 in PBS, for 1 hr at RT on a shaker (700 rpm). Secondary antibody staining was performed with donkey anti-mouse IgG-Alexa Fluor (AF)555 (Life Technologies) and goat anti-rabbit IgG-AF647 (Abcam), both diluted 1:200 in PBS/1%BSA (Sigma Aldrich)/0.5 M NaCl for 30 min at 4°C in the dark, followed by a final wash step and resuspension in PBS/1%BSA/0.5 M NaCl. All fractions were washed and treated with either active substance (proteins or antibodies) or solution only in the same manner. For flow cytometry, data were acquired using a BD Accuri 6 (BD Biosciences, San Jose, CA, USA) and analyzed with FlowJo10. For confocal microcopy, CC were spun onto cytoslides (Shandon, Pittsburg, PA, USA) by a Cytospin centrifuge (Thermo Fisher Scientific, Waltham, MA, USA) and analyzed using Nikon A1R Nala and NIS software (both Nikon, Tokyo, Japan). For imaging flow cytometry, analyses were carried out using ImageStreamX Mark II and IDEAS software (both EMD Millipore, Billerica, MA, USA).

Cell Culture

Peripheral blood mononuclear cells were isolated from fresh buffy coats (Blood Transfusion Centre of the University Hospital Basel, Basel, Switzerland) by density gradient centrifugation using Lymphoprep (Stemcell Technologies, Vancouver, Canada). Monocytes were obtained by CD14+ magnetic-activated cell separation beads (Miltenyi, Bergisch Gladbach, Germany) according to the manufacturer's instructions (yielding an average purity of 95-98% CD14+ monocytes determined by flow cytometry). Monocytes were differentiated into human monocyte-derived macrophages (HMDMs), cultured in DMEM supplemented with 100 U/ml penicillin and 100 μg/ml streptomycin (DMEM+), 10% fetal calf serum (FCS) (all from Life Technologies) and 50 ng/ml GM-CSF (Immunotools, Frisoythe, Germany) at a cell concentration of $0.5x10^6$ cells/ml in 6-well plates (BD Biosciences, Franklin Lakes, NJ, USA) and maintained in 5% CO_2 at 37°C for 7 d.

Treatment with CC Complexes

After 7 d, HMDMs were washed with prewarmed DMEM+, optionally stimulated with 100 ng/ml lipopolysaccharide (LPS) (E. coli O127:B8, Sigma Aldrich), diluted in prewarmed DMEM+, and treated with CC, CC-C1q or CC-C1q-vWF complexes for indicated time points. CC and CC-complexes were prepared as described above, washed once with PBS by centrifugation (1000 x g, 5 min, RT) and resuspended in prewarmed DMEM+ at a final concentration of 0.5 mg/ml before adding to cells.

Surface Receptor Expression

HMDMs were stimulated with LPS and treated with CC, CC-C1q or CC-C1q-vWF complexes as described above. After 18 hr, HMDMs were washed with PBS and incubated with PBS/10 mM EDTA (AppliChem, Darmstadt, Germany) for 30 min at 4°C. Cells were collected in FACS buffer (PBS/0.1% FCS/1 mM EDTA) and resuspended at a cell concentration of $5x10^5$ cells/100 µl and incubated with 2 µg/ml of human IgG for 45 min at 4°C to block unspecific binding of antibodies to Fcγ receptors. Staining was performed for 30 min at 4°C in the dark in PBS using the following antibodies: anti-MHC II-FITC (Immunotools), anti-tyrosine-protein-kinase Mer (MerTK)-PE (R&D Systems, Minneapolis, MN, USA), anti-programmed death ligand 1 (PD-L1/CD274)-APC and anti-CD14-PeCy7 (both from Biolegend, San Diego, CA, USA) (antibody panel 1) or anti-CD86-FITC (Biolegend), anti-lipoprotein receptor-related protein 1 (LRP-1/CD91)-PE (Thermo Fisher Scientific, Waltham, MA, USA), anti-leukocyte-associated immunoglobulin-like receptor 1 (LAIR1/CD305)-AF647 and anti-scavenger receptor A 1 (SR-A1/CD204)-PeCy7 (both from Biolegend) (antibody panel 2). HMDMs were washed and resuspended in FACS buffer. Data were aquired using a BD LSRFortessa (BD Biosciences) and analyzed with FlowJo10. Gating was performed on SSC/CD14+ cells (antibody panel 1) or SSC/CD91+ cells (antibody panel 2), respectively, and geometric mean fluorescence intensity (gMFI) was calculated.

Phagocytosis Assay

Assessment of granularity of HMDMs. HMDMs were kept untreated or treated with CC, CC-C1q or CC-C1q-vWF complexes as described above. After 18 hr, HMDMs were harvested with PBS/10 mM EDTA and resuspended at a cell concentration of $5x10^5$ cells/100 µl in FACS buffer. HMDMs were stained with anti-CD11c-APC (Biolegend) for 30 min at 4°C in the dark. Data were aquired using a BD LSRFortessa

(BD Biosciences) and analyzed with FlowJo10. For the quantification of phagocytosis the percentage of CD11c+ cells with high cell granularity, indicated by a shift into the side scatter $(SSC)^{high}$ gate (gate set according to shift in SSC from CD11c+ untreated to CC treated cells), was determined.

Assessment of phagocytosed pHrodo-dyed CC complexes. HMDMs were harvested with PBS/10mM EDTA and resuspended in phagocytosis buffer (DMEM+/12.5 mM HEPES (Sigma Aldrich)/5 mM $MgCl_2$) at a density of $5x10^5$ cells/100 µl. For pHrodo-dyed CC complexes, 1 mg/ml CC were suspended in 0.1M $NaHCO_3$ buffer (pH 8.3) and incubated with 10 µg/ml pHrodo Red Ester (Thermo Fisher Scientific) for 1 hr in the dark before the addition of C1q or C1q-vWF as described above. After a final wash, pHrodo-dyed CC complexes were added to HMDMs at a concentration of 0.5 mg/ml and incubated at 37°C for 30 min. Unphagocytosed CC complexes were washed away and HMDMs were stained with anti-CD11c-FITC (Bio-Rad, Hercules, CA, USA) for 30 min at 4°C in the dark and resuspended in FACS buffer. Data were aquired using a Beckman Coulter CytoFLEX (Beckman Coulter, Brea, CA, USA) and analyzed with FlowJo10. For the quantification of phagocytosis, the percentage of CD11c+ cells with a shift into the pHrodo Red Ester+ gate (gate set according to shift in pHrodo Red Ester from CD11c+ untreated to CC treated cells) was determined.

Quantification of Secreted Cytokine Levels

HMDMs were stimulated with LPS and treated with CC, CC-C1q or CC-C1q-vWF complexes as described above. After 18 hr, supernatants were collected, centrifuged to remove cellular debris and CC and stored at -80°C until measurement. Analyses of cytokine secretion were carried out in duplicates with ELISA kits according to the manufacturer's instructions. IL-1ß, IL-1α, IL-6 and IL-10 were measured using Biolegend ELISA kits, IL-18 and IL-1RA using Abcam ELISA kits and TNFα using a BD Bioscience ELISA kit.

Cell Viability Assay

HMDMs were kept untreated or treated with CC, CC-C1q or CC-C1q-vWF complexes as described above. After 18 hr, HMDMs were harvested with PBS/10 mM EDTA. HMDMs were stained in Annexin V (AnV) binding buffer using Annexin V-APC (both from Biolegend) for 30 min at 4°C in the dark to assess early apoptosis. Propidium iodide (PI) (Sigma Aldrich) was added to HMDMs immediately before aquiring to assess late apoptosis and necrosis. Data were

aquired using a BD Accuri 6 (BD Biosciences) and analyzed with FlowJo10. Data are expressed relative to the cell viability of HMDMs that were kept untreated which was set to 1.

Caspase-1 Activity Assay

HMDMs were kept untreated or treated with CC, CC-C1q or CC-C1q-vWF complexes as described above. After 18 hr, HMDMs were harvested with PBS/10 mM EDTA and resuspended at a cell concentration of $5x10^5$ cells/ml. Cells were incubated for 1 hr with fluorochrome-labeled inhibitors of caspases (FLICA) probes for caspase-1 detection according to the manufacturer's instruction (FAM FLICA Caspase-1 Assay Kit, Immunochemistry Technology, Bloomington, MN, USA). HMDMs were stained with anti-CD11c-APC (Biolegend) for 30 min at 4°C in the dark. Data were aquired using a BD LSRFortessa (BD Biosciences) and analyzed with FlowJo10. Quantification of caspase-1 activity was determined by the percentage of CD11c+ cells in the FLICA+ gate.

Immunofluorescence of Human Carotid Arteries

Ethical Approval. Collection and use of patient tissue were approved by the local Ethics Committee (EKNZ No. 2019-01490)

Patients and processing of samples. Carotid artery plaque tissue was obtained from patients who underwent thromboendarterectomy procedure at the Department of Vascular Surgery of the University Hospital Basel, Switzerland. Carotid artery tissue without any atherosclerotic manifestation was obtained from patients during autopsy at the Department of Pathology of the University of Basel. Immediately after the procedure, specimens were embedded in optimal cutting temperature (OCT) media (CellPath, Newtown, UK) and snap-frozen in liquid nitrogen. The specimens were cut in 18 μm sections with a cryostat and laid onto SuperFrost Plus slides (Menzel, Braunschweig, Germany).

Immunofluorescence and confocal microscopy analysis. Sections were thawed for 30 min, washed with PBS/0.05% Tween and blocked with PBS/0.05% Tween/1% BSA/1% FCS (PBSTBF) for 30 min. Sections were then incubated with the following primary monoclonal antibodies: mouse anti-human C1q (clone 32A6) and rabbit anti-human vWF (Abcam) or mouse IgG (Southern Biotech) and rabbit IgG (Jackson) as isotype controls in PBSTBF for 1 hr. Afterwards, sections were incubated with the secondary antibodies goat anti-mouse IgG-AF750 (Invitrogen) and goat anti-rabbit IgG-AF647 (Jackson) for 30 min in the dark. Finally, sections were washed with

PBS/0.05% Tween three times and with distilled water once before mounting with Fluoroshield (Sigma Aldrich). All steps were performed at RT. Immunofluorescence was analyzed using a Nikon Ti2 widefield microscope and NIS software. Images were prepared using OMERO software.

Statistical Analysis

Data are expressed as median ± interquartile range (IQR), if not stated otherwise. Wilcoxon matched pairs signed rank test was used to compare two groups of paired data. When more than 2 groups of unpaired data were compared, Kruskal-Wallis test was performed and if significant followed by Mann-Whitney U test for comparison of two specified groups as indicated. Data were analyzed with a statistical package program (GraphPad Prism 8, La Jolla, CA, USA). Differences were considered statistically significant when the p-value was <0.05.

Results

C1q-vWF Complexes Alter the Morphology of HMDMs

Even though a direct interplay between C1q-vWF interaction was proven by our group and described to be functional in terms of allowing complement activation as well as platelet adhesion [171], the impact of C1q-vWF complexes on the immune system has remained unknown to date. First, we established a model where we exposed HMDMs to C1q or C1q-vWF complexes. Therefore, HMDMs were harvested and exposed to different coatings. After 18 hr, cell morphology was assessed by phase-contrast microscopy. HMDMs on C1q coating (**Figure 8A**, left panel) exhibited a circular cell shape with the majority of cells evenly distributed and a minority of cells clustered together. However, HMDMs on coated C1q-vWF complexes displayed augmented cell clusters, forming cell aggregates (**Figure 8A**, right panel). The average cell size of HMDMs exposed to coating with C1q-vWF complexes was significantly higher compared to C1q alone (median cell size (IQR) of HMDMs on C1q coating: 574.7 px² (485.9-1986 px²) vs. C1q-vWF coating: 1124 px² (649.8-2309 px²), p=0.0156) (**Figure 8B**). HMDMs coated on HSA or vWF did not induce cell aggregation (data not shown).

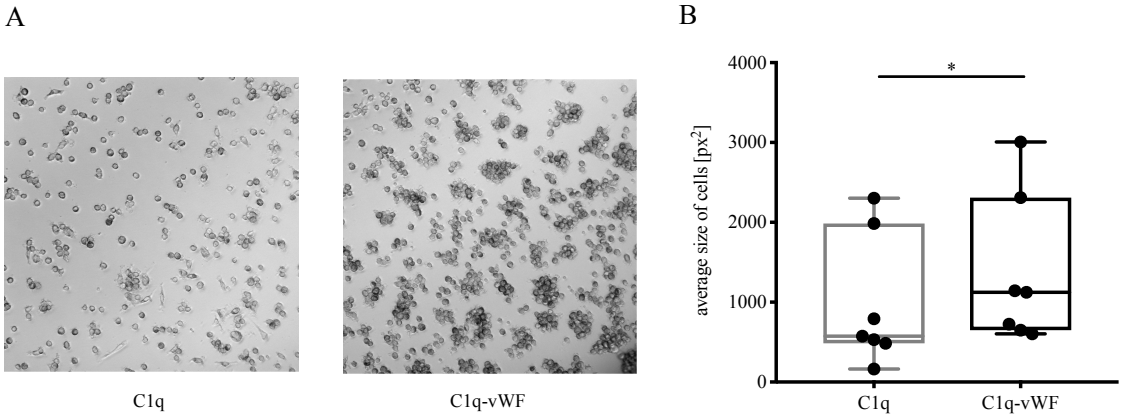

Figure 8: C1q-vWF complexes induce cell aggregation of HMDMs.

(A) HMDMs were incubated on C1q or C1q-vWF complex-coated plates for 18 hr and cell morphology was assessed by phase-contrast microscopy. 10x magnification of one representative out of seven experiments is shown. **(B)** Quantification of the average cell size for pooled data is shown. Horizontal lines in the box plots denote median while whiskers indicate interquartile range. Data points represent independent experiments analyzing seven different healthy donors used to obtain HMDMs (Wilcoxon matched pairs signed rank test, * p<0.05).

vWF Binds to CC in a C1q-Dependent Manner

Whereas C1q is described as a classical opsonin for a variety of DAMPs [154], the molecule has been also shown to adhere to oxidized LDL [116]. In addition, Samstad et. al demonstrated C1q binding on CC after incubation with human plasma [151]. Therefore, we first analyzed whether surface-bound C1q on CC secondarily enables the binding of vWF. We characterized the binding of vWF to C1q on the surface of CC by flow cytometry (**Figure 9A-C**), confocal microscopy (**Figure 9D**) and imaging flow cytometry (**Figure 9E**). C1q deposition on the surface of CC is shown in **Figure 9A**. The incubation of CC with vWF in the absence of C1q showed no vWF deposition on the CC surface (orange histogram in **Figure 9B**, **Figure 9C**). Only in the presence of surface-bound C1q, vWF was enabled to bind (green histogram in **Figure 9B**, **Figure 9C**). The gMFI for vWF binding in the presence of C1q was 50-fold higher compared to CC without C1q (median gMFI (IQR) of C1q+vWF: 115,000 (102,000-175,000) vs. vWF: 2,300 (1,500-2,400), p=0.0079). Furthermore, we analyzed the localization of vWF binding to CC-C1q complex. Using confocal microscopy, C1q and vWF could be visualized on CC. C1q and vWF stainings co-localized (**Figure 9D**). Finally, we used imaging flow cytometry to analyze a larger CC population as CC have a heterogenous structure. Again, we observed a similar staining pattern for C1q and vWF on CC (**Figure 9E**). Taken together, our results demonstrate that bound C1q mediates the binding of vWF to CC, and vWF alone is not able to bind to the surface of CC.

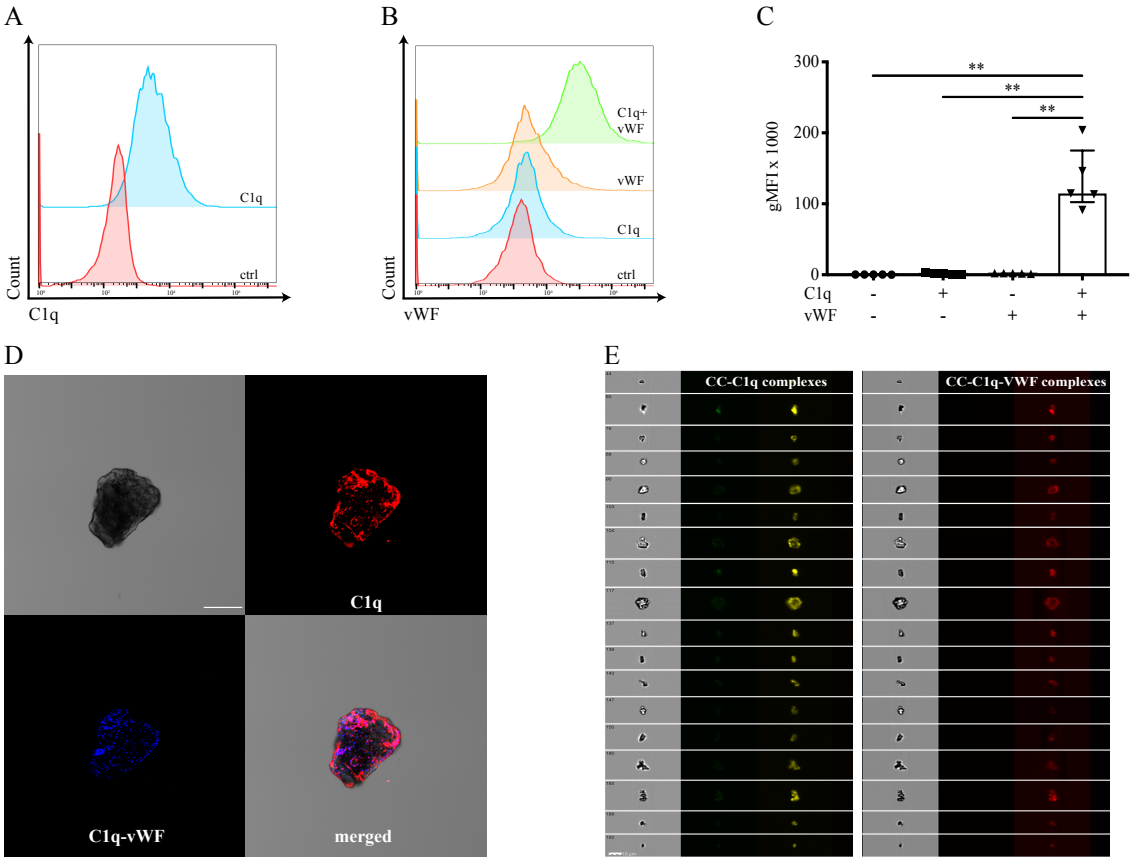

Figure 9: vWF binds to CC in a C1q-dependent manner.

Binding of C1q and vWF to surface-bound C1q on CC was determined by **(A, B, C)** flow cytometry, **(D)** confocal microscopy and **(E)** ImageStreamX. Representative flow cytometry diagrams show the binding of **(A)** C1q or **(B)** C1q-dependent binding of vWF on the surface of CC. Controls (ctrl) represent the presence of secondary antibodies only. **(C)** Flow cytometry data are shown as median gMFI with IQR ($n = 5$, Mann-Whitney U test, ** $p<0.01$). Confocal microscopy depicting a representative CC in brightfield, with C1q (red) or vWF (blue) in the presence of C1q bound to its surface. **(D)** The merged staining patterns visualize the C1q-vWF interaction. One of three independent experiments is shown. Scale bar = 50 µm. **(E)** Fluorescent staining of CC captured by ImageStreamX for C1q (yellow) or C1q-vWF (red). One of two independent experiments is shown. Scale bar = 10 µm.

CC-C1q-vWF Complexes Upregulate the Surface Receptor Expression of HMDMs

Macrophages have a high degree of plasticity, enabling these cells to change their phenotype according to the environmental stimuli [172]. In this context, C1q has been shown to elicit upregulated expression of MerTK receptor, which is involved in efferocytosis [173]. Moreover, it has been described that stimulation of macrophages with C1q leads to a polarization of these cells towards an anti-inflammatory state [168]. Therefore, we aimed to investigate the phenotype of HMDMs in our *in vitro* model. For this purpose, HMDMs were kept untreated or treated with CC, CC-C1q or CC-C1q-vWF complexes for 18 hr. To mimic the inflammatory milieu present in, e.g., atherosclerotic plaques [101], HMDMs were simultaneously exposed to 100 ng/ml LPS for 18 hr. The phenotype was studied by analyzing the expression of surface CD14, CD86, LAIR1, LRP-1, MerTK, MHC II, PD-L1 and SR-A1 (**Figure 10A-H**). HMDMs stimulated with CC-C1q-vWF complexes significantly upregulated the expression of CD14 (p=0.0312), LAIR1 (p=0.0312), LRP-1 (p=0.0312), MerTK (p=0.0312), PD-L1 (p=0.0312) and SR-A1 (p=0.0312) as compared to CC-C1q complexes without vWF. In four out of six donors, CD86 expression was upregulated, while MHC II expression was downregulated in five out of six donors. Neither the median receptor expression of CD86 nor of MHC II was significantly affected. Also, CC treatment did not induce any significant changes in surface receptor expression as compared to untreated HMDMs (data not shown).

Our results demonstrate that CC-C1q-vWF complexes uniquely affect the expression of surface receptors namely an upregulation of efferocytosis receptor MerTK, scavenger receptors LRP-1 and SR-A1 as well as CD14, LAIR1 and PD-L1.

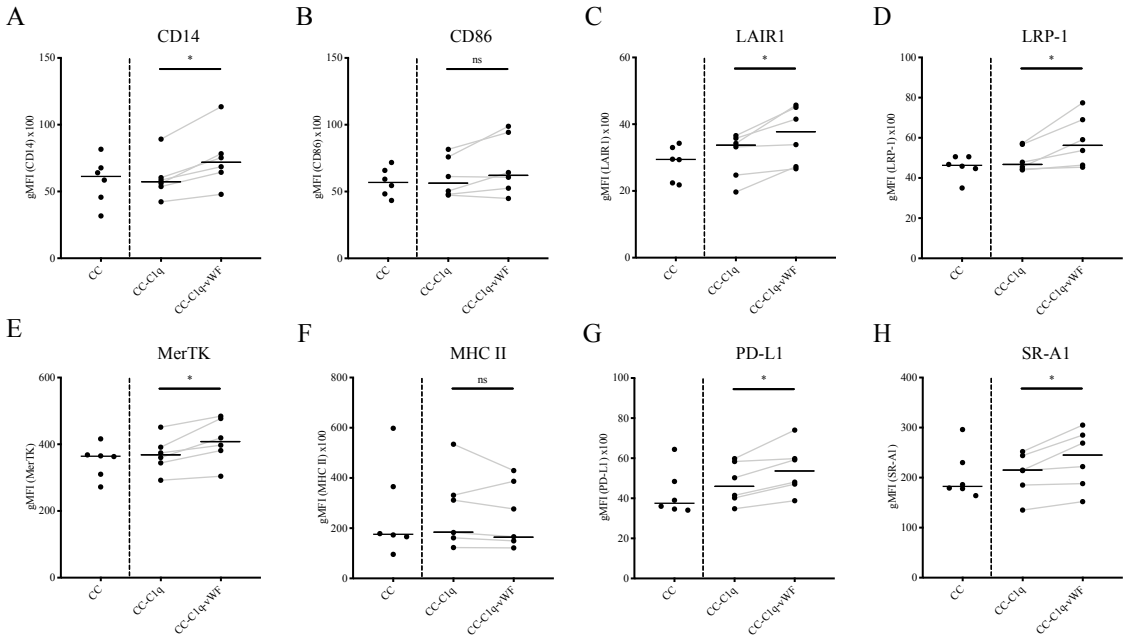

Figure 10: CC-C1q-vWF complexes upregulate the surface receptor expression of HMDMs.

LPS-stimulated HMDMs were treated with CC, CC-C1q or CC-C1q-vWF complexes for 18 hr and analyzed by flow cytometry for surface marker expression of **(A)** CD14, **(B)** CD86, **(C)** LAIR1, **(D)** LRP-1, **(E)** MerTK, **(F)** MHC II, **(G)** PD-L1 and **(H)** SR-A1. Pooled flow cytometry data are shown as gMFI with horizontal lines denoting median. Data points represent independent experiments analyzing six different healthy donors used to obtain HMDMs (Wilcoxon matched pairs signed rank test, * $p<0.05$; ns = not significant).

Phagocytosis of CC-C1q-vWF Complexes by HMDMs is Hampered

Since C1q is involved in the processes of efferocytosis [174] as well as phagocytosis [153] and as the additional presence of vWF upregulates efferocytosis and scavenger receptors (**Figure 10**), we next investigated the role of C1q-vWF binding in the uptake of CC complexes by HMDMs (**Figure 11**). Therefore, HMDMs were kept untreated or treated with CC, CC-C1q or CC-C1q-vWF complexes for 18 hr. The phagocytosis of CC led to an increase in cell granularity, which could be determined by a shift in SSC using flow cytometry. Analyzed as a control, untreated CD11c+ HMDMs did not express a SSC^{high} population. When HMDMs were treated with CC, CC-C1q or CC-C1-vWF complexes, the cells exhibited a SSC^{high} population (**Figure 11A**). HMDMs showed a significant decrease in cells positive for phagocytosis after the treatment with CC-C1q-vWF complexes compared to CC-C1q complexes (median phagocytosis (IQR) in six independent donors of CC-C1q-vWF: 13.65% (5.83-16.35%) vs. CC-C1q: 24.05% (22.55-34.60%), p=0.0312) (**Figure 11B**). To exploit the effect on early phagocytosis, we incubated CC with the pH-dependent pHrodo Red dye (**Figure 11C, D**). Analyzed as a control, unstimulated

CD11c+ HMDMs only exhibited a dim fluorescent signal for pHrodo Red. Fluorescent signal for pHrodo Red increased strongly when HMDMs were treated with pHrodo-dyed CC complexes for 30 min, due to the fusion of phagocytosed CC with the acidic lysosome. For the early phagocytosis, HMDMs had phagocytosed significantly less CC-C1q-vWF complexes than CC-C1q complexes (median phagocytosis (IQR) in six independent donors of CC-C1q-vWF: 54.55% (40.05-60.03%) vs. CC-C1q: 62,40% (49.05-68.78%), p=0.0312) (**Figure 11D**).

In summary, late as well as early phagocytosis, by HMDMs, of CC-C1q-vWF complexes is reduced as compared to CC-C1q complexes.

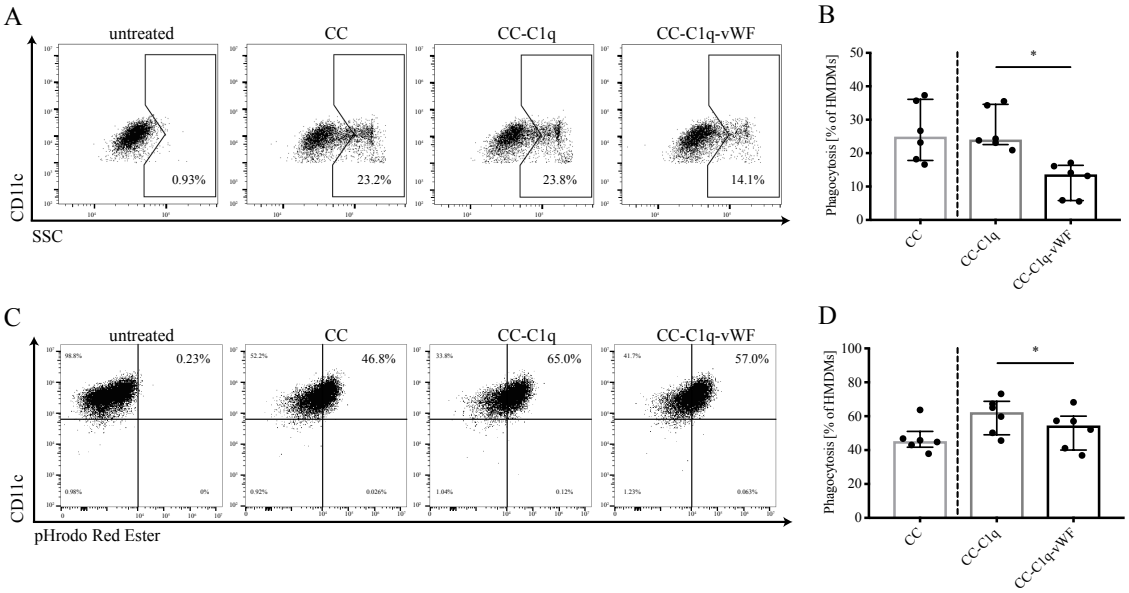

Figure 11: Phagocytosis of CC-C1q-vWF complexes by HMDMs is hampered.

(A, B) HMDMs were kept untreated or treated with CC, CC-C1q or CC-C1q-vWF complexes for 18 hr and analyzed by flow cytometry for the degree of phagocytosis of CC complexes. Phagocytosis was determined by the percentage of CD11c+ cells with a shift into the SSC^{high} gate. **(A)** Flow cytometry dot plots show one out of six independent experiments. **(B)** Quantification of phagocytosis for pooled data is shown. **(C, D)** HMDMs were treated with CC, CC-C1q or CC-C1q-vWF pHrodo-dyed complexes for 30 min and analyzed by flow cytometry for the degree of phagocytosis of CC complexes. Phagocytosis was determined by the percentage of CD11c+ cells with a shift into pHrodo Red Ester+ gate. **(C)** Flow cytometry dot plots show one out of six independent experiments. **(D)** Quantification of phagocytosis for pooled data is shown. Columns denote median while error bars indicate interquartile range. Data points represent independent experiments analyzing six different healthy donors used to obtain HMDMs (Wilcoxon matched pairs signed rank test, * p<0.05).

CC-C1q-vWF Complexes Reduce IL-1 Cytokine Secretion of HMDMs

CC have been repeatedly described as capable inducers of IL-1ß secretion in human monocytes and macrophages [165]. On the contrary, C1q has been shown to dampen pro-inflammatory cytokine secretion for the same cell types [168]. Consequently, we next examined the effect of CC-C1q-vWF complexes on the cytokine profile of HMDMs. For this purpose, HMDMs kept untreated or treated with CC, CC-C1q or CC-C1q-vWF complexes were stimulated with 100 ng/ml LPS for 18 hr and supernatants were analyzed for the secretion of IL-1ß, IL-1α, IL-1RA, IL-18, IL-6, IL-10 and TNFα cytokine levels (**Figure 12**). The CC treatment induced a strong IL-1ß and IL-1α secretion by HMDMs and a moderate increase in IL-18 secretion as compared to untreated HMDMs. A robust decrease in pro-inflammatory cytokines for IL-1ß and IL-1α was observed with CC-C1q complexes, and a decreasing trend for IL-6 and TNFα secretion. The additional presence of vWF on CC-C1q complexes significantly enhanced reduction of IL-1ß secretion ($p=0.0078$), IL-1ß/IL-1RA ratio ($p=0.0078$) and IL-1α/IL-1RA ratio ($p=0.0234$) compared to CC-C1q complexes alone. No other cytokines were significantly changed by vWF bound to CC-C1q complexes.

Taken together, our data show that IL-1ß cytokine secretion and IL-1ß/IL-1RA and IL-1α/IL-1RA ratios by HMDMs after exposure to CC-C1q complexes are diminished further in the presence of vWF. This reduction appears to be IL-1 specific.

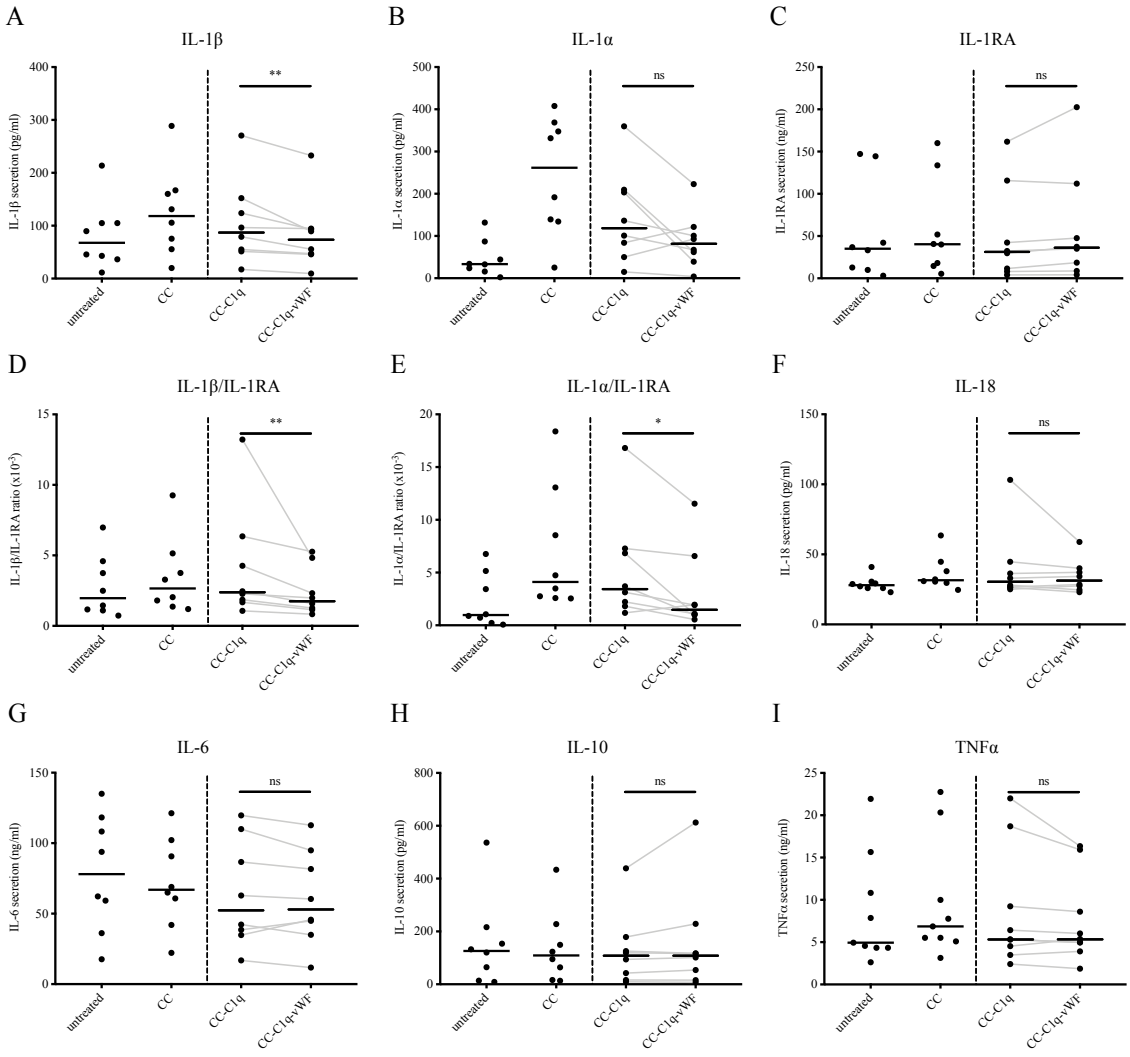

Figure 12: CC-C1q-vWF complexes diminish LPS-induced IL-1 secretion of HMDMs.

LPS-induced HMDMs were kept untreated or treated with CC, CC-C1q or CC-C1q-vWF complexes for 18 hr. Supernatants were analyzed by ELISA for cytokine secretion. Data show median cytokine concentrations of **(A)** IL-1β, **(B)** IL-1α, **(C)** IL-1RA, **(F)** IL-18, **(G)** IL-6, **(H)** IL-10 and **(I)** TNFα levels or median ratios of **(D)** IL-1β/IL-1RA and **(E)** IL-1α/IL-1RA of pooled donors. Data points represent independent experiments analyzing eight different healthy donors used to obtain HMDMs (Wilcoxon matched pairs signed rank test, * $p<0.05$; ** $p<0.01$; ns = not significant).

CC-C1q-vWF Complexes Do Not Alter Cell Viability of HMDMs

DAMPs released by dying cells can influence the viability of neighboring cells [175]. Furthermore, dying cells can secrete cytokines and other cellular components when undergoing apoptosis or necrosis [176]. Therefore, we next determined the cell viability of HMDMs. HMDMs, cultured in the supernatants used in **Figure 12,** were assessed for early apoptosis as well as late apoptosis and necrosis. During apoptosis, phosphatidylserine (PS), which is normally located in the inner leaflet of the cell membrane in viable cells, is translocated to the outer leaflet of the cell membrane. PS on the outer cell surface can be detected by Annexin V staining. During late apoptosis or necrosis, cells lose the integrity of their cell membrane and hence enable dyes to diffuse into these cells. Propidium iodide (PI), which is generally membrane impermanent and excluded from viable cells, intercalates into the DNA of cells when the cell and nucleus membranes are disrupted, and is therefore used to detect late apoptotic and necrotic cells. The percentage of AnV+ as well as PI+ HMDMs did not differ significantly for untreated HMDMs compared to CC, CC-C1q or CC-C1q-vWF complex treated HMDMs (**Figure 13**).

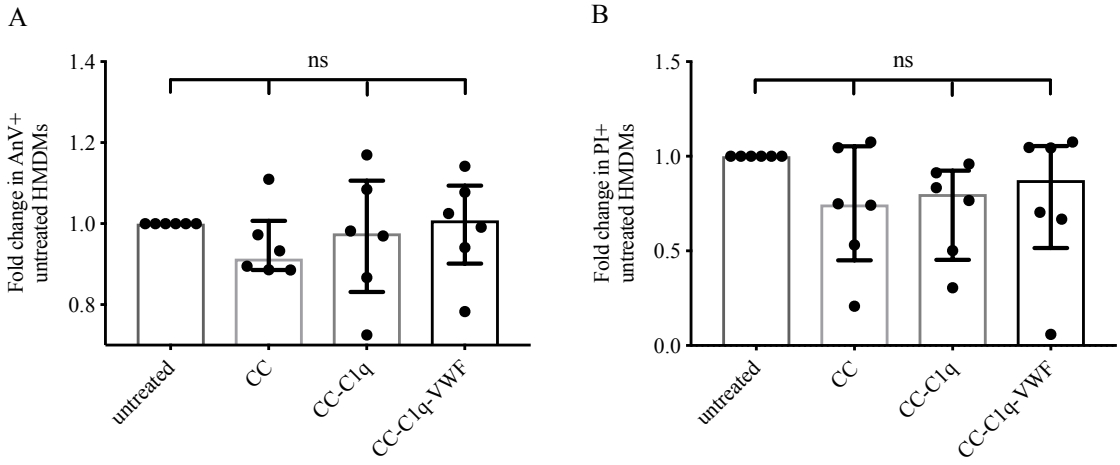

Figure 13: CC-C1q-vWF complexes do not affect the cell viability of HMDMs.

LPS-induced HMDMs were kept untreated or treated with CC, CC-C1q or CC-C1q-vWF complexes for 18 hr. HMDMs were analyzed by flow cytometry for **(A)** AnV, indicating early apoptosis and for **(B)** PI, indicating late apoptosis and necrosis. The percentage of untreated HMDMs positive for AnV+, and for PI+ respectively, was set to 1 and percentage of treated HMDMs expressed as fold change. Columns denote median while data points represent independent experiments analyzing eight different healthy donors used to obtain HMDMs (Wilcoxon matched pairs signed rank test, ns = not significant).

CC-C1q-vWF Complexes Suppress Caspase-1 Activity of HMDMs

It is well known that IL-1 maturation, cleavage and secretion is regulated transcriptionally as well as posttranscriptionally. While a priming signal through pattern recognition receptors is required for pro-IL-1β transcription, the maturation is dependent on the formation of the NLRP3 inflammasome and subsequent caspase-1 activation [177]. Therefore, we aimed to examine whether the observed change in IL-1 cytokine secretion was the result of a preceding NLRP3 inflammasome assembly. To address this point, HMDMs were kept untreated or treated with CC, CC-C1q or CC-C1q-vWF complexes for 18 hr and the effect on caspase-1 activation was quantified with FLICA probes. Upon CC treatment, HMDMs showed a marked increase in FLICA signal, demonstrating caspase-1 activity (**Figure 14A**). While the presence of C1q on CC exhibited only a delicate reduction in caspase-1 activity the additional presence of vWF significantly suppressed caspase-1 activity in HMDMs (median FLICA+ cells (IQR) in six independent donors of CC-C1q: 11.54% (7.29-28.38%) vs. CC-C1q-vWF: 9.37% (5.92-22.73%), p=0.0312)) (**Figure 14B**).

Overall, our data show that HMDMs treated with CC-C1q-vWF complexes exhibit decreased caspase-1 activity that impacts on NLRP3 inflammasome dependent IL-1β secretion.

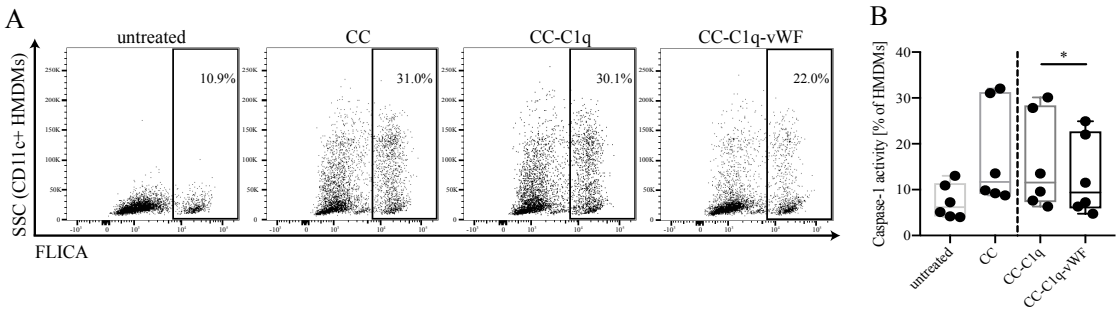

Figure 14: CC-C1q-vWF complexes lead to a reduced caspase-1 activity in HMDMs.

HMDMs were kept untreated or treated with CC, CC-C1q or CC-C1q-vWF complexes for 18 hr and analyzed for caspase-1 activity by flow cytometry. Activity of caspase-1 was determined by the percentage of CD11c+ cells in the FLICA+ gate. **(A)** Flow cytometry dot plots show one out of six independent experiments. **(B)** Quantification of caspase-1 activity for pooled data is shown. Horizontal lines in the box plots denote median while whiskers indicate interquartile range. Data points represent independent experiments analyzing six different healthy donors used to obtain HMDMs (Wilcoxon matched pairs signed rank test, * p<0.05).

C1q and vWF are Present in Human Atherosclerotic Arteries

Since complement components have been described to occur in atherosclerosis but to be absent in healthy arteries, we wanted to examine whether C1q and vWF can be detected in diseased vessels and within atherosclerotic plaques. Therefore, resected human carotid artery specimens from patients with atherosclerotic manifestations and from control patients without atherosclerotic manifestations were stained for C1q and vWF by immunofluorescence, and analyzed for (co-) localization.

In patients without atherosclerotic manifestations, we observed that vWF is localized only within the endothelial layers of the tissues. C1q was mostly absent in those patients (**Figure 15A-C**), but was observed in the subendothelial layer of the carotid arteries to some extent (**Figure 15C**).

On the contrary, in patients with atherosclerotic manifestations (characterized by intima thickening and the presence of atherosclerotic plaques and lesions), vWF was not only present in the endothelial layer but also within the intima and media. Furthermore, C1q could be detected in all three layers: the endothelium, the intima (the center of foam cell formation), and the media. Moreover, we observed a partial overlap of the staining patterns of both proteins, which points to a co-localization and suggests the presence of C1q-vWF complexes in atherosclerotic arteries (**Figure 15D-F**). However, since our specimens did not show CC deposits, the occurrence of CC-C1q-vWF complexes remains to be investigated.

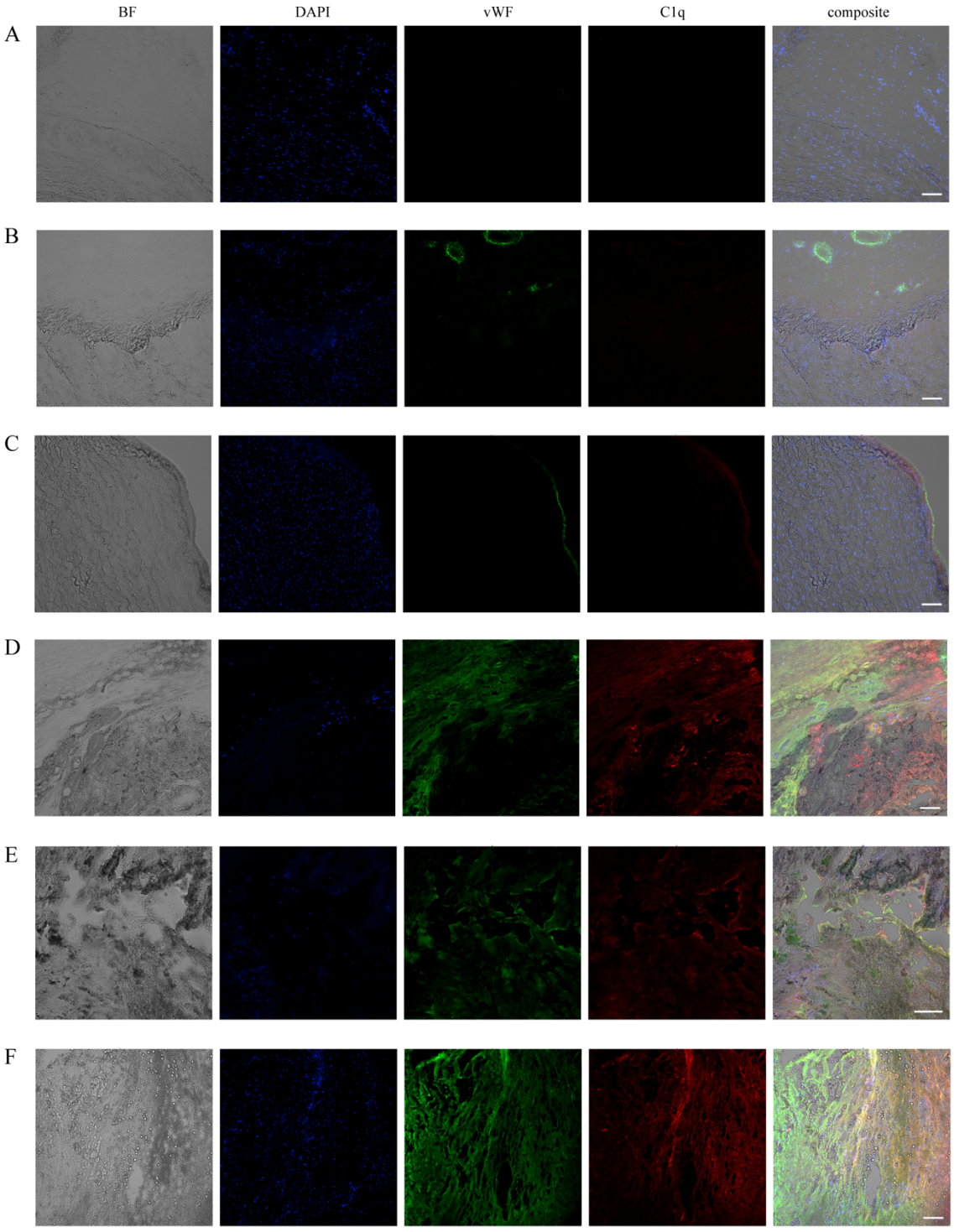

Figure 15: C1q and vWF are Present in Human Atherosclerotic Arteries.

Immunofluorescence of C1q and vWF in human carotid arteries of **(A-C)** patients with healthy arteries or **(D-F)** patients with atherosclerotic arteries. Three representative out of seven donors (for each healthy and diseased) are shown (20x magnification, scale bar=100μm).

Discussion

The cross-talk between the complement and hemostatic systems is extensive and can provide synergistic benefits for the human body [178, 179]. Yet, the role of many of these interplays is still unknown. In particular, even though an interplay between bound complement C1q and vWF has been demonstrated previously [100], its impact on the immune system has remained to be unexplored until now. In our study, we can illustrate that CC provide another physiological surface that allows a C1q-vWF interaction. Moreover, we found that the binding of vWF to bound C1q on CC is capable of modulating the immune response of macrophages by an upregulated expression of phagocytosis-mediating receptors and costimulatory receptors, hampered phagocytosis and enhanced suppression of pro-inflammatory cytokine secretion compared to C1q on CC alone. Deposition of CC is described as a hallmark of atherosclerotic plaques. After recognition as DAMPs and ingestion by phagocytes, CC trigger ROS formation and lysosomal leakage with consecutive NLRP3 inflammasome assembly, caspase-1 generation and IL-1β secretion [164]. IL-1β secretion leads to further recruitment of phagocytes by an amplification loop in a concerted action with other pro-inflammatory cytokines and chemokines [180]. Phagocytes, in particular macrophages, also are responsible for the essential function of recycling LDL and cholesterol in the periphery, but can develop into lipid-laden macrophage-derived foam cells during the course of the disease when their recycling capacity is overwhelmed. First, those foam cells can become apoptotic due to various stimuli, such as prolonged endoplasmic reticulum stress. Second, apoptotic cells that are insufficiently cleared (as occurring in advanced lesions due to defective efferocytosis), advance into cellular necrosis, in turn contributing to the formation of the necrotic core [106]. Consequently, enhanced ingestion of LDL and CC fuels foam cell development, which is thought to be detrimental in later stages of atherosclerosis [109]. Hence, the conclusion that CC induce arterial inflammation and destabilization of atherosclerotic plaques seems to be plausible [181]. The complement molecule C1q can be considered as a double-edged sword in the context of atherosclerosis. Previous studies showed that the clearance of oxidized LDL and modified LDL is enhanced by binding of C1q [116], but simultaneously leads to a polarization of macrophages towards an anti-inflammatory phenotype by a reduction in pro-inflammatory cytokine secretion [119]. In addition, C1q induces mRNA transcription of cholesterol efflux transporters [116]. In contrast to these atheroprotective traits, C1q was

demonstrated to be present on CC from human plasma [182] and found to be complexed to ApoE in human arteries [129], where it enables complement activation and thus is contributing to atheroprogression [183, 184].

With regard to vWF, a number of studies in vWF-deficient animals and patients suffering from von Willebrand factor disease have been performed. Several of those animal studies [139] as well as human studies [140, 141] suggest atheroprogressive effects of vWF. Therefore, one could hypothesize disadvantageous consequences for the additional presence of vWF on CC-C1q complexes on macrophages. However, our findings unexpectedly point to a beneficial effect of vWF in the context of phagocytosis of CC by macrophages, and suggest that the role of vWF in atherosclerosis might be intricate and requires further investigation.

Previously, C1q and vWF have been regarded as separately acting molecules. Here, we identified not only a complex formation of C1q bound to the surface of CC but also the subsequent binding of vWF. Moreover, the treatment of HMDMs with CC-C1q-vWF complexes results in an upregulated expression of surface receptors of efferocytosis (MerTK), scavenger receptors (LRP-1 and SR-A1) as well as CD14, LAIR1 and PD-L1 compared to CC-C1q complexes alone. Studies investigating the role of the phagocytosis-mediating receptors MerTK and LRP-1 indicate atheroprotective features [185, 186] whereas the role of SR-A1 in cardiovascular disease is still controversial (reviewed by Ben and colleagues [187]). Additionally, LAIR1 was described to have beneficial effects on foam cell formation [188]. Therefore, we next sought to determine the effect on the phagocytic capacity of HMDMs. Interestingly, the presence of vWF on CC-C1q complexes strongly diminished the late as well as early phagocytosis of CC by HMDMs, hereby reversing the effect of C1q alone. A possible explanation for this unexpected finding could be that the upregulated expression of phagocytosis-mediating receptors is representing a reinforcing feedback loop that is triggered in order to compensate for the decreased ingestion of CC-C1q-vWF complexes. Last, our data illustrate a significant decrease in IL-1 cytokine secretion by HMDMs when treated with CC-C1q-vWF complexes compared to CC-C1q complexes without vWF. The clinical significance of IL-1 in cardiovascular disease was demonstrated by the anti-IL-1beta antibody Canakinumab Antiinflammatory Thrombosis Outcome Study (CANTOS) [189]. Thus, a reduction in phagocytosis and inflammation could retard plaque progression [190, 191].

One limitation of our study is its *in vitro* character, since the *in vivo* situation in humans is likely to be more complex. C1q's role in human atherosclerosis is

supported by studies that have shown C1q expression in atherosclerotic carotid arteries of patients [113-115] and therefore underlining the relevance of our results. Whereas the majority of C1q is non-covalently bound with serine proteases C1r and C1s to form the C1 complex in plasma and whole blood, free C1q is more prevalent in tissues where it is locally synthesized mainly by macrophages and dendritic cells [10]. Furthermore, it has been demonstrated that vWF binds to a cryptic epitope of C1q, which is only exposed when C1q is surface-bound, while binding of vWF to surface-bound C1 was much weaker [100]. Hence, we assume that the C1q-vWF interaction, especially on CC, primarily occurs in tissue, such as arteries of atherosclerotic patients. In line with this hypothesis, we were able to provide first data on the concomitant presence of C1q and vWF in carotid arteries of such patients **(Figure 15)**. However, further investigation on the occurrence and localization of C1q and vWF, also with regard to CC, in human atherosclerosis is needed.

Second, *in vivo,* shear stress is necessary to unfold the full functional potential of vWF [72]. In our study however, permanent shear stress was not applied, since the physiological occurrence of shear stress would rather reflect the situation during plaque rupture resulting from continuous blood flow but not that inside the plaque itself.

Lastly, alternative ways can be envisaged by which the C1q-vWF interaction, in the form of CC-C1q-vWF complexes, might exert its effect on HMDMs. One of the ways could be partial steric shielding of the C1q molecule by vWF, weakening the effects of C1q (e.g. **Figure 11**). Another way could be an intrinsic effect of vWF (e.g. **Figure 10, Figure 12**). Future studies will have to explore the potential ways responsible for the overall impact of CC-C1q-vWF complexes. In addition, since the mutual interactions between complement and hemostatic systems *in vivo* are likely to be more complex, our *in vitro* model will have to be developed further in order to approach a physiological setting. Recently, Gravastrand et al. have described that CC induce complement-dependent activation of hemostasis [192]. In our group, we have observed that complement activation remains unaffected by the presence of vWF [171]. Hence, downstream complement components, such as C4 and C3, shall be implemented into our system and its effect on HMDMs in the additional presence of platelets addressed in the future.

In conclusion, with this study, we provide new insights into an emerging cross-talk between C1q and hemostasis-initiating vWF. Our findings reveal that binding of vWF to C1q on CC regulates the immune response of HMDMs. We show that CC-

C1q-vWF complexes provoke a hampered phagocytosis together with an accompanied reduction in IL-1 cytokine secretion by macrophages that could prove favorable for decelerating plaque progression.

Part II

C1q-vWF interaction in the context of hemostasis

Abstract

The cross-talk between the inflammatory complement system and hemostasis is becoming increasingly recognized. The interaction between complement C1q, initiation molecule of the classical pathway, and von Willebrand factor (vWF), initiator molecule of primary hemostasis, has been shown to induce platelet rolling and adhesion *in vitro*. As vWF disorders result in prolonged bleeding, a lack of C1q as binding partner for vWF might also lead to an impaired hemostasis. Therefore, this study aimed to investigate the *in vivo* relevance of C1q-dependent binding of vWF in hemostasis.

For this purpose, we analyzed parameters of primary and secondary hemostasis and performed bleeding experiments in wild type (WT) and C1q-deficient ($C1qa^{-/-}$) mice, with reconstitution experiments of C1q in the latter. Bleeding tendency was examined by quantification of bleeding time and blood loss.

First, we found that complete blood counts and plasma vWF levels do not differ between $C1qa^{-/-}$ mice and WT mice. Moreover, platelet aggregation tests indicated that the platelets of both strains of mice are functional. Second, while the prothrombin time was comparable between both groups, the activated partial thromboplastin time was shorter in $C1qa^{-/-}$ mice. In contrast, tail bleeding times of $C1qa^{-/-}$ mice were prolonged accompanied by an increased blood loss. Upon reconstitution of $C1qa^{-/-}$ mice with C1q, parameters of increased bleeding could be reversed.

In conclusion, our data indicate that C1q, a molecule of the first-line of immune defense, actively participates in primary hemostasis by promoting arrest of bleeding. This observation might be of relevance for the understanding of thromboembolic complications in inflammatory disorders, where excess of C1q deposition is observed.

Introduction

Numerous interactions between the complement and the coagulation cascades have been described over the years. Since both pathways are thought to have evolved from a common ancestor, it is not surprising that structural as well as functional similarities exist between them [85]. Structurally, both pathways are composed of potent serine proteases, which are circulating as inactive zymogens. Functionally, both systems belong to the first-line of defense and are intended to act locally at the site of infection/injury in order to limit collateral damage.

The complement system can be activated through the classical, lectin and the alternative pathways, with all three pathways leading to a shared effector response characterized by the formation of C3 and C5 convertases, release of the effector molecules C3a and C5a, and assembly of the membrane-attack complex.

The coagulation system can be characterized by the interaction between primary and secondary hemostasis. During primary hemostasis upon tissue damage, a concerted interplay of von Willebrand factor (vWF), collagen and platelets results in adhesion of platelets at the site of injury. Subsequent platelet activation and aggregation leads to the formation of a primary, instable platelet clot. During secondary hemostasis, exposure of blood to tissue factor (TF) initiates binding of factor VII, which in turn becomes activated. This leads to downstream activation of factors IX and X, with factor Xa being able to convert prothrombin to thrombin. Thrombin can amplify the cascade by activating factors XI, V, VIII as well as platelets themselves. Notably, to enable factor VIII to reach the phospholipid surface of those platelets, vWF is required as a carrier protein. The formation of a factor Xa-Va (prothrombinase) complex propagates the additional generation of thrombin, which then cleaves fibrinogen into insoluble fibrin. Cross-linking of fibrin polymers by factor XIIIa transforms the initial platelet clot into a stable clot. The current view is that primary and secondary hemostasis act in synergy rather than one after the other [193].

To date, experimental studies have described a functional impact of complement components on coagulation [155, 194]. Furthermore, C1q - the pattern recognition molecule of the classical complement pathway - has been attributed a number of complement-independent functions over the years. With regard to coagulation, a number of *in vitro* studies have investigated the interplay between C1q and coagulation components: On the one hand, C1q has been described to interact with platelets but data on this interaction are conflicting. While some studies demonstrate that C1q enhances platelet activation and upregulates P-selectin

expression [31, 195], other studies rather suggest that C1q mitigates coagulation by inhibiting collagen-induced platelet aggregation [196, 197]. On the other hand, C1q has been described to interact with factor XII, hereby proposing an inhibitory effect on clot formation [198]. Moreover, previous findings of our group have demonstrated that a complex of surface-bound C1q and vWF is able to induce platelet rolling and adhesion [100]. This observation is of importance as activated components of complement, including C1q, and coagulation are frequently encountered concomitantly in thrombotic complications that accompany inflammatory disorders such as bacterial sepsis and SLE [199-201].
Therefore, this study aimed to investigate the *in vivo* relevance of C1q-mediated binding of vWF by studying C1q-deficient mice with regard to alterations in hemostasis.

Hypothesis

With the observation in mind that the C1q-vWF interaction possesses the ability to induce platelet rolling and adhesion *in vitro* [100], we sought to investigate the functional consequences of the binding between C1q and vWF *in vivo*. We proposed that the absence of C1q as a binding partner for vWF impairs hemostasis in C1q-deficient mice. Therefore, we speculated that vWF, captured by C1q at sites of tissue damage, is able to induce platelet aggregation and thus contributes to the termination of bleeding. In this way, we assumed that C1q participates in primary hemostasis by inducing vWF-mediated thrombus formation in the context of thromboembolic complications.

Material and Methods

Animals

C57BL/6 mice (animal facility of the Department of Biomedicine, Basel, Switzerland) and C1qa$^{-/-}$ mice on a C57BL/6 genetic background were maintained in our specific-pathogen-free facility at 22°C room temperature (RT) with 12 hr light/12 hr dark cycle and were housed in groups of 2–6 mice. Mice used for experiments were kept for 2 weeks of adaptation period upon transfer. All procedures were approved by the Cantonal Commission for Animal Experiments, and the Federal Food Safety and Veterinary Office (license number 2898/28447). This study was carried out by authorized staff in accordance with the guidelines

and regulations of the Swiss welfare legislation (Animal Welfare Ordinance, Animal Welfare Act and the Animal Experimentation Ordinance).

Tail bleeding time and blood loss

For these experiments, 6-14 week old wild type (WT) or C1qa$^{-/-}$ mice were weighed and injected with a mixture of ketamine (100 mg/kg body weight (BW), xylazine (10 mg/kg BW) and atropine (1.2 mg/kg BW) before 10 mm of the distal tail was amputated and immersed into 0.16% EDTA/PBS, kept at 37°C. Time to cessation of blood flow was evaluated for 15 min. Blood loss was analyzed by i) reduction in body weight, calculated by reweighing the animals including amputated tails before and after tail bleeding, ii) reduction in body weight normalized to total body weight and iii) optical density (OD) of blood-PBS solution obtained from tail bleeding assay. OD was analyzed in 96 well plate using a microplate reader with an emission wavelength of 550 nm. Experimental set-up is shown in **Figure 19**. In all these experiments, the experimenter was blinded to the genetic background of the animals or the substance of reconstitution.

Complete blood counts

Whole blood was obtained from the tail vein, anticoagulated with EDTA and diluted with 0.9% saline (1:3). Blood cell counts and hemoglobin concentration were analyzed by using the ADVIA 2120i Hematology System (Siemens Healthcare, Erlangen, Germany).

vWF plasma levels

Citrated plasma was obtained from the tail vein and analyzed for vWF levels using von Willebrand factor two matched antibody pair kit (Abcam), according to the manufacturer's instructions.

Prothrombin time

Citrated whole blood was obtained from the tail vein and analyzed using Hemochron prothrombin time (PT) citrate cuvettes and Hemochron Jr. Signature+ (both from Accriva Diagnostics, Instrumentation Laboratory, Bedford, MA, USA).

Activated partial thromboplastin time

Citrated plasma was obtained by cardiac puncture and analyzed for activated partial thromboplastin time (aPTT) using ACL Top 750 Las (Instrumentation Laboratory).

Platelet function

Whole blood was obtained from the vena cava, anticoagulated with hirudin and diluted with 0.9% saline (1:1) and analyzed for whole-blood platelet aggregation using the multiple electrode platelet aggregometry (MEA) Multiplate® Analyzer (Roche Diagnostics, Basel, Switzerland). Aggregation (electrical impedance) was induced with the platelet activating agonists ADP (15 μM) or collagen (10 μg/ml) and recorded for 6 min. In order to achieve sufficient amounts of platelets, blood was pooled from three mice per group.

C1q levels and reconstitution of C1q

To determine kinetics of C1q reconstitution, C1qa$^{-/-}$ mice were injected intraperitoneally (*i.p.*) with 500 μg purified human C1q (1 mg/ml, Complement Technology) and blood sampling from the tail vein was carried out at 30 min, 1 hr, 2 hr and 8 hr. Data are shown in **Figure 21.** For the comparison of bleeding diathesis with or without reconstitution, mice were injected *i.p.* with 500 μg purified human C1q or the same volume of 0.9% saline 2 hr prior to tail bleeding. Blood sampling by cardiac puncture was carried out after the tail bleeding experiment. The degree of reconstitution with C1q was quantified from the obtained serum (time point experiments) or plasma (tail bleeding experiments) using a C1q ELISA kit (Hycult Biotech, Unden, Netherlands) according to the manufacturer's instructions. Despite the concentration of administered C1q, the site of injection and the experimenter being constant, we observed considerable interindividual differences in the recovery rate of C1q-reconstituted mice, potentially due to subclinical differences in the intraperitoneal injection site. As a consequence, for the analysis of tail bleeding experiments following C1q reconstitution, only mice in which at least 5 μg/ml of C1q plasma concentration could be achieved were included in the analysis.

Statistical analysis

Data are expressed as median ± interquartile range (IQR), if not stated otherwise. Mann-Whitney test was used to compare two sets of nonparametric, unpaired data.

Correlations were estimated by Spearman's rank correlation coefficient. Data were analyzed with a statistical package program (GraphPad Prism 8, La Jolla, CA, USA). Differences were considered statistically significant when the *p*-value was <0.05.

Results

Complete blood counts and vWF concentrations of C1q-deficient versus WT mice

In order to exclude confounders that can influence bleeding behavior, we first assessed hematologic parameters of the two strains. In detail, blood of WT mice and C1q-deficient mice was analyzed for blood counts (red blood cells, white blood cells, platelets, lymphocytes and hemoglobin) by flow cytometry, and vWF levels were quantified by ELISA. There was no statistically significant difference between WT and C1q-deficient mice for all of these parameters **(Figure 16)**.

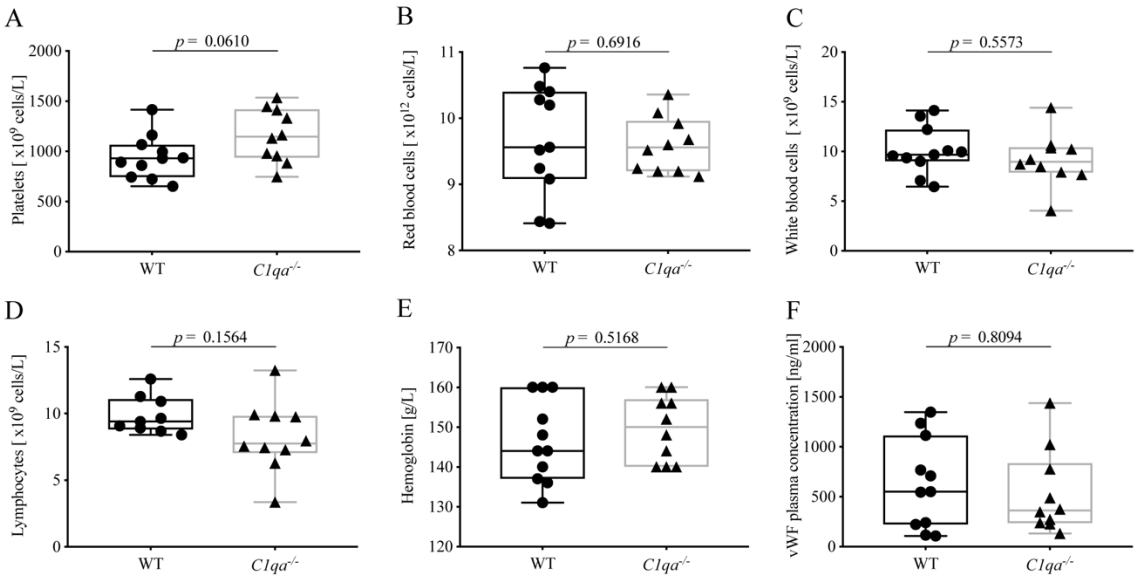

Figure 16: Complete blood counts and vWF levels of C1q-deficient versus WT mice.

EDTA-anticoagulated whole blood of C1q-deficient and WT mice was obtained and quantified by flow cytometry for numbers of **(A)** platelets, **(B)** red blood cells, **(C)** white blood cells, **(D)** lymphocytes and **(E)** amount of hemoglobin. **(F)** From citrated blood, vWF plasma concentration was quantified using ELISA. Horizontal lines in the box plots denote median while the boxes indicate interquartile range and whiskers minimum and maximum values. Data points represent individual mice, **(A), (B), (C), (E), (F)** ●: n= 11, ▲: n=10; **(D)** ●: n= 9, ▲: n=10 (Mann-Whitney test; ns, not significant).

Prothrombin time and activated partial thromboplastin time of C1q-deficient versus WT mice

Secondary hemostasis can be assessed by two different *in vitro* global coagulation tests. The PT provides information on the extrinsic pathway whereas the aPTT

assesses the intrinsic pathway. In this way, abnormalities in coagulation factors of either pathway can be determined [202]. The PT of C1q-deficient mice did not differ significantly from WT mice **(Figure 17A).** However, the aPTT was longer in WT than in C1q-deficient mice (median aPTT (IQR) of C1q-deficient mice: 23.63 s (21.35-26.25 s) vs. WT mice: 28.75 s (23.73-29.65 s), p=0.0486) **(Figure 17B).**

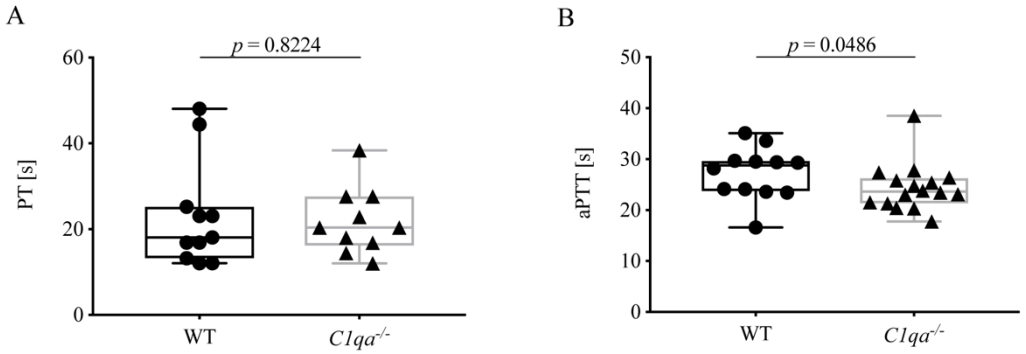

Figure 17: Prothrombin time and activated partial thromboplastin time of C1q-deficient versus WT mice.

(A) Citrated whole blood was analyzed for prothrombin time. Data points represent individual mice, n=10 for each group. **(B)** Citrated blood plasma was analyzed for activated partial thromboplastin time. Horizontal lines in the box plots denote median while the boxes indicate interquartile range and whiskers minimum and maximum values. Data points represent individual mice, ●: n=12, ▲: n=16 (Mann-Whitney test).

Platelet aggregation of C1q-deficient versus WT mice

Platelet function can be assessed by various methods. An elegant way is the impedance whole blood aggregometry. This method allows platelets to adhere to a solid surface, which resembles the physiological function of platelets *in vivo*. Adhesion of platelets to fixed electrodes results in an increase of electrical impedance that is transformed to arbitrary aggregation units (AU) and plotted against time [203], from where the area under the curve (AUC) can be calculated (10 AU * min = AUC [U]). In our study, we obtained hirudin-anticoagulated whole blood and induced platelet aggregation with ADP and collagen. The AUC range in which human platelets are considered to be responsive is from 321-1059 U when platelet aggregation is induced by ADP and from 242-1019 U when platelet aggregation is induced by collagen (Multiplate® analyzer, validated for hospital use). The AUC for ADP-induced platelet aggregation was 574 U for WT mice and 497 U for C1q-deficient mice. For collagen-induced platelet aggregation, an AUC of 745 U for WT mice and 578 U for C1q-deficient mice was observed. For both inducers, the AUC of C1q-deficient mice was slightly lower than the AUC of WT mice **(Figure 18)**. However, based on criteria used in clinics, all AUCs indicate the

functional responsiveness of platelets that were obtained from WT and C1q-deficient mice.

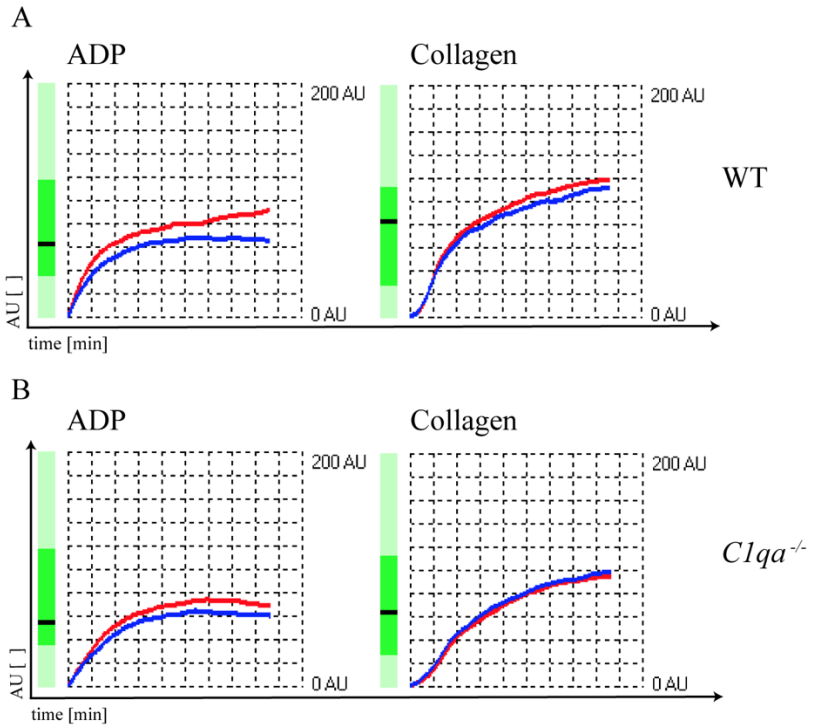

Figure 18: Platelet function of C1q-deficient versus WT mice.

Hirudin-anticoagulated whole blood was obtained for functional platelet aggregation tests using ADP (15 µM) and collagen (10 µg/ml) as inducers of platelet aggregation. Platelet aggregation curve of (A) WT mice and of (B) C1q-deficient mice induced with ADP and collagen are shown. Electrical impedance is expressed as aggregation units (AU) and plotted over time [min]. Representative data of one out of three independent experiments are shown. For each experiment, blood from three mice per group was pooled.

C1q-deficient mice show enhanced bleeding diathesis

Accumulating evidence highlights the cross-talk between complement and coagulation [204, 205]. Previously, our group described the occurrence of C1q-vWF complexes *in vitro* as well as *ex vivo*. Hence, we wanted to investigate whether C1q deficiency also impacts on hemostasis. For this, we conducted a tail bleeding assay **(Figure 19).**

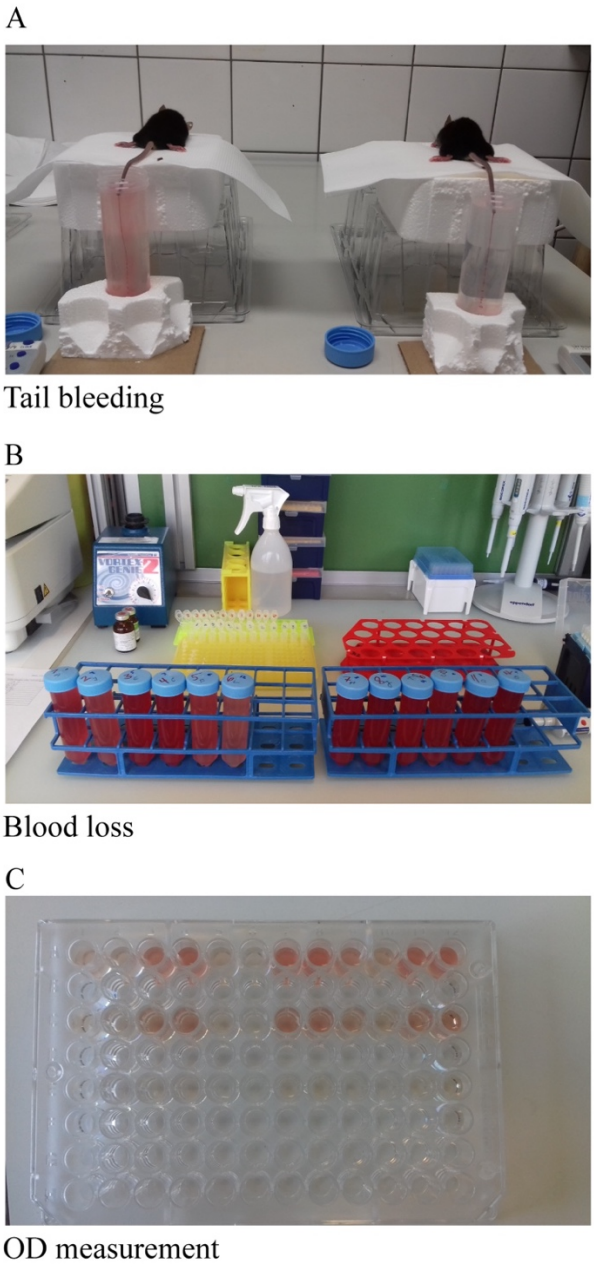

Figure 19: Experimental set-up of tail bleeding assay.

(A) Mice are anaesthetized and placed on individual platforms. 10 mm of the distal tail is cut and tails immersed in 37°C prewarmed PBS solution. Time of bleeding is observed for 15 min. **(B)** Blood-PBS solution obtained from tail bleeding of individual mice is shown. **(C)** Blood-PBS solution is pipetted into a 96 well plate for analysis of OD.

We found that the bleeding time of C1q-deficient mice was significantly prolonged compared to WT mice (median bleeding time (IQR) for C1q-deficient mice: 900 s (750.5-900.0 s) vs. WT mice 750.5 s (651.8-802.0 s), p=0.0226) **(Figure 20A)**. Noteworthy, 900s were equivalent to the upper time limit of the experimental procedure. Moreover, during the tail bleeding assay C1q-deficient mice lost twice the amount of blood (median weight loss (IQR) in mg of C1q-deficient mice 400 mg (225-775 mg) vs. WT mice: 200 mg (100-475 mg), p=0.0511) **(Figure 20B)** and 2.3-fold the amount when normalized to their body weight (median weight loss (IQR) in % of C1q-deficient mice: 2.32% (1.21-3.7%) vs. WT mice: 1.01% (0.49-2.46 %), p=0.0273) **(Figure 20C)** compared to WT mice. The loss of blood could be confirmed when measuring the optical density of the resulting blood-PBS solution. The OD of the obtained solution from C1q-deficient mice showed a 3.2-fold increase compared to WT mice (median OD at 550 nm of C1q-deficient mice: 0.69 (0.33-0.90) vs. WT mice: 0.21 (0.09-0.70), p=0.0173) **(Figure 20D)**. In addition, there was a positive correlation between the OD and the relative weight loss (Spearman r=0.7932, p<0.0001) **(Figure 20E)**. To summarize, C1q-deficient mice exhibit an enhanced bleeding diathesis compared to WT mice.

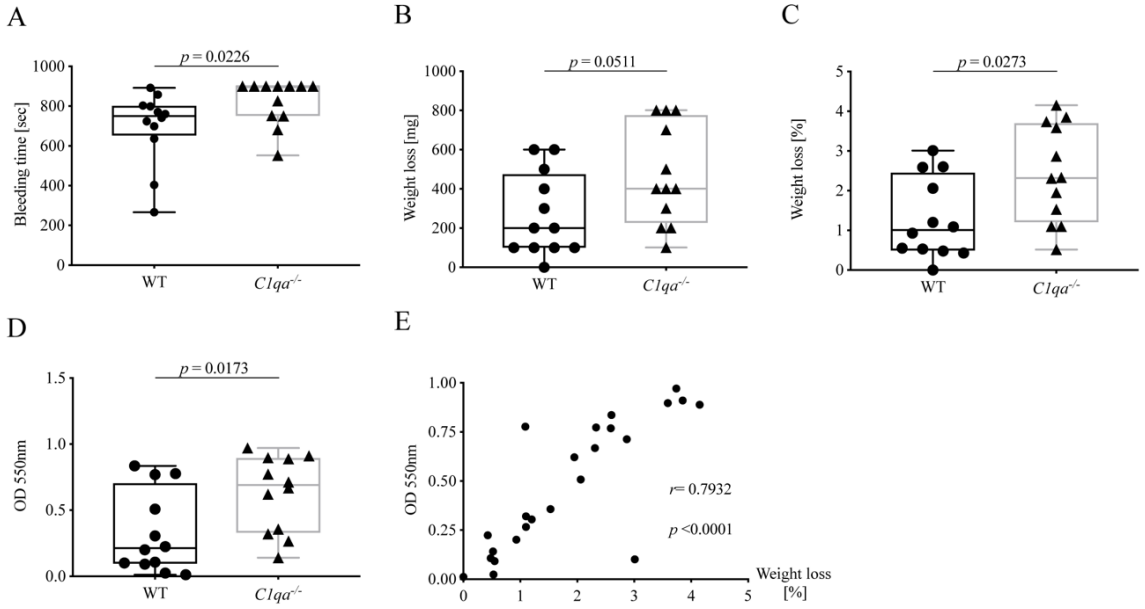

Figure 20: Bleeding tendency of C1q-deficient versus WT mice.

A tail bleeding assay was performed and bleeding tendency of C1q-deficient and WT mice assessed by **(A)** bleeding time, **(B)** weight loss, **(C)** relative weight loss normalized to the total body weight and **(D)** OD of obtained blood-PBS solution. **(E)** Correlation between OD and relative weight loss is depicted. Horizontal lines in the box plots denote median while the boxes indicate interquartile range and whiskers minimum and maximum values. Data points represent individual mice, n=12 per group (Mann-Whitney test; r, Spearman's rank correlation coefficient).

Reconstitution of C1q-deficient mice with purified C1q

To confirm that the prolonged bleeding time in C1q-deficient mice can be attributed to the lack of C1q, we next performed reconstitution experiments. First, we quantified the C1q serum concentration of WT and C1q-deficient mice. The median C1q serum concentration of WT mice was 192.4 μg/ml, whereas the C1q serum concentration of C1q-deficient mice was below the lower limit of detection **(Figure 21A).**

Second, we then investigated the kinetics of recovery for the reconstitution of C1q-deficient mice with human C1q. Injecting the highest administrable dose of C1q, a partial reconstitution, equivalent to approximately 30% of the concentration of murine C1q in WT mice, was achieved with its maximum at 58.75 μg/mL after 2 hr **(Figure 21B)**. Hence, for tail bleeding experiments following C1q reconstitution, C1q-deficient mice were *i.p.* injected with either human C1q or 0.9% saline and tail bleeding experiments carried out after 2 hr.

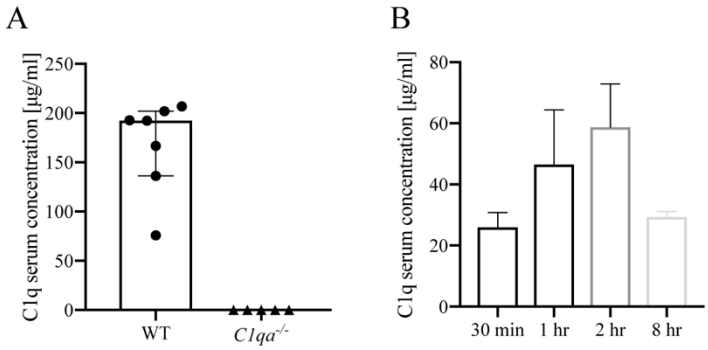

Figure 21: Baseline serum C1q concentrations and concentrations of serum C1q in reconstituted mice over time.

(A) Baseline C1q serum concentration of WT and C1q-deficient mice was quantified by ELISA. **(B)** C1q-deficient mice were *i.p.* injected with purified human C1q and C1q concentration was quantified from serum obtained after 30 min, 1 hr, 2 hr and 8 hr after injection. Columns denote median while errors bars indicate interquartile range. Data points represent individual mice, **(A)** ●: n= 7, ▲: n=5; **(B)** n=2.

C1q reconstituted C1q-deficient mice show a reduced bleeding tendency

In order to investigate whether the observed prolonged bleeding tendency of C1q-deficient mice could be rescued, and thus can be attributed to the lack of C1q, we reconstituted C1q-deficient mice with human C1q or injected 0.9% saline as control and performed tail bleeding experiments in the same manner as described previously. Subsequently, C1q plasma concentrations were analyzed to evaluate the degree of C1q reconstitution.

The bleeding time of C1q-deficient mice reconstituted with C1q was slightly shorter than in non-reconstituted control mice (median bleeding time (IQR) of C1q-injected mice: 865 s (607.0-900.0 s) vs. saline-injected mice 900 s (804-900 s), p=0.4981) **(Figure 22A)**. Strikingly, mice that were reconstituted with C1q lost one fifth of the amount of blood of mice that were injected with saline instead (median weight loss (IQR) in mg of C1q-injected mice: 100 mg (37.5-397.5 mg) vs. saline-injected mice 500 mg (200-645 mg), p=0.0190) **(Figure 22B)** and 4.2-fold less amount of blood when normalized to their body weight (median weight loss (IQR) in % of C1q-injected mice: 0.45% (0.17-1.37 %) vs. saline-injected mice: 1.87% (0.80-2.65 %), p=0.0190) **(Figure 22C)**. Moreover, the OD of obtained blood solution from C1q-reconstituted mice showed a 2.7-fold decrease compared to control mice (median OD at 550 nm of C1q-injected mice: 0.31 (0.06-0.70) vs. saline-injected mice: 0.85 (0.37-1.12), p=0.0503) **(Figure 22D)**. Most strikingly, the relative weight loss of C1q-reconstituted mice during tail bleeding experiment correlated negatively with the achieved C1q concentrations after reconstitution (Spearman r=-0.7461, p=0.0071) **(Figure 22E)**.

Notably, when comparing bleeding tendency of C1q-reconstituted with WT mice, bleeding time of C1q-reconstituted mice approached the times as observed in WT mice, while the absolute as well as relative weight loss was nearly identical between C1q-reconstituted mice and WT mice suggesting that the lack of C1q was fully responsible for differences observed between C1q-deficient and WT mice.

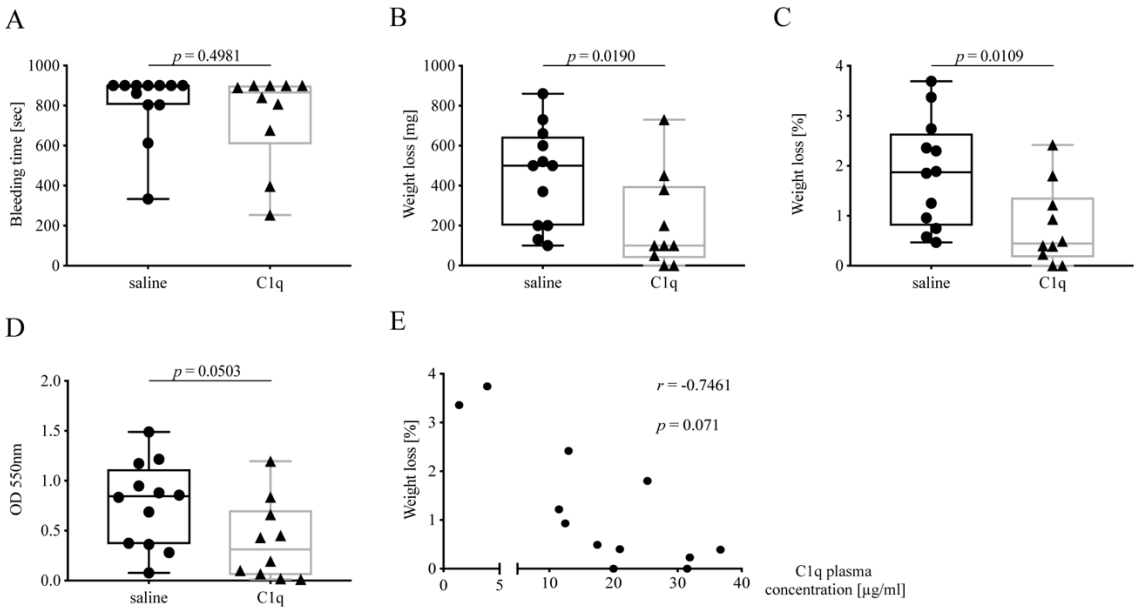

Figure 22: Bleeding tendency of C1q-deficient mice with or without reconstitution with C1q.

Tail bleeding assay was performed and bleeding tendency in C1q-deficient mice injected *i.p.* with either C1q or 0.9% saline 2 hr prior to assessment of **(A)** bleeding time, **(B)** weight loss, **(C)** relative weight loss normalized to the total body weight and **(D)** OD of obtained blood-PBS solution. **(E)** Correlation between relative weight loss and achieved C1q plasma concentration in C1q-reconstituted C1q-deficient mice is shown. Horizontal lines in the box plots denote median while the boxes indicate interquartile range and whiskers minimum and maximum values. Data points represent individual mice, ●: n=12, ▲: n=10 (Mann-Whitney test; *r*, Spearman's rank correlation coefficient).

Discussion

The cross-talk between the complement system and the coagulation system is becoming ever more apparent with many of the interactions still not being fully understood. Our previous research has shown that a complex of C1q and vWF is able to recruit human platelets indicating that C1q has the potential to mediate hemostasis [100]. Therefore, we sought to examine whether C1q can impact on blood coagulability. For this purpose, we compared C1q-deficient mice to WT mice with regard to qualitative and quantitative analyses of parameters of primary and secondary hemostasis. Our study demonstrates that C1q-deficient mice exhibit prolonged bleeding and increased blood loss compared to WT mice during tail bleeding experiments. Performing reconstitution experiments with human purified C1q, the altered bleeding behavior of C1q-deficient mice could be reversed and correlated with the achieved C1q concentration in those mice. These findings highlight that C1q is directly involved in thrombus formation during coagulation.

Similar to humans, clinical conditions characterized by a decline in blood platelets (thrombocytopenia) or vWF levels (von Willebrand factor disease) can lead to

dysfunctional hemostasis and thrombosis in mice [206, 207]. In order to exclude such quantitative differences, we compared complete blood counts and vWF plasma concentrations of C1q-deficient and WT mice. As expected, counts of platelets, red blood cells, white blood cells and lymphocytes as well as levels of hemoglobin and vWF did not differ significantly **(Figure 16)**. Remarkably, the trend of higher platelet counts in C1q-deficient mice, which might rather imply increased coagulability in these mice, could be due to higher platelet consumption during blood collection in WT mice.

PT and aPTT are employed in the clinics to monitor clotting time, e.g. for assessment of anticoagulant therapy, and to diagnose bleeding disorders, e.g. due to deficiencies in coagulation factors. While PT and aPTT both give insight into a functional common pathway involving factors X, V and II, the PT measures the integrity of the extrinsic pathway involving TF and factor VII, whereas the aPTT provides information on the intrinsic pathway involving factors XII, XI, IX, and VIII. While prolonged PT and aPTT usually indicate impaired secondary hemostasis, shortened PT or aPTT due to abnormal levels of coagulation factors, such as factor XII, does not necessarily translate into coagulation disorders [202, 208]. Since no defect in coagulation factors has been described for C1q-deficient mice, we expected the two tested mouse strains to show no significant differences in PT and aPTT. While PT was comparable, unexpectedly, the activated partial thromboplastin time was significantly shorter in C1q-deficient mice compared to WT mice **(Figure 17)**. This finding would be indicative of an increased coagulability of C1q-deficient mice, and thus oppose the enhanced bleeding behavior. Since previous research has demonstrated that C1q exerts an inhibitory effect on factor XII under physiological conditions, absence of C1q might result in an overly active factor XII, hereby shortening the aPTT [198]. Another explanation for the shorter aPTT might be an indirect effect of the formation of C1q-vWF complexes. Physiologically, vWF is necessary for the transport of factor VIII to the site of secondary hemostasis on activated platelets. Thus, deficiency in C1q might result in its omission as a binding partner and hence in a shifted balance of vWF function towards carrying factor VIII, hereby enhancing factor VIII function and leading to a shortened aPTT.

Next to vWF dysfunction or quantitative platelet defects, qualitative platelet defects, such as dysfunctional platelet membrane receptors, can be causative for bleeding disorders [209, 210]. Several studies investigating the effect of C1q on collagen-induced platelet aggregation have shown controversial findings, either weakening or potentiating platelet aggregation [30, 195, 196, 211]. Peerschke and

Ghebrehiwet have repeatedly studied C1q receptors on platelets as well as the consequences of C1q stimulation on platelet activation, concluding that C1q binding to several platelet receptors leads to platelet activation via P-selectin induction and thus increases procoagulant activity [31, 124, 212].

However, Kölm et al. have not observed binding of platelets to C1q, whereas platelets are enabled to adhere to the C1q-vWF complex in an *in vitro* flow-chamber model [100]. Additionally, interaction between C1q and endothelial cells has been demonstrated. C1q has been shown to induce endothelial cell adhesion and spreading, which in turn leads to a prothrombotic phenotype of these cells [213, 214].

In our study, analyzing platelet aggregation induced by collagen and ADP, platelets of WT as well as C1q-deficient mice were found to be functional even though responsiveness of platelets of C1q-deficient mice was slightly lower **(Figure 18)**.

Taken together, we demonstrate that C1q-deficient mice exhibit augmented bleeding **(Figure 20)** that can be partially reversed by reconstitution with C1q **(Figure 22)**.

These results suggest that C1q is directly involved in the maintenance of hemostasis. Conceivably, C1q might represent a binding partner for vWF not only *in vitro* but also *in vivo*. Consequently, the lack of C1q potentially results in reduced vWF binding followed by diminished platelet aggregation and subsequent prolongation of bleeding.

However, considering the substantial body of evidence from C1q-platelet and C1q-endothelial cell interaction studies, we cannot exclude an (maybe additional) interplay between i) C1q and platelets directly, ii) C1q and endothelial cells or iii) a still unknown interplay between C1q and another component of coagulation to participate in hemostasis.

Therefore, a limitation of our study is that, although we propose the C1q-vWF interaction to be responsible for the altered bleeding tendency, the precise mechanism remains to be clarified. Furthermore, our study is limited by the use of human instead of murine C1q for reconstitution experiments due to the lack of availability of the latter. Nevertheless, a 76% sequence homology on DNA level and a 72% homology on protein level exists between human and murine C1q [215]. Although human C1q levels in C1q-reconstituted mice remained lower than murine C1q levels in WT mice **(Figure 21B)**, we observed significant differences in blood loss between C1q-reconstitued and non-reconstituted mice **(Figure 22B,C)**, indicating that human C1q is capable of mimicking functions of murine C1q.

With regard to the clinical relevance of our observations, a well-balanced complement system is crucial to protect against pathogens and fight against infections. In conditions where an overly active complement system results in high consumption and deposition of complement components, such as in bacterial sepsis and SLE, severe thrombotic complications are frequently observed at the same time. Regarding sepsis, it has been demonstrated that gram-positive bacteria-induced sepsis is accompanied by significant C1q consumption [216]. Additionally, C1q has been described to bind to gram-positive and gram-negative bacteria [217].

Downstream activation of complement and generation of inflammatory mediators, such as C3a and C5a, has been shown to stimulate circulating neutrophils and endothelial cells and subsequently upregulates TF expression on these cells [87, 218]. The enhanced TF expression fuels activation of the contact system of hemostasis and thus leads to increased thrombogenicity. This in turn can result in sepsis-associated coagulopathies that have been suggested to negatively affect the outcome by increasing mortality in these patients [219]. In general, inflammation is considered a predisposing factor for thrombosis.

Another example of such cross-talk is SLE, the prototype of systemic autoimmune diseases. SLE is commonly characterized by low plasma levels of C1q due to high consumption and consequent deposition [220, 221]. Strikingly, SLE patients have been described to have a higher risk of thrombotic complications, which cannot be sufficiently explained by traditional risk factors [222, 223]. Those thrombotic complications include platelet hyperfunction [224], thrombotic microangiopathies (TMA) [225], venous thromboembolism (VTE) [226] and atherosclerosis [227]. Moreover, it has been shown that C1q and other complement components are deposited on platelets of SLE patients and are associated with venous as well as arterial thrombotic events in those patients [228-230].

Apart from bacterial sepsis and SLE, C1q has also been found to be present in high concentrations at sites of atherosclerotic, inflammatory and vascular lesions, and vice versa high concentrations of C1q in these conditions have been postulated to be a driver for inflammation and thrombosis [114, 115, 231]. Therefore, future work is warranted to elucidate the clinical relevance of C1q for hemostasis in humans.

In conclusion, our study provides evidence that C1q has a physiological role in hemostasis *in vivo* by promoting arrest of bleeding. With regard to disease, an excess of deposited C1q might be a cause of thrombotic complications in inflammatory diseases such as bacterial sepsis and SLE.

Conclusion

In my doctoral studies, I investigated the consequences of the interaction between C1q and vWF. In my first project, I focused on the immunological consequences of the C1q-vWF interaction in the context of atherosclerosis. For this purpose, we developed and characterized an *in vitro* model of CC-C1q-vWF complexes, which was used to study the modulation of immunological effects on human macrophages derived from healthy donors. I could demonstrate that formation of CC-C1q-vWF complexes occurs by binding of vWF to CC in a C1q-dependent manner. Moreover, CC-C1q-vWF complexes induce an upregulation of macrophage receptor expression, in the same time hamper phagocytosis, and lead to a caspase-1 dependent reduction in IL-1 cytokine secretion by macrophages (**Figure 23**) [232].

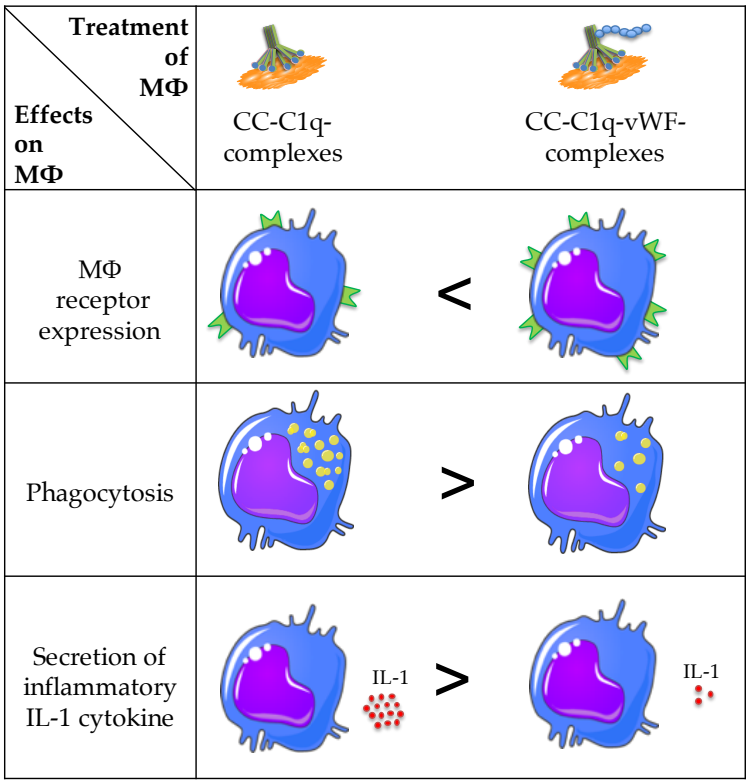

Figure 23: Graphical summary of the effects of CC-C1q-vWF complexes on human-monocyte derived macrophages.

The effects of exposure of human monocyte-derived macrophages to CC-C1q complexes vs. CC-C1q-vWF complexes on i) MΦ receptor expression, ii) phagocytosis and iii) secretion of inflammatory IL-1 cytokine are summarized.
Abbreviations: MΦ: human monocyte-derived macrophages.

Additionally, I investigated the localization of C1q and vWF in human carotid arteries. Here, I observed that C1q and vWF are both localized in the endothelium, intima and media of carotid arteries of patients with atherosclerotic manifestations,

whereas C1q appears to be mostly absent in the intima and media of healthy arteries (Donat et al., in preparation).

In conclusion, our results indicate that the C1q-vWF interaction might be beneficial in dampening inflammation and decelerating plaque progression in the context of atherosclerosis.

In my second project, I focused on the functional consequences of the C1q-vWF interaction in the context of hemostasis *in vivo*.

For this purpose, a thorough analysis of coagulation parameters and assessment of bleeding behavior of C1q-deficient versus WT mice was conducted. Furthermore, in order to investigate whether the observed phenotype of an altered bleeding behavior could be explained by the mere absence of C1q, we carried out reconstitution experiments. In these experiments, I could show that C1q-deficient mice exhibit prolonged bleeding times and increased blood loss compared to WT mice. Upon reconstitution of C1q-deficient animals with human C1q, this blood loss is reduced compared to saline-injected animals (**Figure 24**) (Donat et al., submitted to Frontiers in Immunology).

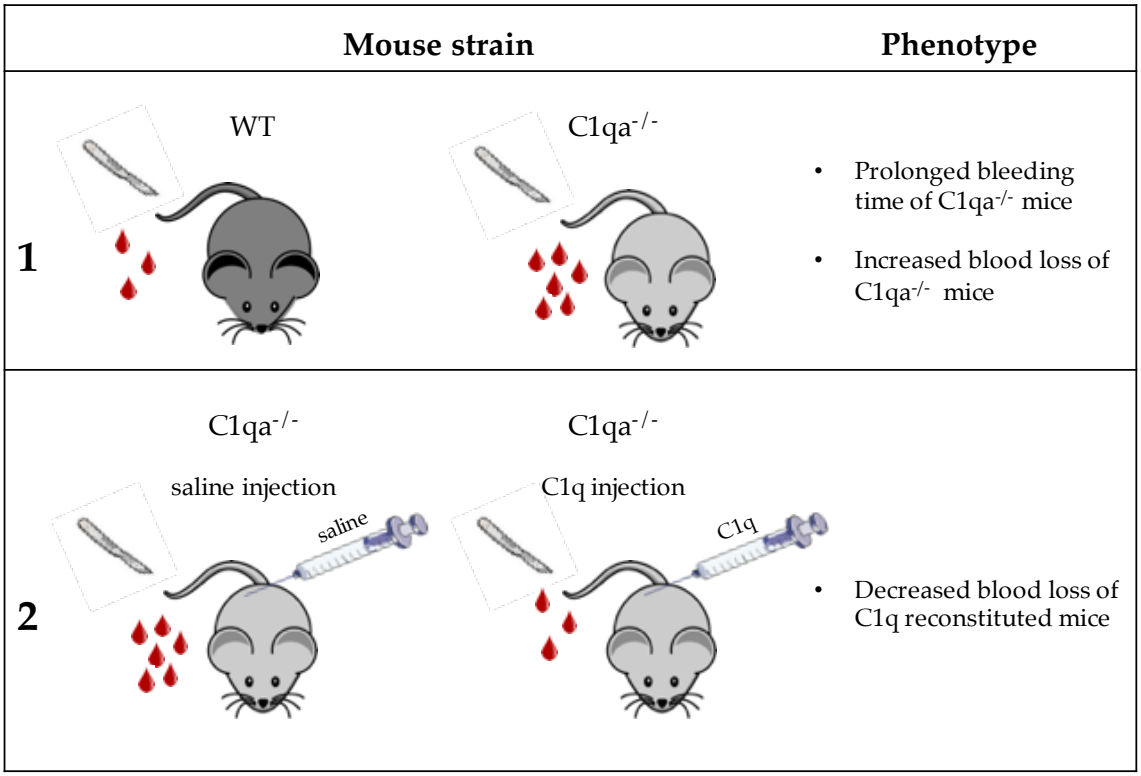

Figure 24: Graphical summary of altered bleeding behavior in C1q-deficient mice.

The observed effects from tail bleeding assays of **1)** wild-type (WT) and C1q-deficient ($C1qa^{-/-}$) mice, as well as of **2)** C1q-deficient ($C1qa^{-/-}$) mice injected with saline (control) or C1q are summarized.

In conclusion, our data indicate that C1q enhances primary hemostasis. These findings might be of relevance for the understanding of thromboembolic complications in inflammatory conditions, where excess C1q deposition is observed.

Overall, immunological and functional consequences of the interaction between C1q and vWF were explored in *in vitro* and *in vivo* models and propose the involvement of C1q-vWF complexes in health (hemostasis) and disease (atherosclerosis and SLE). Since the cross-talk between the complement and coagulation systems has been described to have fundamental clinical implications [233], we predict that the C1q-vWF interaction is also playing a role in other yet unknown physiological as well as pathophysiological settings, such as bacterial sepsis, antibody-mediated hemolytic anemia or acute hemolytic transfusion reaction.

Taken together, the findings of my doctoral research provide a closer insight into the consequences of the interaction between C1q and vWF, which is pivotal for a better understanding of their implications in health and disease. An appreciation of the manifold interplays of both systems holds promise for developing novel diagnostics and therapies for a wide range of diseases that extend beyond those traditionally regarded as complement- or coagulation-mediated.

Outlook

Part I

In vitro

I could show that phagocytosis of CC-C1q-vWF complexes by HMDMs is hampered and secretion of pro-inflammatory IL-1 cytokine is reduced. Consequently, we suggest that detrimental foam cell formation by engulfment of CC-C1q complexes can be retarded by the additional presence of vWF (**Manuscript I**). However, formation of foam cells can be viewed from at least two perspectives, namely i) an increased uptake of lipid structures such as CC and ii) an exhausted efflux of metabolized free cholesterol by transporters such as the ATP-binding cassette transporters ABC-A1 and ABC-G1 [109, 190]. Therefore, we aim to undertake a dual approach to investigate the kinetics of CC-complex uptake by HMDMs on the one hand and the kinetics of efflux of generated free CC as well as expression of efflux transporters on the other hand. For this purpose, live cell imaging of HMDMs treated with CC complexes shall give answers to the question whether foam cell formation can be impeded due to a reduced uptake, an increased efflux or a combination of both. Expression of efflux transporters ABC-A1 and ABC-G1 on mRNA level will be investigated by quantitative polymerase chain reaction (PCR) and on protein level by western blot.

Next to monocyte-derived macrophages, vascular smooth muscle cells [234] as well as endothelial cells [235] can give rise to foam cells. Therefore, in a second step, the use of an *in vitro* model of foam cell formation, including co-culture of three cell types and a microfluidic device exerting stretch forces [236], shall be exploited to provide a deeper understanding of the complex mechanisms of foam cell formation.

Ex vivo

Currently, the number of our obtained specimens of human carotid arteries has not been sufficient to allow for quantification of C1q and vWF expression in healthy compared to diseased individuals. The same accounts for the statistical interpretation of co-localization of C1q and vWF in arteries with atherosclerotic manifestations.

Moreover, since none of our specimens show CC deposits, we are working in collaboration with groups from Milan, Italy, and Trondheim, Norway, to demonstrate the presence of CC-C1q-vWF complexes in human atherosclerosis. So

far, preliminary data indicate that C1q-vWF formation occurs also in areas where CC clefts are present. This part of the project will be finalized in the near future.

Part II

I was able to provide *in vivo* data demonstrating that C1q fulfils an essential role in primary hemostasis by contributing to arrest of bleeding, potentially due to complex formation with vWF (**Manuscript II**).

Even though platelets of C1q-deficient as well as WT mice are functional, the response to platelet aggregation appeared to be slightly constrained for platelets of C1q-deficient mice (Figure 18). To address this point, an in-depth characterization of platelet functionality of C1q-deficient mice could be envisaged. Moreover, up to this point, we were unable to elucidate the exact mechanism of our observations. Future work is needed to clarify the intricate interactions of C1q with vWF and platelets and possibly other not yet considered coagulation factors or cell types.

First, *in vitro* binding experiments with murine vWF (recombinant and plasma-derived) and human C1q shall be carried out to provide evidence that supports our hypothesis of a vWF-dependent C1q-platelet interaction.

Second, functional platelet experiments with normal human serum compared to vWF- and C1q-deficient serum shall be conducted to obtain information about the complex interplay.

With regard to clinical implications, previous studies have pointed out that complement deposition on platelets might be contributing to the thrombotic complications frequently occurring in SLE [228, 237].

Hence, a study investigating platelets of SLE patients, whose C1q serum concentration is strongly decreased, could be conceived. More precisely, platelets of SLE patients and healthy donors shall be examined for the presence of C1q and vWF, by using imaging flow cytometry, and correlated with their ability to form platelet aggregates, by using a reproducible and sensitive platelet aggregation test such as multiple electrode aggregometry (MEA) [238].

Taken together, these future experiments aim to provide a better understanding of the underlying mechanisms of the C1q-hemostasis cross-talk.

References

1. Morgan, B.P. and C.L. Harris, *Complement regulatory proteins.* 1999.
2. Walport, M.J., *Complement. First of two parts.* N Engl J Med, 2001. **344**(14): p. 1058-66.
3. Ricklin, D., et al., *Complement: a key system for immune surveillance and homeostasis.* Nat Immunol, 2010. **11**(9): p. 785-97.
4. Murphy, K. and C. Weaver, *Janeway's immunobiology*. 2017.
5. Sellar, G.C., D.J. Blake, and K.B. Reid, *Characterization and organization of the genes encoding the A-, B- and C-chains of human complement subcomponent C1q. The complete derived amino acid sequence of human C1q.* Biochem J, 1991. **274 (Pt 2)**: p. 481-90.
6. Kishore, U., et al., *Modular organization of the carboxyl-terminal, globular head region of human C1q A, B, and C chains.* J Immunol, 2003. **171**(2): p. 812-20.
7. Calcott, M.A. and H.J. Muller-Eberhard, *C1q protein of human complement.* Biochemistry, 1972. **11**(18): p. 3443-50.
8. Kishore, U. and K.B. Reid, *C1q: structure, function, and receptors.* Immunopharmacology, 2000. **49**(1-2): p. 159-70.
9. De Bracco, M.M. and J.A. Manni, *Serum levels of C1q, C1r and C1s in normal and pathologic sera.* Arthritis Rheum, 1974. **17**(2): p. 121-8.
10. Rabs, U., et al., *Isolation and characterization of macrophage-derived C1q and its similarities to serum C1q.* Eur J Immunol, 1986. **16**(9): p. 1183-6.
11. Colten, H.R., *Biosynthesis of complement.* Adv Immunol, 1976. **22**: p. 67-118.
12. Reid, K.B. and E. Solomon, *Biosynthesis of the first component of complement by human fibroblasts.* Biochem J, 1977. **167**(3): p. 647-60.
13. Morris, K.M., H.R. Colten, and D.H. Bing, *The first component of complement. A quantitative comparison of its biosynthesis in culture by human epithelial and mesenchymal cells.* J Exp Med, 1978. **148**(4): p. 1007-19.
14. Schäfer, M.K.H., et al., *Complement C1q Is Dramatically Up-Regulated in Brain Microglia in Response to Transient Global Cerebral Ischemia.* The Journal of Immunology, 2000. **164**(10): p. 5446.
15. Bulla, R., et al., *Decidual endothelial cells express surface-bound C1q as a molecular bridge between endovascular trophoblast and decidual endothelium.* Mol Immunol, 2008. **45**(9): p. 2629-40.
16. Teo, B.H., et al., *Complement C1q production by osteoclasts and its regulation of osteoclast development.* Biochem J, 2012. **447**(2): p. 229-37.
17. Rubenstein, D.A., et al., *Tobacco and e-cigarette products initiate Kupffer cell inflammatory responses.* Mol Immunol, 2015. **67**(2 Pt B): p. 652-60.
18. van Schaarenburg, R.A., et al., *The production and secretion of complement component C1q by human mast cells.* Mol Immunol, 2016. **78**: p. 164-170.
19. Kaul, M. and M. Loos, *The Fc-recognizing, collagen-like C1q molecule is a putative type II membrane protein of macrophages.* Behring Inst Mitt, 1993(93): p. 171-9.
20. Gohara, D.W. and E. Di Cera, *Allostery in trypsin-like proteases suggests new therapeutic strategies.* Trends in Biotechnology, 2011. **29**(11): p. 577-585.

21. Bobak, D., F. M, and T. A, *C1q acts synergistically with phorbol dibutyrate to activate CR1-mediated phagocytosis by human mononuclear phagocytes.* European Journal of Immunology, 1988. **18**(12): p. 2001-2007.
22. Bobak, D., W. R, and F. M, *C1q enhances the phagocytosis of Cryptococcus neoformans blastospores by human monocytes.* Journal of Immunology, 1988. **141**(2): p. 592-597.
23. Bobak, D.A., et al., *Modulation of FcR function by complement: subcomponent C1q enhances the phagocytosis of IgG-opsonized targets by human monocytes and culture-derived macrophages.* J Immunol, 1987. **138**(4): p. 1150-6.
24. Kishore, U., et al., *Structural and functional anatomy of the globular domain of complement protein C1q.* Immunology Letters, 2004. **95**(2): p. 113-128.
25. Thielens, N.M., et al., *C1q: A fresh look upon an old molecule.* Mol Immunol, 2017. **89**: p. 73-83.
26. Galvan, M.D., M.C. Greenlee-Wacker, and S.S. Bohlson, *C1q and phagocytosis: the perfect complement to a good meal.* J Leukoc Biol, 2012. **92**(3): p. 489-97.
27. Oiki, S. and Y. Okada, *C1q induces chemotaxis and K+ conductance activation coupled to increased cytosolic Ca2+ in mouse fibroblasts.* J Immunol, 1988. **141**(9): p. 3177-85.
28. Bordin, S., B. Ghebrehiwet, and R.C. Page, *Participation of C1q and its receptor in adherence of human diploid fibroblast.* J Immunol, 1990. **145**(8): p. 2520-6.
29. Leigh, E.A.L., et al., *C1q-mediated chemotaxis by human neutrophils: involvement of gClqR and G-protein signalling mechanisms.* Biochemical Journal, 1998. **330**(1): p. 247.
30. Peerschke, E.I. and B. Ghebrehiwet, *C1q augments platelet activation in response to aggregated Ig.* J Immunol, 1997. **159**(11): p. 5594-8.
31. Peerschke, E.I., K.B. Reid, and B. Ghebrehiwet, *Platelet activation by C1q results in the induction of alpha IIb/beta 3 integrins (GPIIb-IIIa) and the expression of P-selectin and procoagulant activity.* J Exp Med, 1993. **178**(2): p. 579-87.
32. Farber, K., et al., *C1q, the recognition subcomponent of the classical pathway of complement, drives microglial activation.* J Neurosci Res, 2009. **87**(3): p. 644-52.
33. Vegh, Z., et al., *Maturation-dependent expression of C1q binding proteins on the cell surface of human monocyte-derived dendritic cells.* Int Immunopharmacol, 2003. **3**(1): p. 39-51.
34. Csomor, E., et al., *Complement protein C1q induces maturation of human dendritic cells.* Mol Immunol, 2007. **44**(13): p. 3389-97.
35. Cutler, A.J., et al., *T cell-dependent immune response in C1q-deficient mice: defective interferon gamma production by antigen-specific T cells.* J Exp Med, 1998. **187**(11): p. 1789-97.
36. van Montfoort, N., et al., *A novel role of complement factor C1q in augmenting the presentation of antigen captured in immune complexes to CD8+ T lymphocytes.* J Immunol, 2007. **178**(12): p. 7581-6.
37. Young, K.R., Jr., et al., *Complement subcomponent C1q stimulates Ig production by human B lymphocytes.* J Immunol, 1991. **146**(10): p. 3356-64.
38. Ferry, H., et al., *Increased Positive Selection of B1 Cells and Reduced B Cell Tolerance to Intracellular Antigens in c1q-Deficient Mice.* The Journal of Immunology, 2007. **178**(5): p. 2916.
39. Stevens, B., et al., *The classical complement cascade mediates CNS synapse elimination.* Cell, 2007. **131**(6): p. 1164-78.

40. Naito, A.T., et al., *Complement C1q activates canonical Wnt signaling and promotes aging-related phenotypes.* Cell, 2012. **149**(6): p. 1298-313.
41. Bossi, F., et al., *C1q as a unique player in angiogenesis with therapeutic implication in wound healing.* Proc Natl Acad Sci U S A, 2014. **111**(11): p. 4209-14.
42. Bulla, R., F. Bossi, and F. Tedesco, *The complement system at the embryo implantation site: friend or foe?* Front Immunol, 2012. **3**: p. 55.
43. Bulla, R., et al., *VE-cadherin is a critical molecule for trophoblast–endothelial cell interaction in decidual spiral arteries.* Experimental Cell Research, 2005. **303**(1): p. 101-113.
44. Mangogna, A., et al., *Is the Complement Protein C1q a Pro- or Anti-tumorigenic Factor? Bioinformatics Analysis Involving Human Carcinomas.* Front Immunol, 2019. **10**: p. 865.
45. Cho, K., *Emerging Roles of Complement Protein C1q in Neurodegeneration.* Aging and disease, 2019. **10**(3): p. 652-663.
46. Walport, M.J., *Complement and systemic lupus erythematosus.* Arthritis research, 2002. **4 Suppl 3**(Suppl 3): p. S279-S293.
47. Stegert, M., M. Bock, and M. Trendelenburg, *Clinical presentation of human C1q deficiency: How much of a lupus?* Mol Immunol, 2015. **67**(1): p. 3-11.
48. Pickering, M.C., et al., *Systemic lupus erythematosus, complement deficiency, and apoptosis.* Adv Immunol, 2000. **76**: p. 227-324.
49. Siegert, C.E., F.C. Breedveld, and M.R. Daha, *Autoantibodies against C1q in systemic lupus erythematosus.* Behring Inst Mitt, 1993(93): p. 279-86.
50. Abu-Shakra, M., et al., *Mortality studies in systemic lupus erythematosus. Results from a single center. I. Causes of death.* J Rheumatol, 1995. **22**(7): p. 1259-64.
51. Ward, M.M., *Premature morbidity from cardiovascular and cerebrovascular diseases in women with systemic lupus erythematosus.* Arthritis Rheum, 1999. **42**(2): p. 338-46.
52. Roman, M.J., et al., *Prevalence and correlates of accelerated atherosclerosis in systemic lupus erythematosus.* N Engl J Med, 2003. **349**(25): p. 2399-406.
53. Afeltra, A., et al., *Thrombosis in systemic lupus erythematosus: congenital and acquired risk factors.* Arthritis Rheum, 2005. **53**(3): p. 452-9.
54. DeLoughery, T.G., *Hemostasis and Thrombosis.* 2015.
55. Cines, D.B., et al., *Endothelial cells in physiology and in the pathophysiology of vascular disorders.* Blood, 1998. **91**(10): p. 3527-61.
56. Heemskerk, J.W., E.M. Bevers, and T. Lindhout, *Platelet activation and blood coagulation.* Thromb Haemost, 2002. **88**(2): p. 186-93.
57. Triplett, D.A., *Coagulation and bleeding disorders: review and update.* Clin Chem, 2000. **46**(8 Pt 2): p. 1260-9.
58. Lasne, D., B. Jude, and S. Susen, *From normal to pathological hemostasis.* Can J Anaesth, 2006. **53**(6 Suppl): p. S2-11.
59. Bermudez, P., M. Beushausen, and M. P. Horan, *Management of Inherited, Acquired, and Iatrogenically Induced Coagulopathies in Oral Surgery*. 2016.
60. Bombeli, T. and D.R. Spahn, *Updates in perioperative coagulation: physiology and management of thromboembolism and haemorrhage.* Br J Anaesth, 2004. **93**(2): p. 275-87.

61. Owens, A.P., 3rd and N. Mackman, *Tissue factor and thrombosis: The clot starts here.* Thromb Haemost, 2010. **104**(3): p. 432-9.
62. Vine, A.K., *Recent advances in haemostasis and thrombosis.* Retina, 2009. **29**(1): p. 1-7.
63. Springer, T.A., *Biology and physics of von Willebrand factor concatamers.* J Thromb Haemost, 2011. **9 Suppl 1**: p. 130-43.
64. Yee, A. and C.A. Kretz, *Von Willebrand factor: form for function.* Semin Thromb Hemost, 2014. **40**(1): p. 17-27.
65. Zhou, Y.F., et al., *Sequence and structure relationships within von Willebrand factor.* Blood, 2012. **120**(2): p. 449-58.
66. Bonthron, D., et al., *Nucleotide sequence of pre-pro-von Willebrand factor cDNA.* Nucleic acids research, 1986. **14**(17): p. 7125-7127.
67. Dong, J.F., et al., *ADAMTS-13 rapidly cleaves newly secreted ultralarge von Willebrand factor multimers on the endothelial surface under flowing conditions.* Blood, 2002. **100**(12): p. 4033-9.
68. Siedlecki, C.A., et al., *Shear-dependent changes in the three-dimensional structure of human von Willebrand factor.* Blood, 1996. **88**(8): p. 2939-50.
69. Jaffe, E.A., L.W. Hoyer, and R.L. Nachman, *Synthesis of von Willebrand factor by cultured human endothelial cells.* Proc Natl Acad Sci U S A, 1974. **71**(5): p. 1906-9.
70. Sporn, L.A., et al., *Biosynthesis of von Willebrand protein by human megakaryocytes.* J Clin Invest, 1985. **76**(3): p. 1102-6.
71. Michaux, G., et al., *The physiological function of von Willebrand's factor depends on its tubular storage in endothelial Weibel-Palade bodies.* Dev Cell, 2006. **10**(2): p. 223-32.
72. Springer, T.A., *von Willebrand factor, Jedi knight of the bloodstream.* Blood, 2014. **124**(9): p. 1412-25.
73. Mazzucato, M., et al., *Identification of domains responsible for von Willebrand factor type VI collagen interaction mediating platelet adhesion under high flow.* J Biol Chem, 1999. **274**(5): p. 3033-41.
74. Savage, B., J.J. Sixma, and Z.M. Ruggeri, *Functional self-association of von Willebrand factor during platelet adhesion under flow.* Proc Natl Acad Sci U S A, 2002. **99**(1): p. 425-30.
75. Xu, E.R., et al., *Structure and dynamics of the platelet integrin-binding C4 domain of von Willebrand factor.* Blood, 2019. **133**(4): p. 366-376.
76. Dong, X., et al., *The von Willebrand factor D'D3 assembly and structural principles for factor VIII binding and concatemer biogenesis.* Blood, 2019. **133**(14): p. 1523-1533.
77. Levy, G.G., et al., *Mutations in a member of the ADAMTS gene family cause thrombotic thrombocytopenic purpura.* Nature, 2001. **413**(6855): p. 488-94.
78. Turner, N.A. and J. Moake, *Assembly and activation of alternative complement components on endothelial cell-anchored ultra-large von Willebrand factor links complement and hemostasis-thrombosis.* PLoS One, 2013. **8**(3): p. e59372.
79. Rauch, A., et al., *On the versatility of von Willebrand factor.* Mediterr J Hematol Infect Dis, 2013. **5**(1): p. e2013046.
80. Leebeek, F.W.G. and J.C.J. Eikenboom, *Von Willebrand's Disease.* N Engl J Med, 2017. **376**(7): p. 701-2.

81. Sanders, Y.V., et al., *Bleeding spectrum in children with moderate or severe von Willebrand disease: Relevance of pediatric-specific bleeding.* Am J Hematol, 2015. **90**(12): p. 1142-8.
82. de Wee, E.M., et al., *Determinants of bleeding phenotype in adult patients with moderate or severe von Willebrand disease.* Thromb Haemost, 2012. **108**(4): p. 683-92.
83. Mehta, R., et al., *Acquired Von Willebrand Syndrome (AVWS) in cardiovascular disease: a state of the art review for clinicians.* J Thromb Thrombolysis, 2019.
84. Lian, E.C.Y., *Pathogenesis of Thrombotic Thrombocytopenic Purpura: ADAMTS13 Deficiency and Beyond.* SEMINARS IN THROMBOSIS AND HEMOSTASIS, 2005. **31**(6): p. 625-632.
85. Krem, M.M. and E. Di Cera, *Evolution of enzyme cascades from embryonic development to blood coagulation.* Trends Biochem Sci, 2002. **27**(2): p. 67-74.
86. Polley, M.J. and R.L. Nachman, *Human platelet activation by C3a and C3a des-arg.* J Exp Med, 1983. **158**(2): p. 603-15.
87. Ikeda, K., et al., *C5a induces tissue factor activity on endothelial cells.* Thromb Haemost, 1997. **77**(2): p. 394-8.
88. Tedesco, F., et al., *The cytolytically inactive terminal complement complex activates endothelial cells to express adhesion molecules and tissue factor procoagulant activity.* J Exp Med, 1997. **185**(9): p. 1619-27.
89. Rezende, S.M., R.E. Simmonds, and D.A. Lane, *Coagulation, inflammation, and apoptosis: different roles for protein S and the protein S-C4b binding protein complex.* Blood, 2004. **103**(4): p. 1192-201.
90. Ghebrehiwet, B., et al., *Mechanisms of activation of the classical pathway of complement by Hageman factor fragment.* The Journal of clinical investigation, 1983. **71**(5): p. 1450-1456.
91. Krisinger, M.J., et al., *Thrombin generates previously unidentified C5 products that support the terminal complement activation pathway.* Blood, 2012. **120**(8): p. 1717-25.
92. Keel, M. and O. Trentz, *Pathophysiology of polytrauma.* Injury, 2005. **36**(6): p. 691-709.
93. Sun, H., *The interaction between pathogens and the host coagulation system.* Physiology (Bethesda), 2006. **21**: p. 281-8.
94. Guo, R.F. and P.A. Ward, *Role of C5a in inflammatory responses.* Annu Rev Immunol, 2005. **23**: p. 821-52.
95. Karpman, D., et al., *Platelet activation in hemolytic uremic syndrome.* Semin Thromb Hemost, 2006. **32**(2): p. 128-45.
96. Wiedmer, T., et al., *Complement-induced vesiculation and exposure of membrane prothrombinase sites in platelets of paroxysmal nocturnal hemoglobinuria.* Blood, 1993. **82**(4): p. 1192-6.
97. Coppola, L., et al., *C1 inhibitor infusion modifies platelet activity in hereditary angioedema patients.* Arch Pathol Lab Med, 2002. **126**(7): p. 842-5.
98. Palatinus, A. and M. Adams, *Thrombosis in systemic lupus erythematosus.* Semin Thromb Hemost, 2009. **35**(7): p. 621-9.
99. Schaller, M., et al., *Autoantibodies against C1q in systemic lupus erythematosus are antigen-driven.* J Immunol, 2009. **183**(12): p. 8225-31.
100. Kölm, R., et al., *Von Willebrand Factor Interacts with Surface-Bound C1q and Induces Platelet Rolling.* J Immunol, 2016. **197**(9): p. 3669-3679.
101. Ross, R., *Atherosclerosis--an inflammatory disease.* N Engl J Med, 1999. **340**(2): p. 115-26.

102. Willis, M., J.W. Homeister, and J.R. Stone, *Cellular and molecular pathobiology of cardiovascular disease.* 2014.
103. Lusis, A.J., *Atherosclerosis.* Nature, 2000. **407**(6801): p. 233-41.
104. Fruchart, J.C., et al., *New risk factors for atherosclerosis and patient risk assessment.* Circulation, 2004. **109**(23 Suppl 1): p. Iii15-9.
105. Libby, P., P.M. Ridker, and G.K. Hansson, *Progress and challenges in translating the biology of atherosclerosis.* Nature, 2011. **473**(7347): p. 317-325.
106. Tabas, I., *Macrophage death and defective inflammation resolution in atherosclerosis.* Nat Rev Immunol, 2010. **10**(1): p. 36-46.
107. Lee, S.E., et al., *Effects of Statins on Coronary Atherosclerotic Plaques: The PARADIGM Study.* JACC Cardiovasc Imaging, 2018. **11**(10): p. 1475-1484.
108. Brophy, M.L., et al., *Eating the Dead to Keep Atherosclerosis at Bay.* Front Cardiovasc Med, 2017. **4**: p. 2.
109. Maguire, E.M., S.W.A. Pearce, and Q. Xiao, *Foam cell formation: A new target for fighting atherosclerosis and cardiovascular disease.* Vascul Pharmacol, 2019. **112**: p. 54-71.
110. Niculescu, F. and H. Rus, *The role of complement activation in atherosclerosis.* Immunologic Research, 2004. **30**(1): p. 73-80.
111. Patzelt, J., A. Verschoor, and H.F. Langer, *Platelets and the complement cascade in atherosclerosis.* Front Physiol, 2015. **6**: p. 49.
112. Speidl, W.S., et al., *Complement in atherosclerosis: friend or foe?* J Thromb Haemost, 2011. **9**(3): p. 428-40.
113. Cao, W., et al., *Dendritic cells in the arterial wall express C1q: potential significance in atherogenesis.* Cardiovasc Res, 2003. **60**(1): p. 175-86.
114. Peerschke, E.I., et al., *Expression of gC1q-R/p33 and its major ligands in human atherosclerotic lesions.* Mol Immunol, 2004. **41**(8): p. 759-66.
115. Vlaicu, R., et al., *Immunoglobulins and complement components in human aortic atherosclerotic intima.* Atherosclerosis, 1985. **55**(1): p. 35-50.
116. Fraser, D.A. and A.J. Tenner, *Innate immune proteins C1q and mannan-binding lectin enhance clearance of atherogenic lipoproteins by human monocytes and macrophages.* J Immunol, 2010. **185**(7): p. 3932-9.
117. Spivia, W., et al., *Complement protein C1q promotes macrophage anti-inflammatory M2-like polarization during the clearance of atherogenic lipoproteins.* Inflamm Res, 2014. **63**(10): p. 885-93.
118. Ho, M.-M. and D.A. Fraser, *Transcriptome data and gene ontology analysis in human macrophages ingesting modified lipoproteins in the presence or absence of complement protein C1q.* Data in brief, 2016. **9**: p. 362-367.
119. Ho, M.M., et al., *Macrophage molecular signaling and inflammatory responses during ingestion of atherogenic lipoproteins are modulated by complement protein C1q.* Atherosclerosis, 2016. **253**: p. 38-46.
120. Pulanco, M.C., et al., *Complement Protein C1q Enhances Macrophage Foam Cell Survival and Efferocytosis.* The Journal of Immunology, 2016.

121. Bhatia, V.K., et al., *Complement C1q reduces early atherosclerosis in low-density lipoprotein receptor-deficient mice.* Am J Pathol, 2007. **170**(1): p. 416-26.
122. Lewis, M.J., et al., *Immunoglobulin M is required for protection against atherosclerosis in low-density lipoprotein receptor-deficient mice.* Circulation, 2009. **120**(5): p. 417-26.
123. Pardo, P.V., et al., *Investigating modulation of inflammation in atherosclerosis by complement protein C1q.* The Journal of Immunology, 2017. **198**(1 Supplement): p. 75.6-75.6.
124. Peerschke, E.I., K.B. Reid, and B. Ghebrehiwet, *Identification of a novel 33-kDa C1q-binding site on human blood platelets.* J Immunol, 1994. **152**(12): p. 5896-901.
125. Pilely, K., et al., *Cholesterol Crystals Activate the Lectin Complement Pathway via Ficolin-2 and Mannose-Binding Lectin: Implications for the Progression of Atherosclerosis.* J Immunol, 2016. **196**(12): p. 5064-74.
126. van der Net, J.B., et al., *Replication study of 10 genetic polymorphisms associated with coronary heart disease in a specific high-risk population with familial hypercholesterolemia.* Eur Heart J, 2008. **29**(18): p. 2195-201.
127. Lewis, R.D., et al., *The membrane attack complex of complement drives the progression of atherosclerosis in apolipoprotein E knockout mice.* Mol Immunol, 2010. **47**(5): p. 1098-105.
128. Schmiedt, W., et al., *Complement C6 deficiency protects against diet-induced atherosclerosis in rabbits.* Arterioscler Thromb Vasc Biol, 1998. **18**(11): p. 1790-5.
129. Yin, C., et al., *ApoE attenuates unresolvable inflammation by complex formation with activated C1q.* Nat Med, 2019. **25**(3): p. 496-506.
130. Niculescu, F., et al., *Quantitative evaluation of the terminal C5b-9 complement complex by ELISA in human atherosclerotic arteries.* Clin Exp Immunol, 1987. **69**(2): p. 477-83.
131. Badimon, L., et al., *Aortic atherosclerosis in pigs with heterozygous von Willebrand disease. Comparison with homozygous von Willebrand and normal pigs.* Arteriosclerosis, 1985. **5**(4): p. 366-70.
132. Fuster, V., et al., *Arteriosclerosis in normal and von Willebrand pigs: long-term prospective study and aortic transplantation study.* Circ Res, 1982. **51**(5): p. 587-93.
133. Fuster, W., et al., *Resistance to arteriosclerosis in pigs with von Willebrand's disease. Spontaneous and high cholesterol diet-induced arteriosclerosis.* The Journal of clinical investigation, 1978. **61**(3): p. 722-730.
134. Griggs, T.R., et al., *Development of coronary atherosclerosis in swine with severe hypercholesterolemia. Lack of influence of von Willebrand factor or acute intimal injury.* Arteriosclerosis, 1986. **6**(2): p. 155-65.
135. Griggs, T.R., et al., *Susceptibility to atherosclerosis in aortas and coronary arteries of swine with von Willebrand's disease.* Am J Pathol, 1981. **102**(2): p. 137-45.
136. Reddick, R.L., et al., *Coronary atherosclerosis in the pig. Induced plaque injury and platelet response.* Arteriosclerosis, 1990. **10**(4): p. 541-50.
137. Methia, N., et al., *Localized reduction of atherosclerosis in von Willebrand factor-deficient mice.* Blood, 2001. **98**(5): p. 1424-8.
138. Qin, F., et al., *Overexpression of von Willebrand factor is an independent risk factor for pathogenesis of intimal hyperplasia: preliminary studies.* J Vasc Surg, 2003. **37**(2): p. 433-9.

139. van Galen, K.P., et al., *Von Willebrand factor deficiency and atherosclerosis.* Blood Rev, 2012. **26**(5): p. 189-96.
140. Bilora, F., et al., *Hemophilia A, von Willebrand disease, and atherosclerosis of abdominal aorta and leg arteries: factor VIII and von Willebrand factor defects appear to protect abdominal aorta and leg arteries from atherosclerosis.* Clin Appl Thromb Hemost, 2001. **7**(4): p. 311-3.
141. Bilora, F., et al., *Do hemophilia A and von Willebrand disease protect against carotid atherosclerosis? A comparative study between coagulopathics and normal subjects by means of carotid echo-color Doppler scan.* Clin Appl Thromb Hemost, 1999. **5**(4): p. 232-5.
142. Sramek, A., et al., *Decreased coagulability has no clinically relevant effect on atherogenesis: observations in individuals with a hereditary bleeding tendency.* Circulation, 2001. **104**(7): p. 762-7.
143. Sramek, A., et al., *Patients with type 3 severe von Willebrand disease are not protected against atherosclerosis: results from a multicenter study in 47 patients.* Circulation, 2004. **109**(6): p. 740-4.
144. Kovacevic, K.D., et al., *Von Willebrand factor antigen levels predict major adverse cardiovascular events in patients with carotid stenosis of the ICARAS study.* Atherosclerosis, 2019. **290**: p. 31-36.
145. Kucharska-Newton, A.M., et al., *Hemostasis, inflammation, and fatal and nonfatal coronary heart disease: long-term follow-up of the atherosclerosis risk in communities (ARIC) cohort.* Arterioscler Thromb Vasc Biol, 2009. **29**(12): p. 2182-90.
146. Villmann, J.M., et al., *Atherosclerosis, myocardial infarction and primary hemostasis: Impact of platelets, von Willebrand factor and soluble glycoprotein VI.* Thromb Res, 2019. **180**: p. 98-104.
147. Zadi, T., et al., *No independent association found between von Willebrand factor and plaque ulceration in carotid artery atherosclerosis.* Thromb Res, 2019. **174**: p. 95-97.
148. Morgan, B.P. and C.L. Harris, *Complement, a target for therapy in inflammatory and degenerative diseases.* Nat Rev Drug Discov, 2015. **14**(12): p. 857-77.
149. Nayak, A., et al., *The non-classical functions of the classical complement pathway recognition subcomponent C1q.* Immunol Lett, 2010. **131**(2): p. 139-50.
150. Bohlson, S.S., D.A. Fraser, and A.J. Tenner, *Complement proteins C1q and MBL are pattern recognition molecules that signal immediate and long-term protective immune functions.* Mol Immunol, 2007. **44**(1-3): p. 33-43.
151. Samstad, E.O., et al., *Cholesterol crystals induce complement-dependent inflammasome activation and cytokine release.* J Immunol, 2014. **192**(6): p. 2837-45.
152. Fraser, D.A., et al., *C1q and MBL, components of the innate immune system, influence monocyte cytokine expression.* J Leukoc Biol, 2006. **80**(1): p. 107-16.
153. Fraser, D.A., et al., *C1q differentially modulates phagocytosis and cytokine responses during ingestion of apoptotic cells by human monocytes, macrophages, and dendritic cells.* J Immunol, 2009. **183**(10): p. 6175-85.
154. Benoit, M.E., et al., *Complement protein C1q directs macrophage polarization and limits inflammasome activity during the uptake of apoptotic cells.* J Immunol, 2012. **188**(11): p. 5682-93.
155. Markiewski, M.M., et al., *Complement and coagulation: strangers or partners in crime?* Trends Immunol, 2007. **28**(4): p. 184-92.

156. van Schooten, C.J., et al., *Macrophages contribute to the cellular uptake of von Willebrand factor and factor VIII in vivo.* Blood, 2008. **112**(5): p. 1704-12.
157. Wohner, N., et al., *Macrophage scavenger receptor SR-AI contributes to the clearance of von Willebrand factor.* Haematologica, 2018. **103**(4): p. 728-737.
158. Feng, S., et al., *The interaction between factor H and Von Willebrand factor.* PLoS One, 2013. **8**(8): p. e73715.
159. Feng, S., et al., *von Willebrand factor is a cofactor in complement regulation.* Blood, 2015. **125**(6): p. 1034-7.
160. Franklin, B.S., M.S. Mangan, and E. Latz, *Crystal Formation in Inflammation.* Annu Rev Immunol, 2016. **34**: p. 173-202.
161. Corr, E.M., C.C. Cunningham, and A. Dunne, *Cholesterol crystals activate Syk and PI3 kinase in human macrophages and dendritic cells.* Atherosclerosis, 2016. **251**: p. 197-205.
162. Zimmer, S., et al., *Cyclodextrin promotes atherosclerosis regression via macrophage reprogramming.* Sci Transl Med, 2016. **8**(333): p. 333ra50.
163. Bakke, S.S., et al., *Cyclodextrin Reduces Cholesterol Crystal-Induced Inflammation by Modulating Complement Activation.* J Immunol, 2017. **199**(8): p. 2910-2920.
164. Rajamaki, K., et al., *Cholesterol crystals activate the NLRP3 inflammasome in human macrophages: a novel link between cholesterol metabolism and inflammation.* PLoS One, 2010. **5**(7): p. e11765.
165. Duewell, P., et al., *NLRP3 inflammasomes are required for atherogenesis and activated by cholesterol crystals.* Nature, 2010. **464**(7293): p. 1357-61.
166. Abela, G.S., *Cholesterol crystals piercing the arterial plaque and intima trigger local and systemic inflammation.* J Clin Lipidol, 2010. **4**(3): p. 156-64.
167. Buono, C., et al., *Influence of C3 deficiency on atherosclerosis.* Circulation, 2002. **105**(25): p. 3025-31.
168. Thanei, S. and M. Trendelenburg, *Anti-C1q Autoantibodies from Systemic Lupus Erythematosus Patients Induce a Proinflammatory Phenotype in Macrophages.* J Immunol, 2016. **196**(5): p. 2063-74.
169. Turecek, P.L., et al., *Development of a plasma- and albumin-free recombinant von Willebrand factor.* Hamostaseologie, 2009. **29 Suppl 1**: p. S32-8.
170. Bigler, C., et al., *Autoantibodies against complement C1q specifically target C1q bound on early apoptotic cells.* J Immunol, 2009. **183**(5): p. 3512-21.
171. Kölm, R., et al., *Von Willebrand factor binds surface-bound C1q and induces platelet rolling.* University of Basel, 2015.
172. Sica, A. and A. Mantovani, *Macrophage plasticity and polarization: in vivo veritas.* J Clin Invest, 2012. **122**(3): p. 787-95.
173. Galvan, M.D., et al., *Complement component C1q regulates macrophage expression of Mer tyrosine kinase to promote clearance of apoptotic cells.* J Immunol, 2012. **188**(8): p. 3716-23.
174. Taylor, P.R., et al., *A hierarchical role for classical pathway complement proteins in the clearance of apoptotic cells in vivo.* J Exp Med, 2000. **192**(3): p. 359-66.
175. Rubartelli, A. and M.T. Lotze, *Inside, outside, upside down: damage-associated molecular-pattern molecules (DAMPs) and redox.* Trends Immunol, 2007. **28**(10): p. 429-36.

176. Place, D.E. and T.D. Kanneganti, *Cell death-mediated cytokine release and its therapeutic implications.* J Exp Med, 2019. **216**(7): p. 1474-1486.
177. Broz, P. and V.M. Dixit, *Inflammasomes: mechanism of assembly, regulation and signalling.* Nat Rev Immunol, 2016. **16**(7): p. 407-20.
178. Rayes, J., et al., *The interaction between factor H and VWF increases factor H cofactor activity and regulates VWF prothrombotic status.* Blood, 2014. **123**(1): p. 121-5.
179. Nissila, E., et al., *Complement Factor H and Apolipoprotein E Participate in Regulation of Inflammation in THP-1 Macrophages.* Front Immunol, 2018. **9**: p. 2701.
180. Libby, P., *Interleukin-1 Beta as a Target for Atherosclerosis Therapy: Biological Basis of CANTOS and Beyond.* J Am Coll Cardiol, 2017. **70**(18): p. 2278-2289.
181. Janoudi, A., et al., *Cholesterol crystal induced arterial inflammation and destabilization of atherosclerotic plaque.* Eur Heart J, 2016. **37**(25): p. 1959-67.
182. Pilely, K., et al., *C-Reactive Protein Binds to Cholesterol Crystals and Co-Localizes with the Terminal Complement Complex in Human Atherosclerotic Plaques.* Frontiers in Immunology, 2017. **8**(1040).
183. Niculescu, F., et al., *Localization of the terminal C5b-9 complement complex in the human aortic atherosclerotic wall.* Immunol Lett, 1985. **10**(2): p. 109-14.
184. Torzewski, M., et al., *Immunohistochemical demonstration of enzymatically modified human LDL and its colocalization with the terminal complement complex in the early atherosclerotic lesion.* Arterioscler Thromb Vasc Biol, 1998. **18**(3): p. 369-78.
185. Cai, B., et al., *MerTK receptor cleavage promotes plaque necrosis and defective resolution in atherosclerosis.* J Clin Invest, 2017. **127**(2): p. 564-568.
186. Mueller, P.A., et al., *Deletion of Macrophage Low-Density Lipoprotein Receptor-Related Protein 1 (LRP1) Accelerates Atherosclerosis Regression and Increases C-C Chemokine Receptor Type 7 (CCR7) Expression in Plaque Macrophages.* Circulation, 2018. **138**(17): p. 1850-1863.
187. Ben, J., et al., *Class A1 scavenger receptors in cardiovascular diseases.* Br J Pharmacol, 2015. **172**(23): p. 5523-30.
188. Yi, X., et al., *Silencing LAIR-1 in human THP-1 macrophage increases foam cell formation by modulating PPARgamma and M2 polarization.* Cytokine, 2018. **111**: p. 194-205.
189. Ridker, P.M., et al., *Antiinflammatory Therapy with Canakinumab for Atherosclerotic Disease.* N Engl J Med, 2017. **377**(12): p. 1119-1131.
190. Moore, K., F. Sheedy, and E. Fisher, *Macrophages in atherosclerosis: a dynamic balance.* Nat Rev Immunol, 2013. **13**(10): p. 709-21.
191. Libby, P., *Inflammation in atherosclerosis.* Nature, 2002. **420**(6917): p. 868-74.
192. Gravastrand, C.S., et al., *Cholesterol Crystals Induce Coagulation Activation through Complement-Dependent Expression of Monocytic Tissue Factor.* J Immunol, 2019.
193. Gale, A.J., *Continuing education course #2: current understanding of hemostasis.* Toxicologic pathology, 2011. **39**(1): p. 273-280.
194. Oikonomopoulou, K., et al., *Interactions between coagulation and complement--their role in inflammation.* Semin Immunopathol, 2012. **34**(1): p. 151-65.

195. Skoglund, C., et al., *C1q induces a rapid up-regulation of P-selectin and modulates collagen- and collagen-related peptide-triggered activation in human platelets.* Immunobiology, 2010. **215**(12): p. 987-995.
196. Cazenave, J.P., et al., *Clq inhibition of the interaction of collagen with human platelets.* J Immunol, 1976. **116**(1): p. 162-3.
197. Skoglund, C., et al., *C-reactive protein and C1q regulate platelet adhesion and activation on adsorbed immunoglobulin G and albumin.* Immunol Cell Biol, 2008. **86**(5): p. 466-74.
198. Rehmus, E.H., et al., *Inhibition of the activation of Hageman factor (factor XII) by complement subcomponent C1q.* J Clin Invest, 1987. **80**(2): p. 516-21.
199. Markiewski, M.M., R.A. DeAngelis, and J.D. Lambris, *Complexity of complement activation in sepsis.* Journal of cellular and molecular medicine, 2008. **12**(6A): p. 2245-2254.
200. Bazzan, M., A. Vaccarino, and F. Marletto, *Systemic lupus erythematosus and thrombosis.* Thromb J, 2015. **13**: p. 16.
201. Al-Homood, I.A., *Thrombosis in systemic lupus erythematosus: a review article.* ISRN Rheumatol, 2012. **2012**: p. 428269.
202. Kamal, A.H., A. Tefferi, and R.K. Pruthi, *How to Interpret and Pursue an Abnormal Prothrombin Time, Activated Partial Thromboplastin Time, and Bleeding Time in Adults.* Mayo Clinic Proceedings, 2007. **82**(7): p. 864-873.
203. Paniccia, R., et al., *Platelet function tests: a comparative review.* Vascular health and risk management, 2015. **11**: p. 133-148.
204. Foley, J.H., *Examining coagulation-complement crosstalk: complement activation and thrombosis.* Thromb Res, 2016. **141 Suppl 2**: p. S50-4.
205. Dzik, S., *Complement and Coagulation: Cross Talk Through Time.* Transfusion Medicine Reviews, 2019.
206. Denis, C., et al., *A mouse model of severe von Willebrand disease: defects in hemostasis and thrombosis.* Proc Natl Acad Sci U S A, 1998. **95**(16): p. 9524-9.
207. Morowski, M., et al., *Only severe thrombocytopenia results in bleeding and defective thrombus formation in mice.* Blood, 2013. **121**(24): p. 4938-47.
208. Chaudhry, L.A., et al., *Factor XII (Hageman Factor) Deficiency: a rare harbinger of life threatening complications.* Pan Afr Med J, 2019. **33**: p. 39.
209. Strassel, C., et al., *Decreased thrombotic tendency in mouse models of the Bernard-Soulier syndrome.* Arterioscler Thromb Vasc Biol, 2007. **27**(1): p. 241-7.
210. Ware, J., *Dysfunctional platelet membrane receptors: from humans to mice.* Thromb Haemost, 2004. **92**(3): p. 478-85.
211. Csako, G., E.A. Suba, and A. Herp, *Effect of collagen-like substances (C1q, acetylcholinesterase and elastin) on collagen-induced platelet aggregation.* Haemostasis, 1982. **11**(4): p. 204-9.
212. Peerschke, E.I., et al., *The soluble recombinant form of a binding protein/receptor for the globular domain of C1q (gC1qR) enhances blood coagulation.* Blood Coagul Fibrinolysis, 1998. **9**(1): p. 29-37.
213. Ghebrehiwet, B., et al., *Complement component C1q induces endothelial cell adhesion and spreading through a docking/signaling partnership of C1q receptors and integrins.* Int Immunopharmacol, 2003. **3**(3): p. 299-310.

214. Yau, J.W., H. Teoh, and S. Verma, *Endothelial cell control of thrombosis.* BMC cardiovascular disorders, 2015. **15**: p. 130-130.
215. Petry, F., K.B. Reid, and M. Loos, *Gene expression of the A- and B-chain of mouse C1q in different tissues and the characterization of the recombinant A-chain.* J Immunol, 1991. **147**(11): p. 3988-93.
216. Dumestre-Perard, C., et al., *Involvement of complement pathways in patients with bacterial septicemia.* Mol Immunol, 2007. **44**(7): p. 1631-8.
217. Brouwer, N., et al., *Mannose-binding lectin (MBL) facilitates opsonophagocytosis of yeasts but not of bacteria despite MBL binding.* J Immunol, 2008. **180**(6): p. 4124-32.
218. Ritis, K., et al., *A novel C5a receptor-tissue factor cross-talk in neutrophils links innate immunity to coagulation pathways.* J Immunol, 2006. **177**(7): p. 4794-802.
219. Kienast, J., et al., *Treatment effects of high-dose antithrombin without concomitant heparin in patients with severe sepsis with or without disseminated intravascular coagulation.* J Thromb Haemost, 2006. **4**(1): p. 90-7.
220. Ghebrehiwet, B. and E.I. Peerschke, *Role of C1q and C1q receptors in the pathogenesis of systemic lupus erythematosus.* Curr Dir Autoimmun, 2004. **7**: p. 87-97.
221. Walport, M.J., K.A. Davies, and M. Botto, *C1q and Systemic Lupus Erythematosus.* Immunobiology, 1998. **199**(2): p. 265-285.
222. Svenungsson, E., et al., *Risk factors for cardiovascular disease in systemic lupus erythematosus.* Circulation, 2001. **104**(16): p. 1887-93.
223. Avina-Zubieta, J.A., et al., *The risk of pulmonary embolism and deep venous thrombosis in systemic lupus erythematosus: A general population-based study.* Semin Arthritis Rheum, 2015. **45**(2): p. 195-201.
224. Dhar, J.P., et al., *Thrombophilic patterns of coagulation factors in lupus.* Lupus, 2009. **18**(5): p. 400-6.
225. Wu, L.H., et al., *Inclusion of renal vascular lesions in the 2003 ISN/RPS system for classifying lupus nephritis improves renal outcome predictions.* Kidney Int, 2013. **83**(4): p. 715-23.
226. Kishore, S., et al., *Systemic Lupus Erythematosus Is Associated With a High Risk of Venous Thromboembolism in Hospitalized Patients Leading to Poor Outcomes and a Higher Cost: Results From Nationwide Inpatient Sample Database 2003-2011.* ACR Open Rheumatology, 2019. **1**(3): p. 194-200.
227. Asanuma, Y., et al., *Premature coronary-artery atherosclerosis in systemic lupus erythematosus.* N Engl J Med, 2003. **349**(25): p. 2407-15.
228. Lood, C., et al., *Increased C1q, C4 and C3 deposition on platelets in patients with systemic lupus erythematosus--a possible link to venous thrombosis?* Lupus, 2012. **21**(13): p. 1423-32.
229. Peerschke, E.I., et al., *Serum complement activation on heterologous platelets is associated with arterial thrombosis in patients with systemic lupus erythematosus and antiphospholipid antibodies.* Lupus, 2009. **18**(6): p. 530-8.
230. Hoiland, II, et al., *Associations between complement pathways activity, mannose-binding lectin, and odds of unprovoked venous thromboembolism.* Thromb Res, 2018. **169**: p. 50-56.
231. Peerschke, E.I. and B. Ghebrehiwet, *Platelet receptors for the complement component C1q: implications for hemostasis and thrombosis.* Immunobiology, 1998. **199**(2): p. 239-49.

232. Donat, C., S. Thanei, and M. Trendelenburg, *Binding of von Willebrand Factor to Complement C1q Decreases the Phagocytosis of Cholesterol Crystals and Subsequent IL-1 Secretion in Macrophages.* Frontiers in Immunology, 2019. **10**(2712).
233. Conway, E.M., *Reincarnation of ancient links between coagulation and complement.* J Thromb Haemost, 2015. **13 Suppl 1**: p. S121-32.
234. Yin, Y.W., et al., *TLR4-mediated inflammation promotes foam cell formation of vascular smooth muscle cell by upregulating ACAT1 expression.* Cell Death & Disease, 2014. **5**(12): p. e1574-e1574.
235. Ivan, L. and F. Antohe, *Hyperlipidemia induces endothelial-derived foam cells in culture.* J Recept Signal Transduct Res, 2010. **30**(2): p. 106-14.
236. Gu, X., et al., *An in vitro model of foam cell formation induced by a stretchable microfluidic device.* Scientific Reports, 2019. **9**(1): p. 7461.
237. Navratil, J.S., et al., *Platelet C4d is highly specific for systemic lupus erythematosus.* Arthritis Rheum, 2006. **54**(2): p. 670-4.
238. Toth, O., et al., *Multiple electrode aggregometry: a new device to measure platelet aggregation in whole blood.* Thromb Haemost, 2006. **96**(6): p. 781-8.

Acknowledgements

Finally, I get to express my gratitude to those who accompanied me on the journey of my PhD:

I would like to thank **Marten** for taking me as a PhD student. I truly acknowledge him for always having an open ear, advocating for me and providing me with scientific independence when wanted and with support when needed.

I would also like to thank **Radek Skoda** and **Verena Schröder** for their valuable input in the PhD advisory committee meetings and for evaluating my dissertation.

I cannot thank my **family** and **friends** enough for their endless love and support throughout the years. I am especially grateful to **Vivi** & **Marc** for the trust they always had in me and for making me a better person.

I am deeply thankful to all of my present and former lab members for their company, myriads of hours of conversations and assistance. A special thank you is addressed to **Sophie** and **Robert** without whom I would have often drowned in self-doubts.

Moreover, I would like to acknowledge the members of **DBM research groups** of Translational Diabetes, Clinical Neurobiology, Diabetes Research, Translational Immunology, Translational Neuroimmunology, Immunodeficiency, of the **DBM PhD Club** and of the **DBM core facilities** for great scientific and even greater non-scientific support.

I would like to thank **Nathalie Niyonzima**, **Shabih Zaidi**, **Bernard Arnolda** and **Jacques Houot** for their invaluable inspiration and motivation.

I am utterly obliged to all of the above for their precious contributions that have made this journey possible.

Appendix

Manuscript I

Binding of von Willebrand factor to complement C1q decreases the phagocytosis of cholesterol crystals and subsequent IL-1 secretion in macrophages

Claudia Donat[1*], Sophia Thanei[1], Marten Trendelenburg[1,2]

[1]Laboratory of Clinical Immunology, Department of Biomedicine, University of Basel, 4031 Basel, Switzerland
[2]Division of Internal Medicine, University Hospital of Basel, 4031 Basel, Switzerland

* **Correspondence:**
Claudia Donat
E- Mail: claudia.donat@unibas.ch

frontiers in Immunology

ORIGINAL RESEARCH
published: 21 November 2019
doi: 10.3389/fimmu.2019.02712

Binding of von Willebrand Factor to Complement C1q Decreases the Phagocytosis of Cholesterol Crystals and Subsequent IL-1 Secretion in Macrophages

Claudia Donat[1]*, *Sophia Thanei*[1] *and Marten Trendelenburg*[1,2]

[1] *Laboratory of Clinical Immunology, Department of Biomedicine, University of Basel, Basel, Switzerland,* [2] *Division of Internal Medicine, University Hospital of Basel, Basel, Switzerland*

Complement C1q, the initiation molecule of the classical pathway, exerts various immunomodulatory functions independent of complement activation. Non-classical functions of C1q include the clearance of apoptotic cells and cholesterol crystals (CC), as well as the modulation of cytokine secretion by immune cells such as macrophages. Moreover, C1q has been shown to act as a binding partner for von Willebrand factor (vWF), initiation molecule of primary hemostasis. However, the consequences of this C1q-vWF interaction on the phagocytosis of CC by macrophages has remained elusive until now. Here, we used CC-C1q-vWF complexes to study immunological effects on human monocyte-derived macrophages (HMDMs). HMDMs were investigated by analyzing surface receptor expression, phagocytosis of CC complexes, cytokine secretion, and caspase-1 activity. We found that vWF only bound to CC in a C1q-dependent manner. Exposure of macrophages to CC-C1q-vWF complexes resulted in an upregulated expression of phagocytosis-mediating receptors MerTK, LRP-1, and SR-A1 as well as CD14, LAIR1, and PD-L1 when compared to CC-C1q without vWF, whereas phagocytosis of CC-C1q complexes was hampered in the presence of vWF. In addition, we observed a diminished caspase-1 activation and subsequent reduction in pro-inflammatory IL-1β cytokine secretion, IL-1β/IL-1RA ratio and IL-1α/IL-1RA ratio. In conclusion, our results demonstrate that vWF binding to C1q substantially modulates the effects of C1q on HMDMs. In this way, the C1q-vWF interaction might be beneficial in dampening inflammation, e.g., in the context of atherosclerosis.

Keywords: macrophages, complement C1q, von Willebrand factor, cholesterol, atherosclerosis, innate immunity

OPEN ACCESS

Edited by:
Uday Kishore,
Brunel University London,
United Kingdom

Reviewed by:
Robert Braidwood Sim,
University of Oxford, United Kingdom
Ansar Ahmed Pathan,
Brunel University London,
United Kingdom

***Correspondence:**
Claudia Donat
claudia.donat@unibas.ch

Specialty section:
This article was submitted to Molecular Innate Immunity, a section of the journal Frontiers in Immunology

Received: *19 August 2019*
Accepted: *05 November 2019*
Published: *21 November 2019*

Citation:
Donat C, Thanei S and Trendelenburg M (2019) Binding of von Willebrand Factor to Complement C1q Decreases the Phagocytosis of Cholesterol Crystals and Subsequent IL-1 Secretion in Macrophages. Front. Immunol. 10:2712. doi: 10.3389/fimmu.2019.02712

INTRODUCTION

The complement system is a highly effective part of the innate immune system. The multiple functions of complement include defense against bacterial infections, bridging innate and adaptive immunity and the clearance of immune complexes, and components of inflammation (1). The complement system can be activated through three distinct pathways: the classical, the lectin and the alternative pathway. All three pathways converge in a shared terminal response resulting in the formation of C5a and C3a as potent inflammatory effector molecules and C5b-9

as membrane attack complex. However, each pathway is initiated through different characteristic recognition molecules (2). The initiation of the classical pathway is triggered by C1q through sensing of bound antibodies as well as pathogen- and damage-associated molecular patterns (PAMPs/DAMPs). In addition, more recent research has shown a number of functions for C1q that are independent of downstream complement activation (3). On the one hand, opsonization with C1q enhances the clearance of diverse structures, namely immune complexes (4) and apoptotic cells (5) as well as atherogenic lipoproteins (6) and cholesterol crystals (CC) (7) by phagocytes. On the other hand, anti-inflammatory properties for C1q have been well-described. For example, bound C1q decreases the release of pro-inflammatory cytokines and increases the production of anti-inflammatory mediators by phagocytes (8, 9). Additionally, the presence of C1q on apoptotic cells skews macrophage polarization toward an anti-inflammatory phenotype (10).

Apart from C1q's extensively studied involvement in immunity, a complex cross-talk between complement and coagulation is becoming more and more evident (11). Complement components have been found to induce hemostasis and *vice versa* coagulation factors can trigger complement activation, thereby combining two powerful plasma cascades. Within the hemostatic cascade, von Willebrand factor (vWF) acts as an important starter molecule by mediating platelet adhesion and aggregation. Immune cells, such as macrophages, are competent to take up and clear vWF through scavenger receptors (12, 13). Moreover, vWF has been shown to interact with complement factor H (14, 15) and therefore can modulate the activation of complement via the alternative pathway (16). Furthermore, a direct interaction between vWF and C1q was found by our group, demonstrating that C1q, bound to surfaces such as apoptotic cells, acts as a binding partner for vWF (17). The C1q-vWF interaction also seems to occur on the surface of CC.

CC can be found as a characteristic feature in the intima of atherosclerotic arteries from early lesions to late plaque (18) and are widely used in *in vitro* models of atherosclerosis (19–21). Formation of CC occurs upon fatty streak development by an increased uptake and exhausted efflux of cholesterol by lipid-laden macrophages known as foam cells. In *in vitro* and *in vivo* models of atherosclerosis, CC have been implicated in the activation of the NOD [nucleotide oligomerization domain]-, LRR [leucine-rich repeat]-, and PYD [pyrin domain]-containing protein 3 (NLRP3) inflammasome and downstream cytokine secretion, consequently triggering local and systemic inflammation (22–24). While the role of CC and macrophages in atherosclerosis appears unambiguous, C1q can play a dual role. On the one hand, C1q bound to oxidized low-density lipoproteins (LDL) or CC has been shown to activate the classical pathway, and in this context to drive the progression of atherosclerosis in animal models (25, 26). On the other hand, C1q has also been described to be protective in early atherosclerosis *in vivo* (27, 28) and to increase cholesterol efflux transporter expression *in vitro* (6), suggesting atheroprotective properties. Similarly, the role of vWF in atherosclerosis is still a matter of debate. Although various studies suggest that vWF deficiency provides protection from atherosclerosis in animals, in humans, an unequivocal protective effect of vWF deficiency on atherosclerosis has not been demonstrated so far (29).

In summary, CC, macrophages, C1q and vWF have all been implicated in atherosclerosis. Nevertheless, the consequences of the interaction between C1q and vWF, especially on phagocytes, remain to be determined. In order to better understand this interaction, the aim of our study was to investigate the immunological effect of complexes consisting of cholesterol crystals, C1q and von Willebrand factor (CC-C1q-vWF complexes) by studying receptor expression, phagocytosis and cytokine secretion of macrophages.

MATERIALS AND METHODS

Preparation of CC

Cholesterol (suitable for cell culture, Sigma Aldrich, St. Louis, MO, USA) was dissolved in 95% ethanol at 60°C (12.5 g/l), sterile filtered and allowed to crystallize at room temperature (RT) for 7 days (d). Excess liquid was removed from the suspension, followed by drying for 5 d. Finally, CC were ground and stored as stock CC at −20°C until use.

Preparation of CC, CC-C1q, and CC-C1q-vWF Complexes for Characterization of C1q and vWF Binding

Dry stock CC were weighed and suspended in PBS (Life Technology, Carlsbad, CA, USA) at a concentration of 1.6 mg/ml, vortexed, and sonicated until a visually homogenous suspension was achieved. This CC suspension was split in three fractions for generation of CC, CC-C1q complexes, and CC-C1q-vWF complexes. Fractions were washed with PBS by centrifugation (1,000 x g, 5 min, RT) and resuspended at the same concentration. For generation of CC-C1q complexes, 50 µg/ml purified C1q (Complement Technology, Tyler, Tx, USA), diluted in PBS, was added and incubated for 1 h at RT on a shaker (700 rpm). Afterwards, CC and CC-C1q complexes were washed (as described above). For generation of CC-C1q-vWF complexes, 10 µg/ml recombinant vWF {provided by Baxalta, Lexington, MA, USA [former Baxter; characterization by Turecek et al. (30)]}, diluted in PBS, was added to washed CC-C1q complexes, vortexed rigorously, and further incubated for 1 h at RT on a shaker (700 rpm). After another washing step, CC complexes were further incubated with monoclonal mouse anti-C1q [clone 32A6 cell supernatant (31)], diluted 1:20 in PBS, or polyclonal rabbit anti-vWF (Abcam, Cambridge, UK), diluted 1:1,000 in PBS, for 1 h at RT on a shaker (700 rpm). Secondary antibody staining was performed with donkey anti-mouse IgG-AlexaFluor (AF)555 (Life Technology) and goat anti-rabbit IgG-AF647 (Abcam), both diluted 1:200 in PBS/1%BSA (Sigma Aldrich)/0.5 M NaCl for 30 min at 4°C in the dark, followed by a final wash step and resuspension in PBS/1%BSA/0.5 M NaCl. All fractions were washed and treated with either active substance (protein or antibodies) or solution only in the same manner. For flow cytometry, data were acquired using a BD Accuri 6 (BD Biosciences, San Jose, CA, USA) and analyzed with FlowJo10.

For confocal microcopy, CC were spun onto cytoslides (Shandon, Pittsburg, PA, USA) by a Cytospin centrifuge (Thermo Fisher Scientific, Waltham, MA, USA) and analyzed using Nikon A1R Nala and NIS software (both Nikon, Tokyo, Japan). For imaging flow cytometry, analyses were carried out using ImageStreamX Mark II and IDEAS software (both EMD Millipore, Billerica, MA, USA).

Cell Culture

Peripheral blood mononuclear cells were isolated from fresh buffy coats (Blood Transfusion Center of the University Hospital Basel, Basel, Switzerland) by density gradient centrifugation using Lymphoprep (Stemcell Technologies, Vancouver, Canada). Monocytes were obtained by CD14+ magnetic-activated cell separation beads (Miltenyi, Bergisch Gladbach, Germany) according to the manufacturer's instructions (yielding an average purity of 95–98% CD14+ monocytes determined by flow cytometry). Monocytes were differentiated into human monocyte-derived macrophages (HMDMs), cultured in DMEM supplemented with 100 U/ml penicillin and 100 µg/ml streptomycin (DMEM+), 10% fetal calf serum (FCS) (all from Life Technology), and 50 ng/ml GM-CSF (Immunotools, Frisoythe, Germany) at a cell concentration of 5×10^5 cells/ml in 6-well plates (BD Biosciences, Franklin Lakes, NJ, USA) and maintained in 5% CO_2 at 37°C for 7 days.

Treatment With CC Complexes

After 7 days, HMDMs were washed with prewarmed DMEM+, optionally stimulated with 100 ng/ml lipopolysaccharide (LPS) (*E. coli* O127:B8, Sigma Aldrich), diluted in prewarmed DMEM+, and treated with CC, CC-C1q, or CC-C1q-vWF complexes for indicated time points. CC and CC-complexes were prepared as described above, washed once with PBS by centrifugation (1,000 × g, 5 min, RT) and resuspended in prewarmed DMEM+ at a final concentration of 0.5 mg/ml before adding to cells.

Surface Receptor Expression

HMDMs were stimulated with LPS and treated with CC, CC-C1q, or CC-C1q-vWF complexes as described above. After 18 h, HMDMs were washed with PBS and incubated with PBS/10 mM EDTA (AppliChem, Darmstadt, Germany) for 30 min at 4°C. Cells were collected in FACS buffer (PBS/0.1% FCS/1 mM EDTA) and resuspended at a cell concentration of 5×10^5 cells/100 µl and incubated with 2 µg/ml of human IgG for 45 min at 4°C to block unspecific binding of antibodies to Fcγ receptors. Staining was performed for 30 min at 4°C in the dark in PBS using the following antibodies: anti-MHC II-FITC (Immunotools), anti-tyrosine-protein-kinase Mer (MerTK)-PE (R&D Systems, Minneapolis, MN, USA), anti-programmed death ligand 1 (PD-L1/CD274)-APC and anti-CD14-PeCy7 (both from Biolegend, San Diego, CA, USA) (antibody panel 1), or anti-CD86-FITC (Biolegend), anti-lipoprotein receptor-related protein 1 (LRP-1/CD91)-PE (Thermo Fisher Scientific, Waltham, MA, USA), anti-leukocyte-associated immunoglobulin-like receptor 1 (LAIR1/CD305)-AF647 and anti-scavenger receptor A 1 (SR-A1/CD204)-PeCy7 (both from Biolegend) (antibody panel 2). HMDMs were washed and resuspended in FACS buffer. Data were aquired using a BD LSRFortessa (BD Biosciences) and analyzed with FlowJo10. Gating was performed on SSC/CD14+ cells (antibody panel 1) or SSC/CD91+ cells (antibody panel 2), respectively, and geometric mean fluorescence intensity (gMFI) was calculated.

Phagocytosis Assay

Assessment of Granularity of HMDMs

HMDMs were kept untreated or treated with CC, CC-C1q or CC-C1q-vWF complexes as described above. After 18 h, HMDMs were harvested with PBS/10 mM EDTA and resuspended at a cell concentration of 5×10^5 cells/100 µl in FACS buffer. HMDMs were stained with anti-CD11c-APC (Biolegend) for 30 min at 4°C in the dark. Data were aquired using a BD LSRFortessa (BD Biosciences) and analyzed with FlowJo10. For the quantification of phagocytosis the percentage of CD11c+ cells with high cell granularity, indicated by a shift into the side scatter (SSC) ^{high} gate (gate set according to shift in SSC from CD11c+ untreated to CC treated cells), was determined.

Assessment of Phagocytosed pHrodo-Dyed CC Complexes

HMDMs were harvested with PBS/10 mM EDTA and resuspended in phagocytosis buffer (DMEM+/12.5 mM HEPES (Sigma Aldrich)/5 mM $MgCl_2$) at a density of 5×10^5 cells/100 µl. For pHrodo-dyed CC complexes, 1 mg/ml CC were suspended in 0.1 M $NaHCO_3$ buffer (pH 8.3) and incubated with 10 µg/ml pHrodo Red Ester (Thermo Fisher Scientific) for 1 h in the dark before the addition of C1q or C1q-vWF as described above. After a final wash, pHrodo-dyed CC complexes were added to HMDMs at a concentration of 0.5 mg/ml and incubated at 37°C for 30 min. Unphagocytosed CC complexes were washed away and HMDMs were stained with anti-CD11c-FITC (Bio-Rad, Hercules, CA, USA) for 30 min at 4°C in the dark and resuspended in FACS buffer. Data were aquired using a Beckman Coulter CytoFLEX (Beckman Coulter, Brea, CA, USA) and analyzed with FlowJo10. For the quantification of phagocytosis, the percentage of CD11c+ cells with a shift into the pHrodo Red Ester+ gate (gate set according to shift in pHrodo Red Ester from CD11c+ untreated to CC treated cells) was determined.

Quantification of Secreted Cytokine Levels

HMDMs were stimulated with LPS and treated with CC, CC-C1q, or CC-C1q-vWF complexes as described above. After 18 h, supernatants were collected, centrifuged to remove cellular debris and CC and stored at −80°C until measurement. Analyses of cytokine secretion were carried out in duplicates with ELISA kits according to the manufacturer's instructions. IL-1ß, IL-1α, IL-6, and IL-10 were measured using Biolegend ELISA kits, IL-18 and IL-1RA using Abcam ELISA kits and TNFα using a BD Bioscience ELISA kit.

Caspase-1 Activity Assay

HMDMs were kept untreated or treated with CC, CC-C1q, or CC-C1q-vWF complexes as described above. After 18 h, HMDMs were harvested with PBS/10 mM EDTA and

resuspended at a cell concentration of 5×10^5 cells/ml. Cells were incubated for 1 h with fluorochrome-labeled inhibitors of caspases (FLICA) probes for caspase-1 detection according to the manufacturer's instruction (FAM FLICA Caspase-1 Assay Kit, Immunochemistry Technology, Bloomington, MN, USA). HMDMs were stained with anti-CD11c-APC (Biolegend) for 30 min at 4°C in the dark. Data were aquired using a BD LSRFortessa (BD Biosciences) and analyzed with FlowJo10. Quantification of caspase-1 activity was determined by the percentage of CD11c+ cells in the FLICA+ gate.

Statistical Analysis

Data are expressed as median ± interquartile range (IQR), if not stated otherwise. Wilcoxon matched pairs signed rank test was used to compare two groups of paired data. When more than 2 groups of unpaired data were compared, Kruskal-Wallis test was performed and if significant followed by Mann-Whitney *U*-test for comparison of two specified groups as indicated. Data were analyzed with a statistical package program (GraphPad Prism 8, La Jolla, CA, USA). Differences were considered statistically significant when the $p < 0.05$.

RESULTS

vWF Binds to CC in a C1q-Dependent Manner

Whereas, C1q is described as a classical opsonin for a variety of DAMPs (10), the molecule has been also shown to adhere to oxidized LDL (6). In addition, Samstad et al. demonstrated C1q binding on CC after incubation with human plasma (7). Therefore, we first analyzed whether surface-bound C1q on CC secondarily enables the binding of vWF. We characterized the binding of vWF to C1q on the surface of CC by flow cytometry (**Figures 1A–C**), confocal microscopy (**Figure 1D**), and imaging flow cytometry (**Figure 1E**). C1q deposition on the surface of CC is shown in **Figure 1A**. The incubation of CC with vWF in the absence of C1q showed no vWF deposition on the CC surface (orange histogram in **Figures 1B,C**). Only in the presence of surface-bound C1q, vWF was enabled to bind (green histogram in **Figures 1B,C**). The gMFI for vWF binding in the presence of C1q was 50-fold higher compared to CC without C1q [median gMFI (IQR) of C1q+vWF: 115,000 (102,000–175,000) vs. vWF: 2,300 (1,500–2,400), $p = 0.0079$]. Furthermore, we analyzed the localization of vWF binding to CC-C1q complex. Using confocal microscopy, C1q and vWF could be visualized on CC. C1q and vWF stainings co-localized (**Figure 1D**). Finally, we used imaging flow cytometry to analyze a larger CC population as CC have a heterogenous structure. Again, we observed a similar staining pattern for C1q and vWF on CC (**Figure 1E**).

Taken together, our results demonstrate that bound C1q mediates the binding of vWF to CC, and vWF alone is not able to bind to the surface of CC.

CC-C1q-vWF Complexes Upregulate the Surface Receptor Expression of HMDMs

Macrophages have a high degree of plasticity, enabling these cells to change their phenotype according to the environmental stimuli (32). In this context, C1q has been shown to elicit upregulated expression of MerTK receptor, which is involved in the process of dead cell removal, termed efferocytosis (33). Moreover, it has been described that stimulation of macrophages with C1q leads to a polarization of these cells toward an anti-inflammatory state (34). Therefore, we aimed to investigate the phenotype of HMDMs in our *in vitro* model. For this purpose, HMDMs were kept untreated or treated with CC, CC-C1q, or CC-C1q-vWF complexes for 18 h. To mimic the inflammatory milieu present in, e.g., atherosclerotic plaques (35), HMDMs were simultaneously exposed to 100 ng/ml LPS for 18 h. The phenotype was studied by analyzing the expression of surface CD14, CD86, LAIR1, LRP-1, MerTK, MHC II, PD-L1, and SR-A1 (**Figures 2A–H**). HMDMs treated with CC-C1q-vWF complexes significantly upregulated the expression of CD14 ($p = 0.0312$), LAIR1 ($p = 0.0312$), LRP-1 ($p = 0.0312$), MerTK ($p = 0.0312$), PD-L1 ($p = 0.0312$), and SR-A1 ($p = 0.0312$) as compared to CC-C1q complexes without vWF. In four out of six donors, CD86 expression was upregulated, while MHC II expression was downregulated in five out of six donors. Neither the median receptor expression of CD86 nor of MHC II was significantly affected. Also, CC treatment did not induce any significant changes in surface receptor expression as compared to untreated HMDMs (data not shown).

Our results demonstrate that CC-C1q-vWF complexes uniquely affect the expression of surface receptors, namely an upregulation of efferocytosis receptor MerTK, scavenger receptors LRP-1 and SR-A1 as well as CD14, LAIR1, and PD-L1.

Phagocytosis of CC-C1q-vWF Complexes by HMDMs Is Hampered

Since C1q is involved in the processes of efferocytosis (36) as well as phagocytosis (9) and as the additional presence of vWF upregulates efferocytosis and scavenger receptors (**Figure 2**), we next investigated the role of C1q-vWF binding in the uptake of CC complexes by HMDMs (**Figure 3**). Therefore, HMDMs were kept untreated or treated with CC, CC-C1q, or CC-C1q-vWF complexes for 18 h. The phagocytosis of CC led to an increase in cell granularity, which could be determined by a shift in SSC using flow cytometry. Analyzed as control, untreated CD11c+ HMDMs did not express a SSC^{high} population. When HDMDs were treated with CC, CC-C1q, or CC-C1-vWF complexes, the cells exhibited a SSC^{high} population (**Figure 3A**). HMDMs showed a significant decrease in cells positive for phagocytosis after the treatment with CC-C1q-vWF complexes compared to CC-C1q complexes [median phagocytosis (IQR) in six independent donors of CC-C1q-vWF: 13.65% (5.83–16.35%) vs. CC-C1q: 24.05% (22.55–34.60%), $p = 0.0312$] (**Figure 3B**). To exploit the effect on early phagocytosis, we incubated CC with the pH-dependent pHrodo Red dye (**Figures 3C,D**). Analyzed as control, unstimulated CD11c+ HMDMs only exhibited a dim fluorescent signal for pHrodo Red. Fluorescent signal for pHrodo Red increased strongly when HMDMs were treated with pHrodo-dyed CC complexes for 30 min, due to the fusion of phagocytosed CC with the acidic lysosome of HMDMs. For the early phagocytosis, HMDMs had phagocytosed significantly

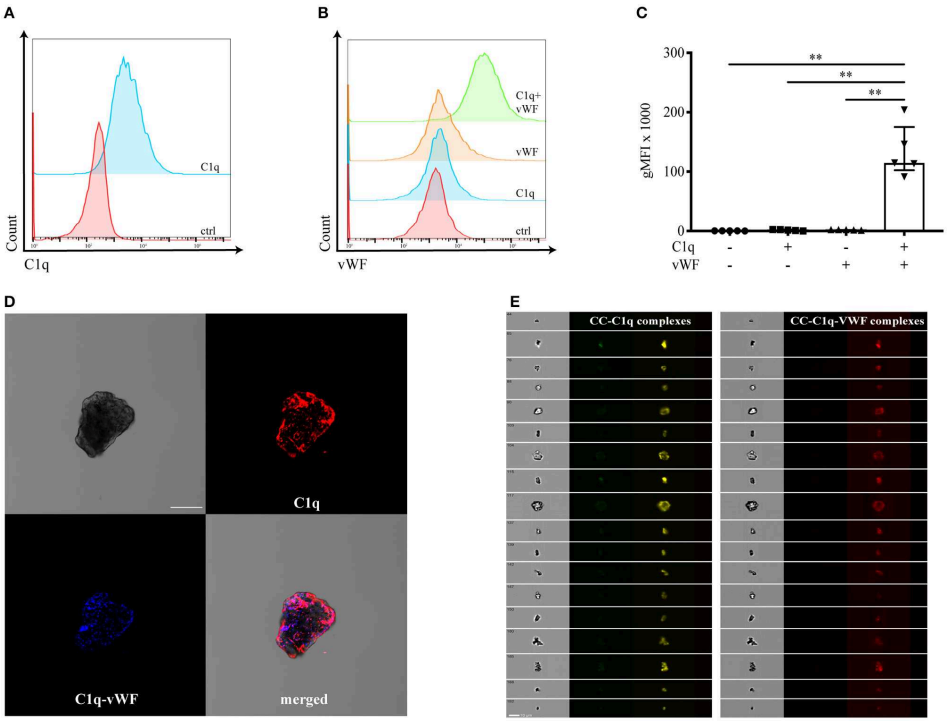

FIGURE 1 | vWF binds to CC in a C1q-dependent manner. Binding of C1q and vWF to surface-bound C1q on CC was determined by **(A–C)** flow cytometry, **(D)** confocal microscopy, and **(E)** ImageStreamX. Representative flow cytometry diagrams show the binding of **(A)** C1q or **(B)** C1q-dependent binding of vWF on the surface of CC. Controls (ctrl) represent the presence of secondary antibodies only. **(C)** Flow cytometry data are shown as median gMFI with IQR ($n = 5$, Mann-Whitney *U*-test, $^{**}p < 0.01$). **(D)** Confocal microscopy depicting a representative CC in brightfield, with C1q (red) or vWF (blue) in the presence of C1q bound to its surface. The merged staining patterns visualize the C1q-vWF interaction. One of three independent experiments is shown. Scale bar = 50 μm. **(E)** Fluorescent staining of CC captured by ImageStreamX for C1q (yellow) or C1q-vWF (red). One of two independent experiments is shown. Scale bar = 10 μm.

less CC-C1q-vWF complexes than CC-C1q complexes [median phagocytosis (IQR) in six independent donors of CC-C1q-vWF: 54.55% (40.05–60.03%) vs. CC-C1q: 62, 40% (49.05–68.78%), $p = 0.0312$] (**Figure 3D**).

In summary, late as well as early phagocytosis, by HMDMs, of CC-C1q-vWF complexes is reduced as compared to CC-C1q complexes.

CC-C1q-vWF Complexes Reduce IL-1 Cytokine Secretion of HMDMs

CC have been repeatedly described as capable inducers of IL-1ß secretion in human monocytes and macrophages (23). On the contrary, C1q has been shown to dampen pro-inflammatory cytokine secretion for the same cell types (34). Consequently, we next examined the effect of CC-C1q-vWF complexes on the cytokine profile of HMDMs. For this purpose, HMDMs kept untreated or treated with CC, CC-C1q, or CC-C1q-vWF complexes were stimulated with 100 ng/ml LPS for 18 h and supernatants were analyzed for the secretion of IL-1ß, IL-1α, IL-1RA, IL-18, IL-6, IL-10, and TNFα cytokine levels (**Figure 4**). The CC treatment induced a strong IL-1ß and IL-1α secretion by HMDMs and a moderate increase in IL-18 secretion as compared to untreated HMDMs. A robust decrease in pro-inflammatory cytokines for IL-1ß and IL-1α was observed with CC-C1q complexes, and a decreasing trend for IL-6 and TNFα secretion. The additional presence of vWF on CC-C1q complexes significantly enhanced reduction of IL-1ß secretion ($p = 0.0078$), IL-1ß/IL-1RA ratio ($p = 0.0078$), and IL-1α/IL-1RA ratio ($p = 0.0234$) compared to CC-C1q complexes alone. No other cytokines were significantly changed by vWF bound to CC-C1q complexes. Differences in cytokine secretion of HMDMs according to the treatment added were not due to differences in

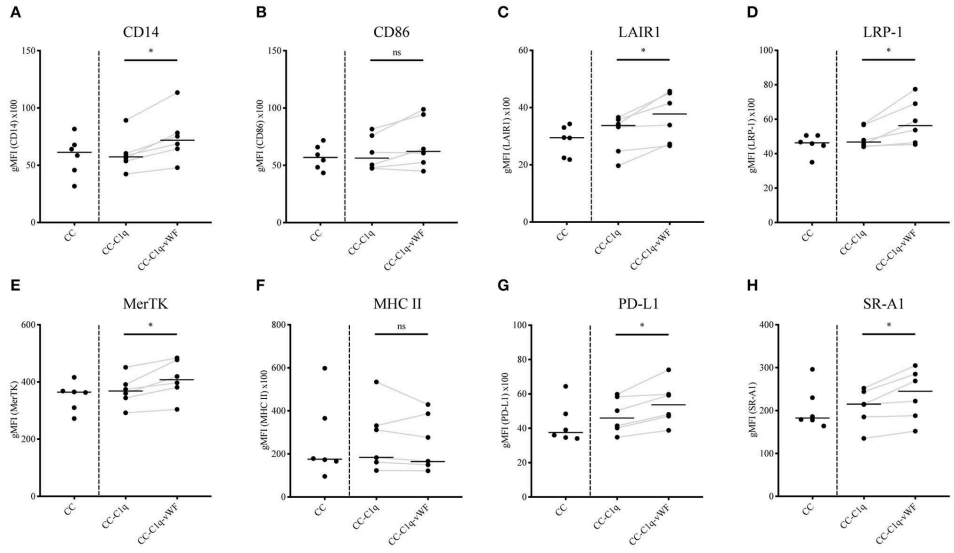

FIGURE 2 | CC-C1q-vWF complexes upregulate the surface receptor expression of HMDMs. LPS-stimulated HMDMs were treated with CC, CC-C1q or CC-C1q-vWF complexes for 18 h and analyzed by flow cytometry for surface marker expression of **(A)** CD14, **(B)** CD86, **(C)** LAIR1, **(D)** LRP-1, **(E)** MerTK, **(F)** MHC II, **(G)** PD-L1, and **(H)** SR-A1. Pooled flow cytometry data are shown as gMFI with horizontal lines denoting median. Data points represent independent experiments analyzing six different healthy donors used to obtain HMDMs (Wilcoxon matched pairs signed rank test, $*p < 0.05$; ns, not significant).

cell death as assessed by quantification of early and late apoptosis or necrosis (data not shown).

Taken together, our data show that IL-1ß cytokine secretion and IL-1ß/IL-1RA and IL-1α/IL-1RA ratio by HMDMs after exposure to CC-C1q complexes are diminished further in the presence of vWF. This reduction appears to be IL-1 specific.

CC-C1q-vWF Complexes Suppress Caspase-1 Activity of HMDMs

It is well-known that IL-1 maturation, cleavage and secretion is regulated transcriptionally as well as post-transcriptionally. While a priming signal through pattern recognition receptors is required for pro-IL-1β transcription, the maturation is dependent on the formation of the NLRP3 inflammasome and subsequent caspase-1 activation (37). Therefore, we aimed to examine whether the observed change in IL-1 cytokine secretion was the result of a preceding NLRP3 inflammasome assembly. To address this point, HMDMs were kept untreated or treated with CC, CC-C1q, or CC-C1q-vWF complexes for 18 h and the effect on caspase-1 activation was quantified with FLICA probes. Upon CC treatment, HMDMs showed a marked increase in FLICA signal, demonstrating caspase-1 activity (**Figure 5A**). While the presence of C1q on CC exhibited only a delicate reduction in caspase-1 activity, the additional presence of vWF significantly suppressed caspase-1 activity in HMDMs [median FLICA+ cells (IQR) in six independent donors of CC-C1q: 11.54% (7.29–28.38%) vs. CC-C1q-vWF: 9.37% (5.92–22.73%), $p = 0.0312$)] (**Figure 5B**).

Overall, our data show that HMDMs treated with CC-C1q-vWF complexes exhibit decreased caspase-1 activity that impacts on NLRP3 inflammasome dependent IL-1β secretion.

DISCUSSION

The cross-talk between the complement and the hemostatic systems is extensive and can provide synergistic benefits for the human body (38, 39). Yet, the role of many of these interplays is still unknown. In particular, even though an interplay between bound complement C1q and vWF has been demonstrated previously (17), its impact on the immune system has remained unexplored until now. In our study, we can illustrate that CC provide another physiological surface that allows a C1q-vWF interaction. Moreover, we found that the binding of vWF to bound C1q on CC is capable of modulating the immune response of macrophages by an upregulated expression of phagocytosis-mediating receptors and costimulatory receptors, a hampered phagocytosis and an enhanced suppression of pro-inflammatory cytokine secretion compared to C1q on CC alone.

Deposition of CC is described as a hallmark of atherosclerotic plaques. After recognition as DAMPs and ingestion by

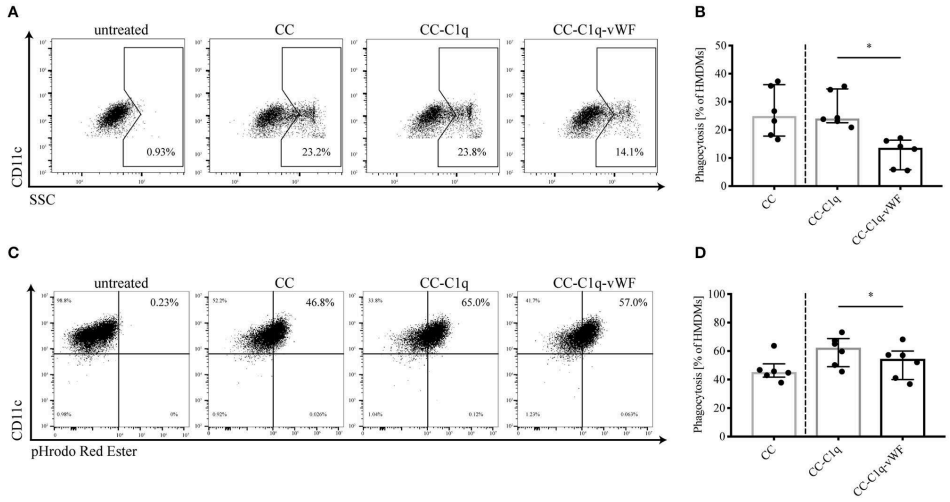

FIGURE 3 | Phagocytosis of CC-C1q-vWF complexes by HMDMs is hampered. **(A,B)** HMDMs were kept untreated or treated with CC, CC-C1q or CC-C1q-vWF complexes for 18 h and analyzed by flow cytometry for the degree of phagocytosis of CC complexes. Phagocytosis was determined by the percentage of CD11c+ cells with a shift into the SSC^{high} gate. **(A)** Flow cytometry dot plots show one out of six independent experiments. **(B)** Quantification of phagocytosis for pooled data is shown. **(C,D)** HMDMs were treated with CC, CC-C1q or CC-C1q-vWF pHrodo-dyed complexes for 30 min and analyzed by flow cytometry for the degree of phagocytosis of CC complexes. Phagocytosis was determined by the percentage of CD11c+ cells with a shift into pHrodo Red Ester+ gate. **(C)** Flow cytometry dot plots show one out of six independent experiments. **(D)** Quantification of phagocytosis for pooled data is shown. Columns denote median while error bars indicate interquartile range. Data points represent independent experiments analyzing six different healthy donors used to obtain HMDMs (Wilcoxon matched pairs signed rank test, $^*p < 0.05$).

phagocytes, CC trigger ROS formation and lysosomal leakage with consecutive NLRP3 inflammasome assembly, caspase-1 generation and IL-1β secretion (24). IL-1β secretion leads to further recruitment of phagocytes by an amplification loop in a concerted action with other pro-inflammatory cytokines and chemokines (40). Phagocytes, in particular macrophages, also are responsible for the essential function of recycling LDL and cholesterol in the periphery, but can develop into lipid-laden macrophage-derived foam cells during the course of the disease when their recycling capacity is overwhelmed. First, those foam cells can become apoptotic due to various stimuli, such as prolonged endoplasmic reticulum stress. Second, apoptotic cells that are insufficiently cleared (as occurring in advanced lesions due to defective efferocytosis), advance into cellular necrosis, in turn contributing to the formation of the necrotic core (41). Consequently, enhanced ingestion of LDL and CC fuels foam cell development, which is thought to be detrimental in later stages of atherosclerosis (42). Hence, the conclusion that CC induce arterial inflammation and destabilization of atherosclerotic plaques seems to be plausible (43). The complement molecule C1q can be considered as a double-edged sword in the context of atherosclerosis. Previous studies showed that the clearance of oxidized LDL and modified LDL is enhanced by binding of C1q (6), but simultaneously leads to a polarization of macrophages toward an anti-inflammatory phenotype through a reduction in pro-inflammatory cytokine secretion (44). In addition, C1q induces mRNA transcription of cholesterol efflux transporters (6). In contrast to these atheroprotective traits, C1q was demonstrated to be present on CC from human plasma (45) and found to be complexed to ApoE in human arteries (46), where it enables complement activation and thus contributes to atheroprogression (47, 48).

With regard to vWF, a number of studies in vWF-deficient animals and in patients suffering from Von Willebrand disease have been performed. Several of those animal studies (29) as well as human studies (49, 50) suggest atheroprogressive effects of vWF. Therefore, one could hypothesize disadvantageous consequences for the additional presence of vWF on CC-C1q complexes on macrophages. However, our findings unexpectedly point to a beneficial effect of vWF in the context of phagocytosis of CC by macrophages, and suggest that the role of vWF in atherosclerosis might be intricate and requires further investigation.

Previously, C1q and vWF have been regarded as separately acting molecules. Here, we identified not only a complex formation of C1q bound to the surface of CC but also the subsequent binding of vWF. Moreover, the treatment of HMDMs with CC-C1q-vWF complexes results in an upregulated

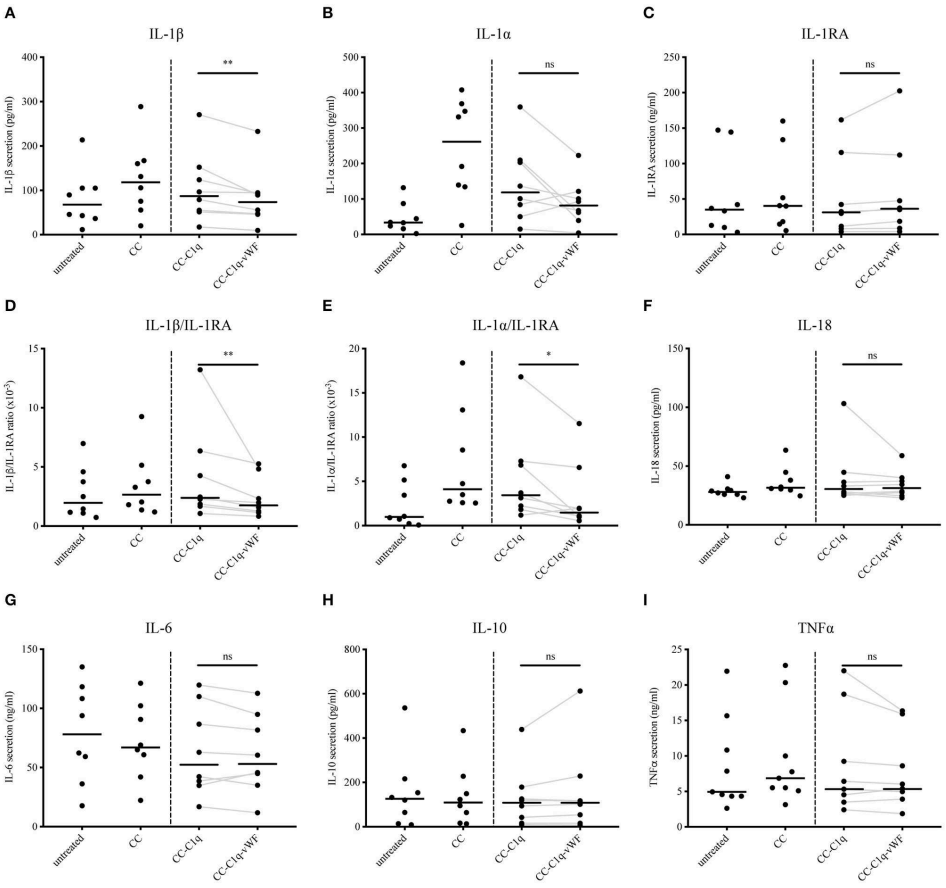

FIGURE 4 | CC-C1q-vWF complexes diminish LPS-induced IL-1 secretion of HMDMs. LPS-induced HMDMs were kept untreated or treated with CC, CC-C1q, or CC-C1q-vWF complexes for 18 h. Supernatants were analyzed by ELISA for cytokine secretion. Data show median cytokine concentrations of **(A)** IL-1β, **(B)** IL-1α, **(C)** IL-1RA, **(F)** IL-18, **(G)** IL-6, **(H)** IL-10, and **(I)** TNFα levels or median ratios of **(D)** IL-1β/IL-1RA and **(E)** IL-1α/IL-1RA of pooled donors. Data points represent independent experiments analyzing eight different healthy donors used to obtain HMDMs (Wilcoxon matched pairs signed rank test, $*p < 0.05$; $**p < 0.01$; ns, not significant).

expression of surface receptors of efferocytosis (MerTK), scavenger receptors (LRP-1 and SR-A1) as well as CD14, LAIR1, and PD-L1 compared to CC-C1q complexes alone. Studies investigating the role of the phagocytosis-mediating receptors MerTK and LRP-1 indicate atheroprotective features (51, 52), whereas the role of SR-A1 in cardiovascular disease is still controversial [reviewed by Ben et al. (53)]. Additionally, LAIR1 was described to have beneficial effects on foam cell formation (54). Therefore, we next sought to determine the effect on the phagocytic capacity of HMDMs. Interestingly, the presence of vWF on CC-C1q complexes strongly diminished the late as well as early phagocytosis of CC by HMDMs, hereby reversing the effect of C1q alone. A possible explanation for this unexpected finding could be that the upregulated expression of phagocytosis-mediating receptors is representing a reinforcing feedback loop that is triggered in order to compensate for the decreased ingestion of CC-C1q-vWF complexes. Last, our data illustrate a significant decrease in IL-1 cytokine secretion by HMDMs when

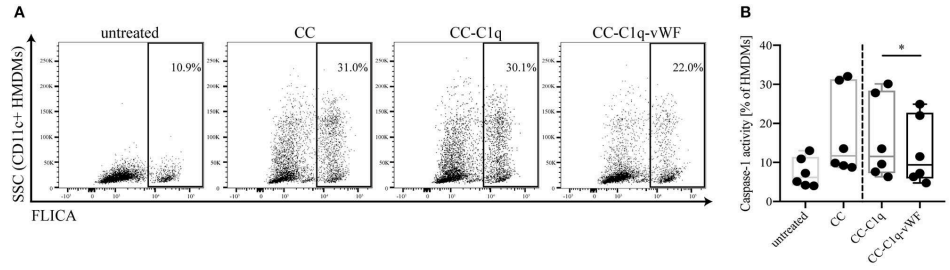

FIGURE 5 | CC-C1q-vWF complexes lead to a reduced caspase-1 activity in HMDMs. HMDMs were kept untreated or treated with CC, CC-C1q, or CC-C1q-vWF complexes for 18 h and analyzed for caspase-1 activity by flow cytometry. Activity of caspase-1 was determined by the percentage of CD11c+ cells in the FLICA+ gate. **(A)** Flow cytometry dot plots show one out of six independent experiments. **(B)** Quantification of caspase-1 activity for pooled data is shown. Horizontal lines in the box plots denote median while the boxes indicate interquartile range and whiskers minimum and maximum values. Data points represent independent experiments analyzing six different healthy donors used to obtain HMDMs (Wilcoxon matched pairs signed rank test, $*p < 0.05$).

treated with CC-C1q-vWF complexes compared to CC-C1q complexes without vWF. The clinical significance of IL-1 in cardiovascular disease was demonstrated by the anti-IL-1beta antibody Canakinumab Antiinflammatory Thrombosis Outcome Study (CANTOS) (55). Thus, a reduction in phagocytosis and inflammation could retard plaque progression (56, 57).

One limitation of our study is its *in vitro* character, since the *in vivo* situation in humans is likely to be more complex. C1q's role in human atherosclerosis is supported by studies that have shown C1q expression in atherosclerotic carotid arteries of patients (58–60) and therefore underlines the relevance of our results. Whereas the majority of C1q is non-covalently bound with serine proteases C1r and C1s to form the C1 complex in plasma and whole blood, free C1q is more prevalent in tissues where it is locally synthesized mainly by macrophages and dendritic cells (61). Furthermore, it has been demonstrated that vWF binds to a cryptic epitope of C1q, which is only exposed when C1q is surface-bound, while binding of vWF to surface-bound C1 was much weaker (17). Hence, we assume that the C1q-vWF interaction, especially on CC, primarily occurs in tissue, such as arteries of atherosclerotic patients. Nevertheless, further investigation on the occurrence of CC-C1q-vWF complexes in human atherosclerosis is needed.

Second, *in vivo,* shear stress is necessary to unfold the full functional potential of vWF (62). In our study however, permanent shear stress was not applied, since the physiological occurrence of shear stress would rather reflect the situation during plaque rupture resulting from continuous blood flow but not that inside the plaque itself.

Lastly, alternative ways can be envisaged by which the C1q-vWF interaction, in the form of CC-C1q-vWF complexes, might exert its effect on HMDMs. One of the ways could be partial steric shielding of the C1q molecule by vWF, weakening the effects of C1q (e.g., **Figure 3**). Another way could be an intrinsic effect of vWF (e.g., **Figures 2**, **4**). Future studies will have to explore the potential ways responsible for the overall impact of CC-C1q-vWF complexes. In addition, since the mutual interactions between complement and hemostatic systems *in vivo* are likely to be more complex, our *in vitro* model will have to be developed further in order to approach a physiological setting. Recently, Gravastrand et al. have described that CC induce complement-dependent activation of hemostasis (63). In our group, we have observed that complement activation remains unaffected by the presence of vWF (64). Hence, downstream complement components, such as C4 and C3, shall be implemented into our system and its effect on HMDMs in the additional presence of platelets addressed in the future.

In conclusion, with this study, we provide new insights into an emerging cross-talk between C1q and hemostasis-initiating vWF. Our findings reveal that binding of vWF to C1q on CC regulates the immune response of HMDMs. We show that CC-C1q-vWF complexes provoke a hampered phagocytosis together with an accompanied reduction of IL-1 cytokine secretion by macrophages that could prove favorable for retarding foam cell formation and decelerating plaque progression.

DATA AVAILABILITY STATEMENT

All datasets generated for this study are included in the article/supplementary material.

AUTHOR CONTRIBUTIONS

CD designed and performed the study, collected and analyzed data, and wrote the manuscript. ST and MT designed and supervised the study, and critically revised the manuscript.

FUNDING

This work was funded by a project grant from the Swiss National Science Foundation (Grant No. 310030_172956).

ACKNOWLEDGMENTS

We would like to thank Baxalta US Inc., a member of the Takeda group of companies for providing recombinant vWF under IIR grant H16-36024. Additionally, we are thankful for the valuable input and help from research labs of the Department of Biomedicine, Basel and from the research lab of Prof. Terje Espevik, especially Nathalie Niyonzima, CEMIR, NTNU, Trondheim, Norway.

REFERENCES

1. Walport MJ. Complement. *First* of two parts. *N Engl J Med*. (2001) 344:1058–66. doi: 10.1056/NEJM200104053441406
2. Morgan BP, Harris CL. Complement, a target for therapy in inflammatory and degenerative diseases. *Nat Rev Drug Discov*. (2015) 14:857–77. doi: 10.1038/nrd4657
3. Nayak A, Ferluga J, Tsolaki AG, Kishore U. The non-classical functions of the classical complement pathway recognition subcomponent C1q. *Immunol Lett*. (2010) 131:139–50. doi: 10.1016/j.imlet.2010.03.012
4. Bobak DA, Gaither TA, Frank MM, Tenner AJ. Modulation of FcR function by complement: subcomponent C1q enhances the phagocytosis of IgG-opsonized targets by human monocytes and culture-derived macrophages. *J Immunol*. (1987) 138:1150–6.
5. Bohlson SS, Fraser DA, Tenner AJ. Complement proteins C1q and MBL are pattern recognition molecules that signal immediate and long-term protective immune functions. *Mol Immunol*. (2007) 44:33–43. doi: 10.1016/j.molimm.2006.06.021
6. Fraser DA, Tenner AJ. Innate immune proteins C1q and mannan-binding lectin enhance clearance of atherogenic lipoproteins by human monocytes and macrophages. *J Immunol*. (2010) 185:3932–9. doi: 10.4049/jimmunol.1002080
7. Samstad EO, Niyonzima N, Nymo S, Aune MH, Ryan L, Bakke SS, et al. Cholesterol crystals induce complement-dependent inflammasome activation and cytokine release. *J Immunol*. (2014) 192:2837–45. doi: 10.4049/jimmunol.1302484
8. Fraser DA, Bohlson SS, Jasinskiene N, Rawal N, Palmarini G, Ruiz S, et al. C1q and MBL, components of the innate immune system, influence monocyte cytokine expression. *J Leukoc Biol*. (2006) 80:107–16. doi: 10.1189/jlb.1105683
9. Fraser DA, Laust AK, Nelson EL, Tenner AJ. C1q differentially modulates phagocytosis and cytokine responses during ingestion of apoptotic cells by human monocytes, macrophages, and dendritic cells. *J Immunol*. (2009) 183:6175–85. doi: 10.4049/jimmunol.0902232
10. Benoit ME, Clarke EV, Morgado P, Fraser DA, Tenner AJ. Complement protein C1q directs macrophage polarization and limits inflammasome activity during the uptake of apoptotic cells. *J Immunol*. (2012) 188:5682–93. doi: 10.4049/jimmunol.1103760
11. Markiewski MM, Nilsson B, Ekdahl KN, Mollnes TE, Lambris JD. Complement and coagulation: strangers or partners in crime? *Trends Immunol*. (2007) 28:184–92. doi: 10.1016/j.it.2007.02.006
12. van Schooten CJ, Shahbazi S, Groot E, Oortwijn BD, van den Berg HM, Denis CV, et al. Macrophages contribute to the cellular uptake of von Willebrand factor and factor VIII *in vivo*. *Blood*. (2008) 112:1704–12. doi: 10.1182/blood-2008-01-133181
13. Wohner N, Muczynski V, Mohamadi A, Legendre P, Proulle V, Ayme G, et al. Macrophage scavenger receptor SR-AI contributes to the clearance of von Willebrand factor. *Haematologica*. (2018) 103:728–37. doi: 10.3324/haematol.2017.175216
14. Feng S, Liang X, Cruz MA, Vu H, Zhou Z, Pemmaraju N, et al. The interaction between factor H and Von Willebrand factor. *PLoS ONE*. (2013) 8:e73715. doi: 10.1371/journal.pone.0073715
15. Turner NA, Moake J. Assembly and activation of alternative complement components on endothelial cell-anchored ultra-large von Willebrand factor links complement and hemostasis-thrombosis. *PLoS ONE*. (2013) 8:e59372. doi: 10.1371/journal.pone.0059372
16. Feng S, Liang X, Kroll MH, Chung DW, Afshar-Kharghan V. von Willebrand factor is a cofactor in complement regulation. *Blood*. (2015) 125:1034–7. doi: 10.1182/blood-2014-06-585430
17. Kölm R, Schaller M, Roumenina LT, Niemiec I, Kremer Hovinga JA, Khanicheh E, et al. Von willebrand factor interacts with surface-bound C1q and induces platelet rolling. *J Immunol*. (2016) 197:3669–79. doi: 10.4049/jimmunol.1501876
18. Franklin BS, Mangan MS, Latz E. Crystal formation in inflammation. *Annu Rev Immunol*. (2016) 34:173–202. doi: 10.1146/annurev-immunol-041015-055539
19. Corr EM, Cunningham CC, Dunne A. Cholesterol crystals activate Syk and PI3 kinase in human macrophages and dendritic cells. *Atherosclerosis*. (2016) 251:197–205. doi: 10.1016/j.atherosclerosis.2016.06.035
20. Zimmer S, Grebe A, Bakke SS, Bode N, Halvorsen B, Ulas T, et al. Cyclodextrin promotes atherosclerosis regression via macrophage reprogramming. *Sci Transl Med*. (2016) 8:333ra350. doi: 10.1126/scitranslmed.aad6100
21. Bakke SS, Aune MH, Niyonzima N, Pilely K, Ryan L, Skjelland M, et al. Cyclodextrin reduces cholesterol crystal-induced inflammation by modulating complement activation. *J Immunol*. (2017) 199:2910–20. doi: 10.4049/jimmunol.1700302
22. Abela GS. Cholesterol crystals piercing the arterial plaque and intima trigger local and systemic inflammation. *J Clin Lipidol*. (2010) 4:156–64. doi: 10.1016/j.jacl.2010.03.003
23. Duewell P, Kono H, Rayner KJ, Sirois CM, Vladimer G, Bauernfeind FG, et al. NLRP3 inflammasomes are required for atherogenesis and activated by cholesterol crystals. *Nature*. (2010) 464:1357–61. doi: 10.1038/nature08938
24. Rajamaki K, Lappalainen J, Oorni K, Valimaki E, Matikainen S, Kovanen PT, et al. Cholesterol crystals activate the NLRP3 inflammasome in human macrophages: a novel link between cholesterol metabolism and inflammation. *PLoS ONE*. (2010) 5:e11765. doi: 10.1371/journal.pone.0011765
25. Schmiedt W, Kinscherf R, Deigner HP, Kamencic H, Nauen O, Kilo J, et al. Complement C6 deficiency protects against diet-induced atherosclerosis in rabbits. *Arterioscler Thromb Vasc Biol*. (1998) 18:1790–5. doi: 10.1161/01.ATV.18.11.1790
26. Lewis RD, Jackson CL, Morgan BP, Hughes TR. The membrane attack complex of complement drives the progression of atherosclerosis in apolipoprotein E knockout mice. *Mol Immunol*. (2010) 47:1098–105. doi: 10.1016/j.molimm.2009.10.035
27. Bhatia VK, Yun S, Leung V, Grimsditch DC, Benson GM, Botto MB, et al. Complement C1q reduces early atherosclerosis in low-density lipoprotein receptor-deficient mice. *Am J Pathol*. (2007) 170:416–26. doi: 10.2353/ajpath.2007.060406
28. Lewis MJ, Malik TH, Ehrenstein MR, Boyle JJ, Botto M, Haskard DO. Immunoglobulin M is required for protection against atherosclerosis in low-density lipoprotein receptor-deficient mice. *Circulation*. (2009) 120:417–26. doi: 10.1161/CIRCULATIONAHA.109.868158
29. van Galen KP, Tuinenburg A, Smeets EM, Schutgens RE. Von Willebrand factor deficiency and atherosclerosis. *Blood Rev*. (2012) 26:189–96. doi: 10.1016/j.blre.2012.05.002
30. Turecek PL, Mitterer A, Matthiessen HP, Gritsch H, Varadi K, Siekmann J, et al. Development of a plasma- and albumin-free recombinant von Willebrand factor. *Hamostaseologie*. (2009) 29 (Suppl. 1):S32–38. doi: 10.1055/s-0037-1617202
31. Bigler C, Schaller M, Perahud I, Osthoff M, Trendelenburg M. Autoantibodies against complement C1q specifically target C1q bound on early apoptotic cells. *J Immunol*. (2009) 183:3512–21. doi: 10.4049/jimmunol.0803573
32. Sica A, Mantovani A. Macrophage plasticity and polarization: *in vivo* veritas. *J Clin Invest*. (2012) 122:787–95. doi: 10.1172/JCI59643
33. Galvan MD, Foreman DB, Zeng E, Tan JC, Bohlson SS. Complement component C1q regulates macrophage expression of Mer tyrosine kinase to promote clearance of apoptotic cells. *J Immunol*. (2012) 188:3716–23. doi: 10.4049/jimmunol.1102920

34. Thanei S, Trendelenburg M. Anti-C1q autoantibodies from systemic lupus erythematosus patients induce a proinflammatory phenotype in macrophages. *J Immunol*. (2016) 196:2063–74. doi: 10.4049/jimmunol.1501659
35. Ross R. Atherosclerosis–an inflammatory disease. *N Engl J Med*. (1999) 340:115–26. doi: 10.1056/NEJM199901143400207
36. Taylor PR, Carugati A, Fadok VA, Cook HT, Andrews M, Carroll MC, et al. A hierarchical role for classical pathway complement proteins in the clearance of apoptotic cells *in vivo*. *J Exp Med*. (2000) 192:359–66. doi: 10.1084/jem.192.3.359
37. Broz P, Dixit VM. Inflammasomes: mechanism of assembly, regulation and signaling. *Nat Rev Immunol*. (2016) 16:407–20. doi: 10.1038/nri.2016.58
38. Rayes J, Roumenina LT, Dimitrov JD, Repesse Y, Ing M, Christophe O, et al. The interaction between factor H and VWF increases factor H cofactor activity and regulates VWF prothrombotic status. *Blood*. (2014) 123:121–5. doi: 10.1182/blood-2013-04-495853
39. Nissila E, Hakala P, Leskinen K, Roig A, Syed S, Van Kessel KPM, et al. Complement factor H and apolipoprotein E participate in regulation of inflammation in THP-1 macrophages. *Front Immunol*. (2018) 9:2701. doi: 10.3389/fimmu.2018.02701
40. Libby P. Interleukin-1 beta as a target for atherosclerosis therapy: biological basis of CANTOS and beyond. *J Am Coll Cardiol*. (2017) 70:2278–89. doi: 10.1016/j.jacc.2017.09.028
41. Tabas I. Macrophage death and defective inflammation resolution in atherosclerosis. *Nat Rev Immunol*. (2010) 10:36–46. doi: 10.1038/nri2675
42. Maguire EM, Pearce SWA, Xiao Q. Foam cell formation: A new target for fighting atherosclerosis and cardiovascular disease. *Vascul Pharmacol*. (2019) 112:54–71. doi: 10.1016/j.vph.2018.08.002
43. Janoudi A, Shamoun FE, Kalavakunta JK, Abela GS. Cholesterol crystal induced arterial inflammation and destabilization of atherosclerotic plaque. *Eur Heart J*. (2016) 37:1959–67. doi: 10.1093/eurheartj/ehv653
44. Ho MM, Manughian-Peter A, Spivia WR, Taylor A, Fraser DA. Macrophage molecular signaling and inflammatory responses during ingestion of atherogenic lipoproteins are modulated by complement protein C1q. *Atherosclerosis*. (2016) 253:38–46. doi: 10.1016/j.atherosclerosis.2016.08.019
45. Pilely K, Fumagalli S, Rosbjerg A, Genster N, Skjoedt M-O, Perego C, et al. C-reactive protein binds to cholesterol crystals and co-localizes with the terminal complement complex in human atherosclerotic plaques. *Front Immunol*. (2017) 8:1040. doi: 10.3389/fimmu.2017.01040
46. Yin C, Ackermann S, Ma Z, Mohanta SK, Zhang C, Li Y, et al. ApoE attenuates unresolvable inflammation by complex formation with activated C1q. *Nat Med*. (2019) 25:496–506. doi: 10.1038/s41591-018-0336-8
47. Niculescu F, Rus H, Cristea A, Vlaicu R. Localization of the terminal C5b-9 complement complex in the human aortic atherosclerotic wall. *Immunol Lett*. (1985) 10:109–14. doi: 10.1016/0165-2478(85)90185-3
48. Torzewski M, Klouche M, Hock J, Messner M, Dorweiler B, Torzewski J, et al. Immunohistochemical demonstration of enzymatically modified human LDL and its colocalization with the terminal complement complex in the early atherosclerotic lesion. *Arterioscler Thromb Vasc Biol*. (1998) 18:369–78. doi: 10.1161/01.ATV.18.3.369
49. Bilora F, Dei Rossi C, Girolami B, Casonato A, Zanon E, Bertomoro A, et al. Do hemophilia A and von Willebrand disease protect against carotid atherosclerosis? A comparative study between coagulopathics and normal subjects by means of carotid echo-color Doppler scan. *Clin Appl Thromb Hemost*. (1999) 5:232–5. doi: 10.1177/107602969900500405
50. Bilora F, Boccioletti V, Zanon E, Petrobelli F, Girolami A. Hemophilia A, von Willebrand disease, and atherosclerosis of abdominal aorta and leg arteries: factor VIII and von Willebrand factor defects appear to protect abdominal aorta and leg arteries from atherosclerosis. *Clin Appl Thromb Hemost*. (2001) 7:311–3. doi: 10.1177/107602960100700411
51. Cai B, Thorp EB, Doran AC, Sansbury BE, Daemen MJ, Dorweiler B, et al. MerTK receptor cleavage promotes plaque necrosis and defective resolution in atherosclerosis. *J Clin Invest*. (2017) 127:564–8. doi: 10.1172/JCI90520
52. Mueller PA, Zhu L, Tavori H, Huynh K, Giunzioni I, Stafford JM, et al. Deletion of macrophage low-density lipoprotein receptor-related protein 1 (LRP1) accelerates atherosclerosis regression and increases C-C chemokine receptor type 7 (CCR7) expression in plaque macrophages. *Circulation*. (2018) 138:1850–63. doi: 10.1161/CIRCULATIONAHA.117.031702
53. Ben J, Zhu X, Zhang H, Chen Q. Class A1 scavenger receptors in cardiovascular diseases. *Br J Pharmacol*. (2015) 172:5523–30. doi: 10.1111/bph.13105
54. Yi X, Zhang J, Zhuang R, Wang S, Cheng S, Zhang D, et al. Silencing LAIR-1 in human THP-1 macrophage increases foam cell formation by modulating PPARgamma and M2 polarization. *Cytokine*. (2018) 111:194–205. doi: 10.1016/j.cyto.2018.08.028
55. Ridker PM, Everett BM, Thuren T, MacFadyen JG, Chang WH, Ballantyne C, et al. Antiinflammatory therapy with canakinumab for atherosclerotic disease. *N Engl J Med*. (2017) 377:1119–31. doi: 10.1056/NEJMoa1707914
56. Libby P. Inflammation in atherosclerosis. *Nature*. (2002) 420:868–74. doi: 10.1038/nature01323
57. Moore K, Sheedy F, Fisher E. Macrophages in atherosclerosis: a dynamic balance. *Nat Rev Immunol*. (2013) 13:709–21. doi: 10.1038/nri3520
58. Vlaicu R, Rus HG, Niculescu F, Cristea A. Immunoglobulins and complement components in human aortic atherosclerotic intima. *Atherosclerosis*. (1985) 55:35–50. doi: 10.1016/0021-9150(85)90164-9
59. Cao W, Bobryshev YV, Lord RS, Oakley RE, Lee SH, Lu J. Dendritic cells in the arterial wall express C1q: potential significance in atherogenesis. *Cardiovasc Res*. (2003) 60:175–86. doi: 10.1016/S0008-6363(03)00345-6
60. Peerschke EI, Minta JO, Zhou SZ, Bini A, Gotlieb A, Colman RW, et al. Expression of gC1q-R/p33 and its major ligands in human atherosclerotic lesions. *Mol Immunol*. (2004) 41:759–66. doi: 10.1016/j.molimm.2004.04.020
61. Rabs U, Martin H, Hitschold T, Golan MD, Heinz HP, Loos M. Isolation and characterization of macrophage-derived C1q and its similarities to serum C1q. *Eur J Immunol*. (1986) 16:1183–6. doi: 10.1002/eji.1830160926
62. Springer TA. von Willebrand factor, Jedi knight of the bloodstream. *Blood*. (2014) 124:1412–25. doi: 10.1182/blood-2014-05-378638
63. Gravastrand CS, Steinkjer B, Halvorsen B, Landsem A, Skjelland M, Jacobsen EA, et al. Cholesterol crystals induce coagulation activation through complement-dependent expression of monocytic tissue factor. *J Immunol*. (2019) 203:853–63. doi: 10.4049/jimmunol.1900503
64. Kölm R, De Libero G, Palmer E, Trendelenburg M. *Von Willebrand Factor Binds Surface-Bound C1q and Induces Platelet Rolling*. Basel: University of Basel (2015).

Conflict of Interest: The authors declare that the research was conducted in the absence of any commercial or financial relationships that could be construed as a potential conflict of interest.

Manuscript II

Complement C1q enhances primary hemostasis

Claudia Donat[1*], Robert Kölm[1], Kinga Csorba[1], Eylul Tuncer[1], Dimitrios A. Tsakiris[2], Marten Trendelenburg[1,3]

[1]Laboratory of Clinical Immunology, Department of Biomedicine, University of Basel, 4031 Basel, Switzerland

[2]Department of Diagnostic Hematology, University Hospital Basel, 4031 Basel, Switzerland

[3]Division of Internal Medicine, University Hospital Basel, 4031 Basel, Switzerland

* **Correspondence:**
Claudia Donat
E- Mail: claudia.donat@unibas.ch

Complement C1q enhances primary hemostasis

Claudia Donat[1]*, Robert Kölm[1], Kinga Csorba[1], Eylul Tuncer[1], Dimitrios A. Tsakiris[2] Marten Trendelenburg[1,3]

[1]Laboratory of Clinical Immunology, Department of Biomedicine, University of Basel, 4031 Basel, Switzerland

[2]Department of Diagnostic Hematology, University Hospital Basel, 4031 Basel, Switzerland

[3]Division of Internal Medicine, University Hospital Basel, 4031 Basel, Switzerland

*** Correspondence:**

Claudia Donat,

E- Mail: claudia.donat@unibas.ch

Keywords: complement system, complement C1q, hemostasis, von Willebrand factor, coagulation, thrombosis, bleeding time

Abstract

The cross-talk between the inflammatory complement system and hemostasis is becoming increasingly recognized. The interaction between complement C1q, initiation molecule of the classical pathway, and von Willebrand factor (vWF), initiator molecule of primary hemostasis, has been shown to induce platelet rolling and adhesion *in vitro*. As vWF disorders result in prolonged bleeding, a lack of C1q as binding partner for vWF might also lead to an impaired hemostasis. Therefore, this study aimed to investigate the *in vivo* relevance of C1q-dependent binding of vWF in hemostasis. For this purpose, we analyzed parameters of primary and secondary hemostasis and performed bleeding experiments in wild type (WT) and C1q-deficient (C1qa$^{-/-}$) mice, with reconstitution experiments of C1q in the latter. Bleeding tendency was examined by quantification of bleeding time and blood loss.

First, we found that complete blood counts and plasma vWF levels do not differ between C1qa$^{-/-}$ mice and WT mice. Moreover, platelet aggregation tests indicated that the platelets of both strains of mice are functional. Second, while the prothrombin time was comparable between both groups, the activated partial thromboplastin time was shorter in C1qa$^{-/-}$ mice. In contrast, tail bleeding times of C1qa$^{-/-}$ mice were prolonged accompanied by an increased blood loss. Upon reconstitution of C1qa$^{-/-}$ mice with C1q, parameters of increased bleeding could be reversed.

In conclusion, our data indicate that C1q, a molecule of the first-line of immune defense, actively participates in primary hemostasis by promoting arrest of bleeding. This observation might be of relevance for the understanding of thromboembolic complications in inflammatory disorders, where excess of C1q deposition is observed.

Introduction

Numerous interactions between the complement and the coagulation cascades have been described over the years. Since both pathways are thought to have evolved from a common ancestor, it is not surprising that structural as well as functional similarities exist between them (Krem and Di Cera, 2002). Structurally, both pathways are composed of potent serine proteases, which are circulating as inactive zymogens. Functionally, both systems belong to the first-line of defense and are intended to act locally at the site of infection/injury in order to limit collateral damage.

The complement system can be activated through the classical, lectin and the alternative pathways, with all three pathways leading to a shared effector response characterized by the formation of C3 and C5 convertases, release of the effector molecules C3a and C5a, and assembly of the membrane-attack complex.

The coagulation system can be characterized by the interaction between primary and secondary hemostasis. During primary hemostasis upon tissue damage, a concerted interplay of von Willebrand factor (vWF), collagen and platelets results in adhesion of platelets at the site of injury. Subsequent platelet activation and aggregation leads to the formation of a primary, instable platelet clot. During secondary hemostasis, exposure of blood to tissue factor (TF) initiates binding of factor VII, which in turn becomes activated. This leads to downstream activation of factors IX and X, with factor Xa being able to convert prothrombin to thrombin. Thrombin can amplify the cascade by activating factors XI, V, and VIII, as well as platelets themselves. Notably, to enable factor VIII to reach the phospholipid surface of those platelets, vWF is required as a carrier protein. The formation of a factor Xa-Va (prothrombinase) complex propagates the additional generation of thrombin, which then cleaves fibrinogen into insoluble fibrin. Cross-linking of fibrin polymers by factor XIIIa transforms the initial platelet clot into a stable clot. The current view is that primary and secondary hemostasis act in synergy rather than one after the other (Gale, 2011).

To date, experimental studies have described a functional impact of complement components on coagulation (Markiewski et al., 2007; Oikonomopoulou et al., 2012). Furthermore, C1q - the pattern-recognition molecule of the classical complement pathway – has been attributed a number of complement-independent functions over the years. With regard to coagulation, a

number of *in vitro* studies have investigated the interplay between C1q and coagulation components: On the one hand, C1q has been described to interact with platelets but data on this interaction are conflicting. While some studies demonstrate that C1q enhances platelet activation and upregulates P-selectin expression (Peerschke et al., 1993; Skoglund et al., 2010), other studies rather suggest that C1q mitigates coagulation by inhibiting collagen-induced platelet aggregation (Cazenave et al., 1976; Skoglund et al., 2008). On the other hand, C1q has been described to interact with factor XII, hereby proposing an inhibitory effect on clot formation (Rehmus et al., 1987). Moreover, previous findings of our group have demonstrated that a complex of surface-bound C1q and vWF is able to induce platelet rolling and adhesion (Kölm et al., 2016). This observation is of importance as activated components of complement, including C1q, and coagulation are frequently encountered concomitantly in thrombotic complications that accompany inflammatory disorders such as bacterial sepsis and systemic lupus erythematosus (SLE) (Markiewski et al., 2008; Al-Homood, 2012; Bazzan et al., 2015). Therefore, this study aimed to investigate the *in vivo* relevance of C1q-mediated binding of vWF by studying C1q-deficient mice with regard to alterations in hemostasis.

Material and Methods

Animals

C57BL/6 mice (animal facility of the Department of Biomedicine, Basel, Switzerland) and C1qa$^{-/-}$ mice on a C57BL/6 genetic background were maintained in our specific-pathogen-free facility at 22 °C room temperature (RT) with 12 h light/12 h dark cycle and were housed in groups of 2–6 mice. Mice used for experiments were kept for 2 weeks of adaptation period upon transfer. All procedures were approved by the Cantonal Commission for Animal Experiments, and the Federal Food Safety and Veterinary Office (license number 2898/28447). This study was carried out by authorized staff in accordance with the guidelines and regulations of the Swiss welfare legislation (Animal Welfare Ordinance, Animal Welfare Act and the Animal Experimentation Ordinance).

Tail bleeding time and blood loss

For these experiments, 6-14 week old wild type (WT) or C1qa$^{-/-}$ mice were weighed and injected with a mixture of ketamine (100 mg/kg body weight (BW), xylazine (10 mg/kg BW) and atropine (1.2 mg/kg BW) before 10 mm of the distal tail was amputated and immersed into 0.16% EDTA/PBS, kept at 37°C. Time to cessation of blood flow was evaluated for 15 min. Blood loss was analyzed by i) reduction in body weight, calculated by reweighing the animals including amputated tails before and after tail bleeding, ii) reduction in body weight normalized to total body weight and iii) optical density (OD) of blood-PBS solution obtained from tail bleeding assay. OD was analyzed in 96 well plate using a microplate reader with an emission wavelength of 550 nm. Experimental set-up is shown in **Supplementary Figure 1**. In all these experiments, the experimenter was blinded to the genetic background of the animals or the substance of reconstitution.

Complete blood counts

Whole blood was obtained from the tail vein, anticoagulated with EDTA and diluted with 0.9% saline (1:3). Blood cell counts and hemoglobin concentration were analyzed by using the ADVIA 2120i Hematology System (Siemens Healthcare, Erlangen, Germany).

vWF plasma levels

Citrated plasma was obtained from the tail vein and analyzed for vWF levels using von Willebrand factor two matched antibody pair kit (Abcam), according to the manufacturer's instructions.

Prothrombin time (PT)

Citrated whole blood was obtained from the tail vein and analyzed using Hemochron PT citrate cuvettes and Hemochron Jr. Signature+ (both from Accriva Diagnostics, Instrumentation Laboratory, Bedford, MA, USA).

Activated partial thromboplastin time (aPTT)

Citrated plasma was obtained by cardiac puncture and analyzed for aPTT using ACL Top 750 Las (Instrumentation Laboratory).

Platelet function

Whole blood was obtained from the vena cava, anticoagulated with hirudin and diluted with 0.9% saline (1:1) and analyzed for whole-blood platelet aggregation using the multiple electrode platelet aggregometry (MEA) Multiplate® Analyzer (Roche Diagnostics, Basel, Switzerland). Aggregation (electrical impedance) was induced with the platelet activating agonists ADP (15 µM) or collagen (10 µg/ml) and recorded for 6 min. In order to achieve sufficient amounts of platelets, blood was pooled from three mice per group.

C1q levels and reconstitution of C1q

To determine kinetics of C1q reconstitution, C1qa$^{-/-}$ mice were injected intraperitoneally (*i.p.*) with 500 µg purified human C1q (1 mg/ml, Complement Technology) and blood sampling from the tail vein was carried out at 30 min, 1 h, 2 h and 8 h. Data are shown in **Supplementary Figure 2**. For the comparison of bleeding diathesis with or without reconstitution, mice were injected *i.p.* with 500 µg purified human C1q or the same volume of 0.9% saline 2 h prior to tail bleeding. Blood sampling by cardiac puncture was carried out after the tail bleeding experiment. The degree of reconstitution with C1q was quantified from the obtained serum (time point experiments) or plasma (tail bleeding experiments) using a C1q ELISA kit (Hycult Biotech, Unden, Netherlands) according to the manufacturer's instructions. Despite the concentration of administered C1q, the site of injection and the experimenter being constant,

we observed considerable interindividual differences in the recovery rate of C1q-reconstituted mice, potentially due to subclinical differences in the intraperitoneal injection site. As a consequence, for the analysis of tail bleeding experiments following C1q reconstitution, only mice in which at least 5 µg/ml of C1q plasma concentration could be achieved were included in the analysis.

Statistical analysis

Data are expressed as median ± interquartile range (IQR), if not stated otherwise. Mann-Whitney test was used to compare two sets of nonparametric, unpaired data. Correlations were estimated by Spearman's rank correlation coefficient. Data were analyzed with a statistical package program (GraphPad Prism 8, La Jolla, CA, USA). Differences were considered statistically significant when the *p*-value was <0.05.

Results

Complete blood counts and vWF concentrations of C1q-deficient versus WT mice

In order to exclude confounders that can influence bleeding behavior, we first assessed hematologic parameters of the two strains. In detail, blood of WT mice and C1q-deficient mice was analyzed for blood counts (red blood cells, white blood cells, platelets, lymphocytes and hemoglobin) by flow cytometry, and vWF levels were quantified by ELISA. There was no statistically significant difference between WT and C1q-deficient mice for all of these parameters **(Figure 1)**.

Prothrombin time and activated partial thromboplastin time of C1q-deficient versus WT mice

Secondary hemostasis can be assessed by two different *in vitro* global coagulation tests. The PT provides information on the extrinsic pathway whereas the aPTT assesses the intrinsic pathway. In this way, abnormalities in coagulation factors of either pathway can be determined (Kamal et al., 2007). The PT of C1q-deficient mice did not differ significantly from WT mice **(Figure 2A)**. However, the aPTT was longer in WT than in C1q-deficient mice (median aPTT (IQR) of C1q-deficient mice: 23.63 s (21.35-26.25 s) vs. WT mice: 28.75 s (23.73-29.65 s), p=0.0486) **(Figure 2B)**.

Platelet aggregation of C1q-deficient versus WT mice

Platelet function can be assessed by various methods. An elegant way is the impedance whole blood aggregometry. This method allows platelets to adhere to a solid surface, which resembles the physiological function of platelets *in vivo*. Adhesion of platelets to fixed electrodes results in an increase of electrical impedance that is transformed to arbitrary aggregation units (AU) and plotted against time (Paniccia et al., 2015), from where the area under the curve (AUC) can be calculated (10 AU * min = AUC [U]). In our study, we obtained hirudin-anticoagulated whole blood and induced platelet aggregation with ADP and collagen. The AUC range in which human platelets are considered to be responsive is from 321-1059 U when platelet aggregation is induced by ADP and from 242-1019 U when platelet aggregation is induced by collagen (Multiplate® analyzer, validated for hospital use). The AUC for ADP-induced platelet aggregation was 574 U for WT mice and 497 U for C1q-deficient mice. For collagen-induced

platelet aggregation, an AUC of 745 U for WT mice and 578 U for C1q-deficient mice was observed. For both inducers, the AUC of C1q-deficient mice was slightly lower than the AUC of WT mice **(Figure 3)**. However, based on criteria used in clinics, all AUCs indicate the functional responsiveness of platelets that were obtained from WT and C1q-deficient mice.

C1q-deficient mice show enhanced bleeding diathesis

Accumulating evidence highlights the cross-talk between complement and coagulation (Foley, 2016; Dzik, 2019). Previously, our group described the occurrence of C1q-vWF complexes *in vitro* as well as *ex vivo*. Hence, we wanted to investigate whether C1q deficiency also impacts on hemostasis. For this, we conducted a tail bleeding assay and found that the bleeding time of C1q-deficient mice was significantly prolonged compared to WT mice (median bleeding time (IQR) for C1q-deficient mice: 900 s (750.5-900.0 s) vs. WT mice 750.5 s (651.8-802.0 s), p=0.0226) **(Figure 4A)**. Noteworthy, 900s were equivalent to the upper time limit of the experimental procedure. Moreover, during the tail bleeding assay C1q-deficient mice lost twice the amount of blood (median weight loss (IQR) in mg of C1q-deficient mice 400 mg (225-775 mg) vs. WT mice: 200 mg (100-475 mg), p=0.0511) **(Figure 4B)** and 2.3-fold the amount when normalized to their body weight (median weight loss (IQR) in % of C1q-deficient mice: 2.32% (1.21-3.7%) vs. WT mice: 1.01% (0.49-2.46 %), p=0.0273) **(Figure 4C)** compared to WT mice. The loss of blood could be confirmed when measuring the optical density of the resulting blood-PBS solution. The OD of the obtained solution from C1q-deficient mice showed a 3.2-fold increase compared to WT mice (median OD at 550 nm of C1q-deficient mice: 0.69 (0.33-0.90) vs. WT mice: 0.21 (0.09-0.70), p=0.0173) **(Figure 4D)**. In addition, there was a positive correlation between the OD and the relative weight loss (Spearman r=0.7932, p<0.0001) **(Figure 4E)**.

To summarize, C1q-deficient mice exhibit an enhanced bleeding diathesis compared to WT mice.

Reconstitution of C1q-deficient mice with purified C1q

To confirm that the prolonged bleeding time in C1q-deficient mice can be attributed to the lack of C1q, we next performed reconstitution experiments. First, we quantified the C1q serum concentration of WT and C1q-deficient mice. The median C1q serum concentration of WT

mice was 192.4 µg/ml, whereas the C1q serum concentration of C1q-deficient mice was below the lower limit of detection **(Suppl. Figure 2A)**.

Second, we then investigated the kinetics of recovery for the reconstitution of C1q-deficient mice with human C1q. Injecting the highest administrable dose of C1q, a partial reconstitution, equivalent to approximately 30% of the concentration of murine C1q in WT mice, was achieved with its maximum at 58.75 µg/mL after 2 h **(Suppl. Figure 2B)**. Hence, for tail bleeding experiments following C1q reconstitution, C1q-deficient mice were *i.p.* injected with either human C1q or 0.9% saline and tail bleeding experiments carried out after 2 h.

C1q reconstituted C1q-deficient mice show a reduced bleeding tendency

In order to investigate whether the observed prolonged bleeding tendency of C1q-deficient mice could be rescued, and thus can be attributed to the lack of C1q, we reconstituted C1q-deficient mice with human C1q or injected 0.9% saline as control and performed tail bleeding experiments in the same manner as described previously. Subsequently, C1q plasma concentrations were analyzed to evaluate the degree of C1q reconstitution.

The bleeding time of C1q-deficient mice reconstituted with C1q was slightly shorter than in non-reconstituted control mice (median bleeding time (IQR) of C1q injected mice: 865 s (607.0-900.0 s) vs. saline injected mice 900 s (804-900 s), p=0.4981) **(Figure 5A)**. Strikingly, mice that were reconstituted with C1q lost one fifth of the amount of blood of mice that were injected with saline instead (median weight loss (IQR) in mg of C1q injected mice: 100 mg (37.5-397.5 mg) vs. saline injected mice 500 mg (200-645 mg), p=0.0190) **(Figure 5B)** and 4.2-fold less amount of blood when normalized to their body weight (median weight loss (IQR) in % of C1q injected mice: 0.45% (0.17-1.37 %) vs. saline injected mice: 1.87% (0.80-2.65 %), p=0.0190) **(Figure 5C)**. Moreover, the OD of obtained blood solution from C1q reconstituted mice showed a 2.7-fold decrease compared to control mice (median OD at 550 nm of C1q injected mice: 0.31 (0.06-0.70) vs. saline injected mice: 0.85 (0.37-1.12), p=0.0503) **(Figure 5D)**. Most strikingly, the relative weight loss of C1q reconstituted mice during tail bleeding experiment correlated negatively with the achieved C1q concentrations after reconstitution (Spearman r=-0.7461, p=0.0071) **(Figure 5E)**.

Notably, when comparing bleeding tendency of C1q-reconstituted with WT mice, bleeding time of C1q-reconstituted mice approached the times as observed in WT mice, while the

absolute as well as relative weight loss was nearly identical between C1q-reconstituted mice and WT mice suggesting that the lack of C1q was fully responsible for differences observed between C1q-deficient and WT mice.

11

Discussion

The cross-talk between the complement system and the coagulation system is becoming ever more apparent with many of the interactions still not being fully understood. Our previous research has shown that a complex of C1q and vWF is able to recruit human platelets indicating that C1q has the potential to mediate hemostasis (Kölm et al., 2016). Therefore, we sought to examine whether C1q can impact on blood coagulability. For this purpose, we compared C1q-deficient mice to WT mice with regard to qualitative and quantitative analyses of parameters of primary and secondary hemostasis. Our study demonstrates that C1q-deficient mice exhibit prolonged bleeding and increased blood loss compared to WT mice during tail bleeding experiments. Performing reconstitution experiments with human purified C1q, the altered bleeding behavior of C1q-deficient mice could be reversed and correlated with the achieved C1q concentration in those mice. These findings highlight that C1q is directly involved in thrombus formation during coagulation.

Similar to humans, clinical conditions characterized by a decline in blood platelets (thrombocytopenia) or vWF levels (von Willebrand factor disease) can lead to dysfunctional hemostasis and thrombosis in mice (Denis et al., 1998; Morowski et al., 2013). In order to exclude such quantitative differences, we compared complete blood counts and vWF plasma concentrations of C1q-deficient and WT mice. As expected, counts of platelets, red blood cells, white blood cells and lymphocytes as well as levels of hemoglobin and vWF did not differ significantly **(Figure 1)**. Remarkably, the trend of higher platelet counts in C1q-deficient mice, which might rather imply increased coagulability in these mice, could be due to higher platelet consumption during blood collection in WT mice.

PT and aPTT are employed in the clinics to monitor clotting time, e.g. for assessment of anticoagulant therapy, and to diagnose bleeding disorders, e.g. due to deficiencies in coagulation factors. While PT and aPTT both give insight into a functional common pathway involving factors X, V and II, the PT measures the integrity of the extrinsic pathway involving TF and factor VII, whereas the aPTT provides information on the intrinsic pathway involving factors XII, XI, IX, and VIII. While prolonged PT and aPTT usually indicate impaired secondary hemostasis, shortened PT or aPTT due to abnormal levels of coagulation factors, such as factor XII, does not necessarily translate into coagulation disorders (Kamal et al., 2007;

Chaudhry et al., 2019). Since no defect in coagulation factors has been described for C1q-deficient mice, we expected the two tested mouse strains to show no significant differences in PT and aPTT. While PT was comparable, unexpectedly, the activated partial thromboplastin time was significantly shorter in C1q-deficient mice compared to WT mice **(Figure 2)**. This finding would be indicative of an increased coagulability of C1q-deficient mice, and thus oppose the enhanced bleeding behavior. Since previous research has demonstrated that C1q exerts an inhibitory effect on factor XII under physiological conditions, absence of C1q might result in an overly active factor XII, hereby shortening the aPTT (Rehmus et al., 1987). Another explanation for the shorter aPTT might be an indirect effect of the formation of C1q-vWF complexes. Physiologically, vWF is necessary for the transport of factor VIII to the site of secondary hemostasis on activated platelets. Thus, deficiency in C1q might result in its omission as a binding partner and hence in a shifted balance of vWF function towards carrying factor VIII, hereby enhancing factor VIII function and leading to a shortened aPTT.

Next to vWF dysfunction or quantitative platelet defects, qualitative platelet defects, such as dysfunctional platelet membrane receptors, can be causative for bleeding disorders (Ware, 2004; Strassel et al., 2007). Several studies investigating the effect of C1q on collagen-induced platelet aggregation have shown controversial findings, either weakening or potentiating platelet aggregation (Cazenave et al., 1976; Csako et al., 1982; Peerschke and Ghebrehiwet, 1997; Skoglund et al., 2010). Peerschke and Ghebrehiwet have repeatedly studied C1q receptors on platelets as well as the consequences of C1q stimulation on platelet activation, concluding that C1q binding to several platelet receptors leads to platelet activation via P-selectin induction and thus increases procoagulant activity (Peerschke et al., 1993; 1994; Peerschke et al., 1998).

However, Kölm et al. have not observed binding of platelets to C1q, whereas platelets are enabled to adhere to the C1q-vWF complex in an *in vitro* flow-chamber model (Kölm et al., 2016). Additionally, interaction between C1q and endothelial cells has been demonstrated. C1q has been shown to induce endothelial cell adhesion and spreading, which in turn leads to a prothrombotic phenotype of these cells (Ghebrehiwet et al., 2003; Yau et al., 2015).

In our study, analyzing platelet aggregation induced by collagen and ADP, platelets of WT as well as C1q-deficient mice were found to be functional even though responsiveness of platelets of C1q-deficient mice was slightly lower **(Figure 3)**.

Taken together, we demonstrate that C1q-deficient mice exhibit augmented bleeding **(Figure 4)** that can be partially reversed by reconstitution with C1q **(Figure 5)**.

These results suggest that C1q is directly involved in the maintenance of hemostasis. Conceivably, C1q might represent a binding partner for vWF not only *in vitro* but also *in vivo*. Consequently, the lack of C1q potentially results in reduced vWF binding followed by diminished platelet aggregation and subsequent prolongation of bleeding.

However, considering the substantial body of evidence from C1q-platelet and C1q-endothelial cell interaction studies, we cannot exclude an (maybe additional) interplay between i) C1q and platelets directly, ii) C1q and endothelial cells or iii) a still unknown interplay between C1q and another component of coagulation to participate in hemostasis.

Therefore, a limitation of our study is that, even though we propose the C1q-vWF interaction to be responsible for the altered bleeding tendency, the precise mechanism remains to be clarified. Furthermore, our study is limited by the use of human instead of murine C1q for reconstitution experiments due to the lack of availability of the latter. Nevertheless, a 76% sequence homology on DNA level and a 72% homology on protein level exists between human and murine C1q (Petry et al., 1991). Although human C1q levels in C1q-reconstituted mice remained lower than murine C1q levels in WT mice **(Suppl. Figure 2B)**, we observed significant differences in blood loss between C1q-reconstitued and non-reconstituted mice **(Figure 5B,C)**, indicating that human C1q is capable of mimicking functions of murine C1q.

With regard to the clinical relevance of our observations, a well-balanced complement system is crucial to protect against pathogens and fight against infections. In conditions where an overly active complement system results in high consumption and deposition of complement components, such as in bacterial sepsis and SLE, severe thrombotic complications are frequently observed at the same time. Regarding sepsis, it has been demonstrated that gram-positive bacteria-induced sepsis is accompanied by significant C1q consumption (Dumestre-Perard et al., 2007). Additionally, C1q has been described to bind to gram-positive and gram-negative bacteria (Brouwer et al., 2008).

Downstream activation of complement and generation of inflammatory mediators, such as C3a and C5a, has been shown to stimulate circulating neutrophils and endothelial cells and subsequently upregulates TF expression on these cells (Ikeda et al., 1997; Ritis et al., 2006). The enhanced TF expression fuels activation of the contact system of hemostasis and thus leads to increased thrombogenicity. This in turn can result in sepsis-associated coagulopathies that have been suggested to negatively affect the outcome by increasing mortality in these patients (Kienast et al., 2006). In general, inflammation is considered a predisposing factor for thrombosis.

Another example of such cross-talk is SLE, the prototype of systemic autoimmune diseases. SLE is commonly characterized by low plasma levels of C1q due to high consumption and consequent deposition (Walport et al., 1998; Ghebrehiwet and Peerschke, 2004). Strikingly, SLE patients have been described to have a higher risk of thrombotic complications, which cannot be sufficiently explained by traditional risk factors (Svenungsson et al., 2001; Avina-Zubieta et al., 2015). Those thrombotic complications include platelet hyperfunction (Dhar et al., 2009), thrombotic microangiopathies (TMA) (Wu et al., 2013), venous thromboembolism (VTE) (Kishore et al., 2019) and atherosclerosis (Asanuma et al., 2003). Moreover, it has been shown that C1q and other complement components are deposited on platelets of SLE patients and are associated with venous as well as arterial thrombotic events in those patients (Peerschke et al., 2009; Lood et al., 2012; Hoiland et al., 2018).

Apart from bacterial sepsis and SLE, C1q has also been found to be present in high concentrations at sites of atherosclerotic, inflammatory and vascular lesions, and vice versa high concentrations of C1q in these conditions have been postulated to be a driver for inflammation and thrombosis (Vlaicu et al., 1985; Peerschke and Ghebrehiwet, 1998; Peerschke et al., 2004). Therefore, future work is warranted to elucidate the clinical relevance of C1q for hemostasis in humans.

In conclusion, our study provides evidence that C1q has a physiological role in hemostasis *in vivo* by promoting arrest of bleeding. With regard to disease, an excess of deposited C1q might be a cause of thrombotic complications in inflammatory diseases such as bacterial sepsis and SLE.

Conflict of Interest

The authors declare no conflict of interest.

Author Contributions

CD, RK, DT and MT designed the study. CD, KC, ET performed experiments and CD collected and analyzed data and wrote the manuscript. MT supervised the study and all authors critically revised the manuscript.

Funding

The work was funded by a project grant from the Swiss National Science Foundation (Grant No. 310030_172956).

Acknowledgments

We would like to thank Denise Dubler and Angela Bosch from the Department of Biomedicine, Basel and the staff of the Department of Diagnostic Hematology, Basel for their technical assistance.

References

Al-Homood, I.A. (2012). Thrombosis in systemic lupus erythematosus: a review article. *ISRN Rheumatol* 2012**,** 428269. doi: 10.5402/2012/428269.

Asanuma, Y., Oeser, A., Shintani, A.K., Turner, E., Olsen, N., Fazio, S., et al. (2003). Premature coronary-artery atherosclerosis in systemic lupus erythematosus. *N Engl J Med* 349(25)**,** 2407-2415. doi: 10.1056/NEJMoa035611.

Avina-Zubieta, J.A., Vostretsova, K., De Vera, M.A., Sayre, E.C., and Choi, H.K. (2015). The risk of pulmonary embolism and deep venous thrombosis in systemic lupus erythematosus: A general population-based study. *Semin Arthritis Rheum* 45(2)**,** 195-201. doi: 10.1016/j.semarthrit.2015.05.008.

Bazzan, M., Vaccarino, A., and Marletto, F. (2015). Systemic lupus erythematosus and thrombosis. *Thromb J* 13**,** 16. doi: 10.1186/s12959-015-0043-3.

Brouwer, N., Dolman, K.M., van Houdt, M., Sta, M., Roos, D., and Kuijpers, T.W. (2008). Mannose-binding lectin (MBL) facilitates opsonophagocytosis of yeasts but not of bacteria despite MBL binding. *J Immunol* 180(6)**,** 4124-4132. doi: 10.4049/jimmunol.180.6.4124.

Cazenave, J.P., Assimeh, S.N., Painter, R.H., Pachham, M.A., and Mustard, J.F. (1976). Clq inhibition of the interaction of collagen with human platelets. *J Immunol* 116(1)**,** 162-163.

Chaudhry, L.A., El-Sadek, W.Y.M., Chaudhry, G.A., and Al-Atawi, F.E. (2019). Factor XII (Hageman Factor) Deficiency: a rare harbinger of life threatening complications. *Pan Afr Med J* 33**,** 39. doi: 10.11604/pamj.2019.33.39.18117.

Csako, G., Suba, E.A., and Herp, A. (1982). Effect of collagen-like substances (C1q, acetylcholinesterase and elastin) on collagen-induced platelet aggregation. *Haemostasis* 11(4)**,** 204-209. doi: 10.1159/000214664.

Denis, C., Methia, N., Frenette, P.S., Rayburn, H., Ullman-Cullere, M., Hynes, R.O., et al. (1998). A mouse model of severe von Willebrand disease: defects in hemostasis and thrombosis. *Proc Natl Acad Sci U S A* 95(16)**,** 9524-9529.

Dhar, J.P., Andersen, J., Essenmacher, L., Ager, J., Bentley, G., and Sokol, R.J. (2009). Thrombophilic patterns of coagulation factors in lupus. *Lupus* 18(5)**,** 400-406. doi: 10.1177/0961203308097566.

Dumestre-Perard, C., Doerr, E., Colomb, M.G., and Loos, M. (2007). Involvement of complement pathways in patients with bacterial septicemia. *Mol Immunol* 44(7)**,** 1631-1638. doi: 10.1016/j.molimm.2006.08.008.

Dzik, S. (2019). Complement and Coagulation: Cross Talk Through Time. *Transfusion Medicine Reviews*. doi: https://doi.org/10.1016/j.tmrv.2019.08.004.

Foley, J.H. (2016). Examining coagulation-complement crosstalk: complement activation and thrombosis. *Thromb Res* 141 Suppl 2**,** S50-54. doi: 10.1016/s0049-3848(16)30365-6.

Gale, A.J. (2011). Continuing education course #2: current understanding of hemostasis. *Toxicologic pathology* 39(1)**,** 273-280. doi: 10.1177/0192623310389474.

Ghebrehiwet, B., Feng, X., Kumar, R., and Peerschke, E.I. (2003). Complement component C1q induces endothelial cell adhesion and spreading through a docking/signaling partnership of C1q receptors and integrins. *Int Immunopharmacol* 3(3)**,** 299-310. doi: 10.1016/s1567-5769(02)00270-9.

Ghebrehiwet, B., and Peerschke, E.I. (2004). Role of C1q and C1q receptors in the pathogenesis of systemic lupus erythematosus. *Curr Dir Autoimmun* 7**,** 87-97. doi: 10.1159/000075688.

Hoiland, II, Liang, R.A., Hindberg, K., Latysheva, N., Brekke, O.L., Mollnes, T.E., et al. (2018). Associations between complement pathways activity, mannose-binding lectin, and odds of unprovoked venous thromboembolism. *Thromb Res* 169**,** 50-56. doi: 10.1016/j.thromres.2018.06.019.

Ikeda, K., Nagasawa, K., Horiuchi, T., Tsuru, T., Nishizaka, H., and Niho, Y. (1997). C5a induces tissue factor activity on endothelial cells. *Thromb Haemost* 77(2)**,** 394-398.

Kamal, A.H., Tefferi, A., and Pruthi, R.K. (2007). How to Interpret and Pursue an Abnormal Prothrombin Time, Activated Partial Thromboplastin Time, and Bleeding Time in Adults. *Mayo Clinic Proceedings* 82(7)**,** 864-873. doi: 10.4065/82.7.864.

Kienast, J., Juers, M., Wiedermann, C.J., Hoffmann, J.N., Ostermann, H., Strauss, R., et al. (2006). Treatment effects of high-dose antithrombin without concomitant heparin in patients with severe sepsis with or without disseminated intravascular coagulation. *J Thromb Haemost* 4(1)**,** 90-97. doi: 10.1111/j.1538-7836.2005.01697.x.

Kishore, S., Jatwani, S., Malhotra, B., Lirette, S.T., Mittal, V., and Majithia, V. (2019). Systemic Lupus Erythematosus Is Associated With a High Risk of Venous Thromboembolism in Hospitalized Patients Leading to Poor Outcomes and a Higher Cost: Results From Nationwide Inpatient Sample Database 2003-2011. *ACR Open Rheumatology* 1(3)**,** 194-200. doi: 10.1002/acr2.1030.

Kölm, R., Schaller, M., Roumenina, L.T., Niemiec, I., Kremer Hovinga, J.A., Khanicheh, E., et al. (2016). Von Willebrand Factor Interacts with Surface-Bound C1q and Induces Platelet Rolling. *J Immunol* 197(9)**,** 3669-3679. doi: 10.4049/jimmunol.1501876.

Krem, M.M., and Di Cera, E. (2002). Evolution of enzyme cascades from embryonic development to blood coagulation. *Trends Biochem Sci* 27(2)**,** 67-74.

Lood, C., Eriksson, S., Gullstrand, B., Jonsen, A., Sturfelt, G., Truedsson, L., et al. (2012). Increased C1q, C4 and C3 deposition on platelets in patients with systemic lupus erythematosus--a possible link to venous thrombosis? *Lupus* 21(13)**,** 1423-1432. doi: 10.1177/0961203312457210.

Markiewski, M.M., DeAngelis, R.A., and Lambris, J.D. (2008). Complexity of complement activation in sepsis. *Journal of cellular and molecular medicine* 12(6A)**,** 2245-2254. doi: 10.1111/j.1582-4934.2008.00504.x.

Markiewski, M.M., Nilsson, B., Ekdahl, K.N., Mollnes, T.E., and Lambris, J.D. (2007). Complement and coagulation: strangers or partners in crime? *Trends Immunol* 28(4)**,** 184-192. doi: 10.1016/j.it.2007.02.006.

Morowski, M., Vogtle, T., Kraft, P., Kleinschnitz, C., Stoll, G., and Nieswandt, B. (2013). Only severe thrombocytopenia results in bleeding and defective thrombus formation in mice. *Blood* 121(24)**,** 4938-4947. doi: 10.1182/blood-2012-10-461459.

Oikonomopoulou, K., Ricklin, D., Ward, P.A., and Lambris, J.D. (2012). Interactions between coagulation and complement--their role in inflammation. *Semin Immunopathol* 34(1)**,** 151-165. doi: 10.1007/s00281-011-0280-x.

Paniccia, R., Priora, R., Liotta, A.A., and Abbate, R. (2015). Platelet function tests: a comparative review. *Vascular health and risk management* 11**,** 133-148. doi: 10.2147/VHRM.S44469.

Peerschke, E.I., and Ghebrehiwet, B. (1997). C1q augments platelet activation in response to aggregated Ig. *J Immunol* 159(11)**,** 5594-5598.

Peerschke, E.I., and Ghebrehiwet, B. (1998). Platelet receptors for the complement component C1q: implications for hemostasis and thrombosis. *Immunobiology* 199(2)**,** 239-249. doi: 10.1016/s0171-2985(98)80030-2.

Peerschke, E.I., Jesty, J., Reid, K.B., and Ghebrehiwet, B. (1998). The soluble recombinant form of a binding protein/receptor for the globular domain of C1q (gC1qR) enhances blood coagulation. *Blood Coagul Fibrinolysis* 9(1)**,** 29-37. doi: 10.1097/00001721-199801000-00004.

Peerschke, E.I., Minta, J.O., Zhou, S.Z., Bini, A., Gotlieb, A., Colman, R.W., et al. (2004). Expression of gC1q-R/p33 and its major ligands in human atherosclerotic lesions. *Mol Immunol* 41(8)**,** 759-766. doi: 10.1016/j.molimm.2004.04.020.

Peerschke, E.I., Reid, K.B., and Ghebrehiwet, B. (1993). Platelet activation by C1q results in the induction of alpha IIb/beta 3 integrins (GPIIb-IIIa) and the expression of P-selectin and procoagulant activity. *J Exp Med* 178(2)**,** 579-587. doi: 10.1084/jem.178.2.579.

Peerschke, E.I., Reid, K.B., and Ghebrehiwet, B. (1994). Identification of a novel 33-kDa C1q-binding site on human blood platelets. *J Immunol* 152(12)**,** 5896-5901.

Peerschke, E.I., Yin, W., Alpert, D.R., Roubey, R.A., Salmon, J.E., and Ghebrehiwet, B. (2009). Serum complement activation on heterologous platelets is associated with arterial thrombosis in patients with systemic lupus erythematosus and antiphospholipid antibodies. *Lupus* 18(6)**,** 530-538. doi: 10.1177/0961203308099974.

Petry, F., Reid, K.B., and Loos, M. (1991). Gene expression of the A- and B-chain of mouse C1q in different tissues and the characterization of the recombinant A-chain. *J Immunol* 147(11)**,** 3988-3993.

Rehmus, E.H., Greene, B.M., Everson, B.A., and Ratnoff, O.D. (1987). Inhibition of the activation of Hageman factor (factor XII) by complement subcomponent C1q. *J Clin Invest* 80(2)**,** 516-521. doi: 10.1172/jci113100.

Ritis, K., Doumas, M., Mastellos, D., Micheli, A., Giaglis, S., Magotti, P., et al. (2006). A novel C5a receptor-tissue factor cross-talk in neutrophils links innate immunity to coagulation pathways. *J Immunol* 177(7)**,** 4794-4802. doi: 10.4049/jimmunol.177.7.4794.

Skoglund, C., Wettero, J., Skogh, T., Sjowall, C., Tengvall, P., and Bengtsson, T. (2008). C-reactive protein and C1q regulate platelet adhesion and activation on adsorbed immunoglobulin G and albumin. *Immunol Cell Biol* 86(5)**,** 466-474. doi: 10.1038/icb.2008.9.

Skoglund, C., Wetterö, J., Tengvall, P., and Bengtsson, T. (2010). C1q induces a rapid up-regulation of P-selectin and modulates collagen- and collagen-related peptide-triggered activation in human platelets. *Immunobiology* 215(12)**,** 987-995. doi: https://doi.org/10.1016/j.imbio.2009.11.004.

Strassel, C., Nonne, C., Eckly, A., David, T., Leon, C., Freund, M., et al. (2007). Decreased thrombotic tendency in mouse models of the Bernard-Soulier syndrome. *Arterioscler Thromb Vasc Biol* 27(1)**,** 241-247. doi: 10.1161/01.Atv.0000251992.47053.75.

Svenungsson, E., Jensen-Urstad, K., Heimburger, M., Silveira, A., Hamsten, A., de Faire, U., et al. (2001). Risk factors for cardiovascular disease in systemic lupus erythematosus. *Circulation* 104(16)**,** 1887-1893. doi: 10.1161/hc4101.097518.

Vlaicu, R., Rus, H.G., Niculescu, F., and Cristea, A. (1985). Immunoglobulins and complement components in human aortic atherosclerotic intima. *Atherosclerosis* 55(1)**,** 35-50.

Walport, M.J., Davies, K.A., and Botto, M. (1998). C1q and Systemic Lupus Erythematosus. *Immunobiology* 199(2)**,** 265-285. doi: https://doi.org/10.1016/S0171-2985(98)80032-6.

Ware, J. (2004). Dysfunctional platelet membrane receptors: from humans to mice. *Thromb Haemost* 92(3)**,** 478-485. doi: 10.1160/th04-05-0308.

Wu, L.H., Yu, F., Tan, Y., Qu, Z., Chen, M.H., Wang, S.X., et al. (2013). Inclusion of renal vascular lesions in the 2003 ISN/RPS system for classifying lupus nephritis improves renal outcome predictions. *Kidney Int* 83(4)**,** 715-723. doi: 10.1038/ki.2012.409.

Yau, J.W., Teoh, H., and Verma, S. (2015). Endothelial cell control of thrombosis. *BMC cardiovascular disorders* 15**,** 130-130. doi: 10.1186/s12872-015-0124-z.

Figure Legends

Figure 1: Complete blood counts and vWF levels of C1q-deficient versus WT mice.
EDTA-anticoagulated whole blood of C1q-deficient and WT mice was obtained and quantified by flow cytometry for numbers of **(A)** platelets, **(B)** red blood cells, **(C)** white blood cells, **(D)** lymphocytes and **(E)** amount of hemoglobin. **(F)** From citrated blood, vWF plasma concentration was quantified using ELISA. Horizontal lines in the box plots denote median while the boxes indicate interquartile range and whiskers minimum and maximum values. Data points represent individual mice, **(A), (B), (C), (E), (F)** ●: n= 11, ▲: n=10; **(D)** ●: n= 9, ▲: n=10 (Mann-Whitney test; ns, not significant).

Figure 2: Prothrombin time and activated partial thromboplastin time of C1q-deficient versus WT mice.
(A) Citrated whole blood was analyzed for prothrombin time. Data points represent individual mice, n=10 for each group. **(B)** Citrated blood plasma was analyzed for activated partial thromboplastin time. Horizontal lines in the box plots denote median while the boxes indicate interquartile range and whiskers minimum and maximum values. Data points represent individual mice, ●: n=12, ▲: n=16 (Mann-Whitney test).

Figure 3: Platelet function of C1q-deficient versus WT mice.
Hirudin-anticoagulated whole blood was obtained for functional platelet aggregation tests using ADP (15 µM) and collagen (10 µg/ml) as inducers of platelet aggregation. Platelet aggregation curve of **(A)** WT mice and of **(B)** C1q-deficient mice induced with ADP and collagen are shown. Electrical impedance is expressed as aggregation units (AU) and plotted over time [min]. Representative data of one out of three independent experiments are shown. For each experiment, blood from three mice per group was pooled.

Figure 4: Bleeding tendency of C1q-deficient versus WT mice.
A tail bleeding assay was performed and bleeding tendency of C1q-deficient and WT mice assessed by **(A)** bleeding time, **(B)** weight loss, **(C)** relative weight loss normalized to the total body weight and **(D)** OD of obtained blood-PBS solution. **(E)** Correlation between OD and relative weight loss is depicted. Horizontal lines in the box plots denote median while the boxes indicate interquartile range and whiskers minimum and maximum values. Data points represent

individual mice, n=12 per group (Mann-Whitney test; *r*, Spearman's rank correlation coefficient).

Figure 5: Bleeding tendency of C1q-deficient mice with or without reconstitution with C1q.

Tail bleeding assay was performed and bleeding tendency in C1q-deficient mice injected *i.p.* with either C1q or 0.9% saline 2 h prior to assessment of **(A)** bleeding time, **(B)** weight loss, **(C)** relative weight loss normalized to the total body weight and **(D)** OD of obtained blood-PBS solution. **(E)** Correlation between relative weight loss and achieved C1q plasma concentration in C1q-reconstituted C1q-deficient mice is shown. Horizontal lines in the box plots denote median while the boxes indicate interquartile range and whiskers minimum and maximum values. Data points represent individual mice, ●: n=12, ▲: n=10 (Mann-Whitney test; *r*, Spearman's rank correlation coefficient).

Supplementary Figure 1: Experimental set-up of tail bleeding assay.

(A) Mice are anaesthetized and placed on individual platforms. 10 mm of the distal tail is cut and tails immersed in 37°C prewarmed PBS solution. Time of bleeding is observed for 15 min. **(B)** Blood-PBS solution obtained from tail bleeding of individual mice is shown. **(C)** Blood-PBS solution is pipetted into a 96 well plate for analysis of OD.

Supplementary Figure 2: Baseline serum C1q concentrations and concentrations of serum C1q in reconstituted mice over time.

(A) Baseline C1q serum concentration of WT and C1q-deficient mice was quantified by ELISA. **(B)** C1q-deficient mice were *i.p.* injected with purified human C1q and C1q concentration was quantified from serum obtained after 30 min, 1 h, 2 h and 8 h after injection. Columns denote median while errors bars indicate IQR. Data points represent individual mice, **(A)** ●: n= 7, ▲: n=5; **(B)** n=2.

Figure 1

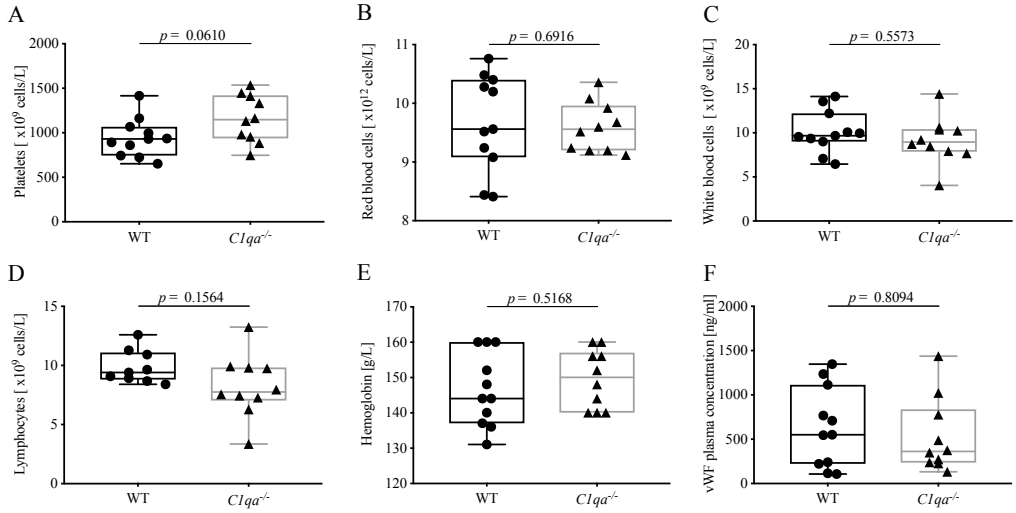
A
p = 0.0610
Platelets [x10^9 cells/L]
2000
1500
1000
500
0
WT
C1qa-/-
B
p = 0.6916
Red blood cells [x10^12 cells/L]
11
10
9
8
WT
C1qa-/-
C
p = 0.5573
White blood cells [x10^9 cells/L]
20
15
10
5
0
WT
C1qa-/-
D
p = 0.1564
Lymphocytes [x10^9 cells/L]
15
10
5
0
WT
C1qa-/-
E
p = 0.5168
Hemoglobin [g/L]
170
160
150
140
130
120
WT
C1qa-/-
F
p = 0.8094
vWF plasma concentration [ng/ml]
2000
1500
1000
500
0
WT
C1qa-/-

Figure 2

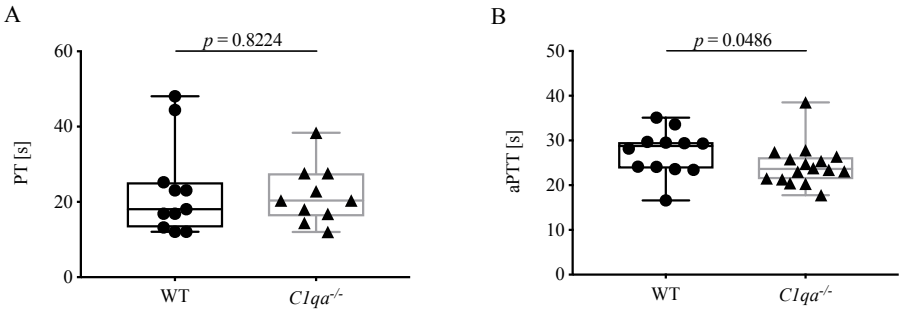
A
p = 0.8224
PT [s]
60
40
20
0
WT
C1qa-/-
B
p = 0.0486
aPTT [s]
50
40
30
20
10
0
WT
C1qa-/-

Figure 3

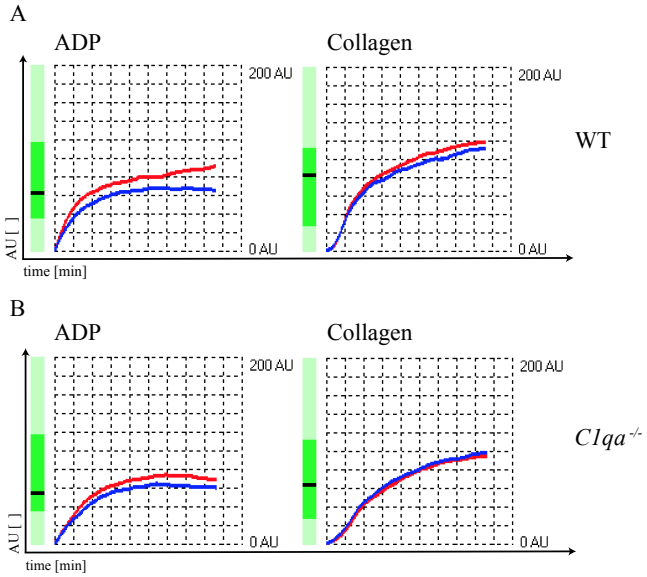
A
ADP
Collagen
200 AU
200 AU
WT
0 AU
0 AU
AU [ ]
time [min]
B
ADP
Collagen
200 AU
200 AU
C1qa-/-
0 AU
0 AU
AU [ ]
time [min]

Figure 4

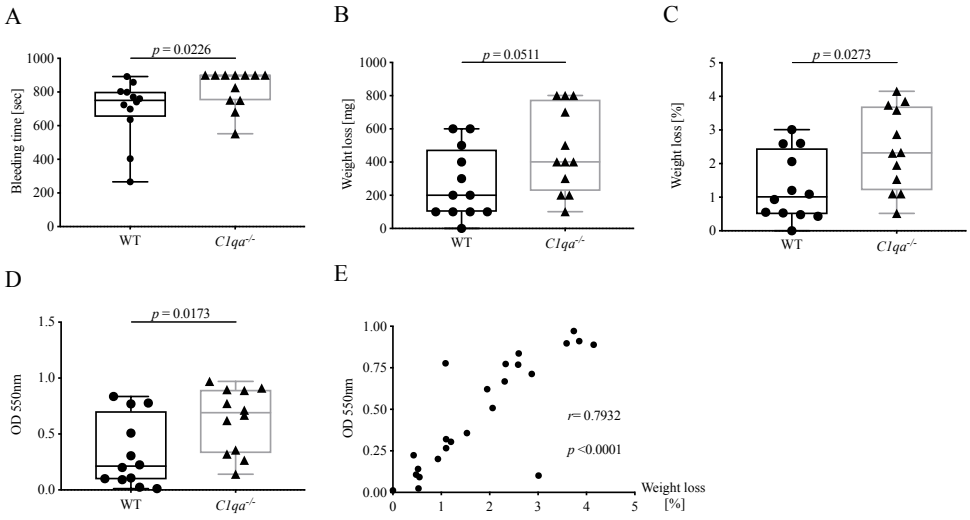
A
p = 0.0226
Bleeding time [sec]
1000
800
600
400
200
0
WT
C1qa-/-
B
p = 0.0511
Weight loss [mg]
1000
800
600
400
200
0
WT
C1qa-/-
C
p = 0.0273
Weight loss [%]
5
4
3
2
1
0
WT
C1qa-/-
D
p = 0.0173
OD 550nm
1.5
1.0
0.5
0.0
WT
C1qa-/-
E
OD 550nm
1.00
0.75
0.50
0.25
0.00
r= 0.7932
p <0.0001
0
1
2
3
4
5
Weight loss
[%]

Figure 5

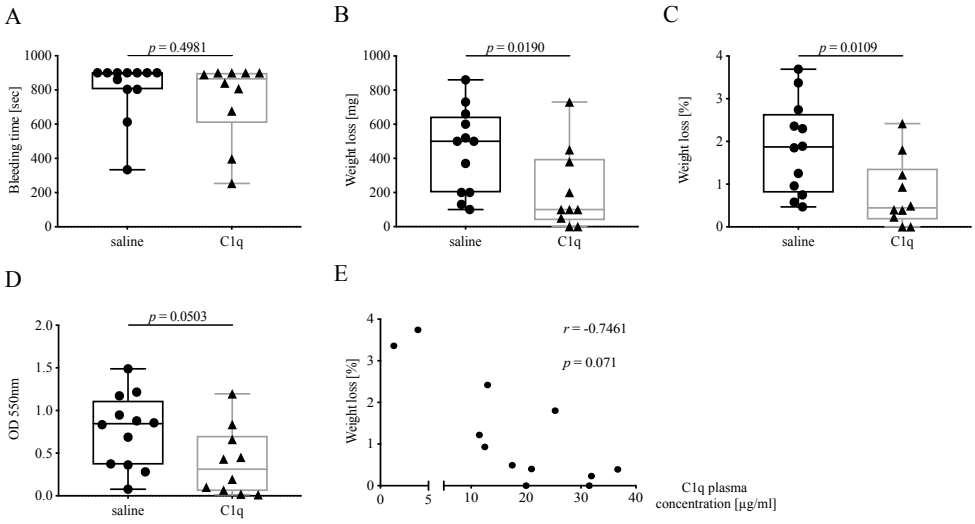
A
p = 0.4981
Bleeding time [sec]
1000
800
600
400
200
0
saline
C1q
B
p = 0.0190
Weight loss [mg]
1000
800
600
400
200
0
saline
C1q
C
p = 0.0109
Weight loss [%]
4
3
2
1
0
saline
C1q
D
p = 0.0503
OD 550nm
2.0
1.5
1.0
0.5
0.0
saline
C1q
E
r = -0.7461
p = 0.071
Weight loss [%]
4
3
2
1
0
0
5
10
20
30
40
C1q plasma
concentration [µg/ml]

Supplementary Figure 1

A

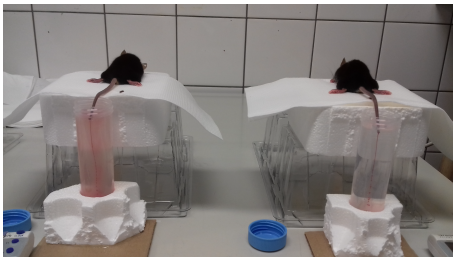

Tail bleeding

B

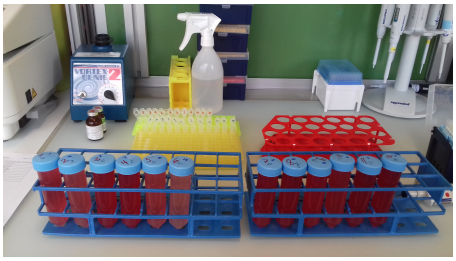

Blood loss

C

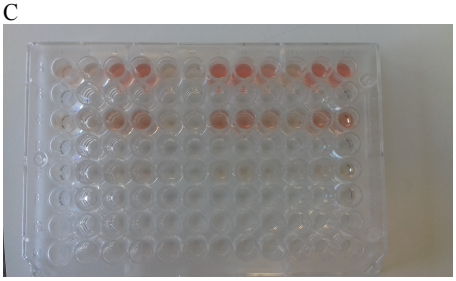

OD measurement

Supplementary Figure 2